FACULTY OF SCIENCE AND TECHNOLOGY

MASTER THESIS

Study program/specialization:
Petroleum Engineering/Drilling and Well Engineering

The spring semester, 2022

Open

Author: Camilla Abrahamsen

C.A
.....
(Signature author)

Course coordinator: Kjell Kåre Fjelde

Supervisor: Kjell Kåre Fjelde

Thesis title: **Comparison Between a Numerical Model and an Analytical Model for Drag Prediction**

Credits (ECTS): 30

Keywords:

- Drag
- Analytical Model
- Numerical Model
- MATLAB

Pages: 96

+ appendix: 15

Stavanger, June 13/2022

Abstract

High torque and drag create problems in directional wells. Directional wells have increased in inclination and length over the years, whereas the extended reach wells (ERW) are particularly prone to torque and drag limitations. Using friction models during well planning, drilling, and completion of the well will ease these issues by predicting and preventing problems at an early stage.

In this thesis, an analytical model, and a numerical model for drag prediction will be compared. Normally, the normal force consists of two components. One component is due to weight, and another component is due to tension effects (Capstan effect). In the numerical model, the normal force contribution due to the weight component perpendicular to the pipe axis is taken into consideration. The analytical model has been simplified where this term is neglected.

When comparing the models, results show that the models calculate equally for both straight inclined sections and vertical sections. The deviation between the models is within curved sections, as the friction in curved sections is modeled differently. The models increase in difference when having a large friction coefficient. A large friction coefficient increases the tension effect (Capstan effect) within a bend. The Capstan effect also increases as the bottom force increases. However, the difference between the models is maybe not very large when one takes into account that the friction coefficient is a calibration factor that can change the model results more than maybe the choice of the model.

The analytical model was implemented in Excel while the numerical model was implemented in MATLAB. More details can be found in the appendix.

Acknowledgement

This thesis was written as a final product before completing a Master of Science degree in Petroleum Engineering at the University of Stavanger, specializing in Drilling & Well Engineering.

I would like to express my gratitude to Professor Kjell Kåre Fjelde for being a motivator throughout the process, and for your knowledge sharing, guidance, and feedback. You have been of great help.

I would also thank my family and my fiancé Kjartan for your support and continuous encouragement throughout my years of study. Thank you for always believing in me and being there for me every step of the way.

Camilla Abrahamsen

Table of Content

Abstract ..... **III**

Acknowledgement ..... **IV**

List of Figures ..... **VIII**

List of Tables ..... **X**

Abbreviations ..... **XIII**

Symbols ..... **XIV**

1 Introduction **1**

1.1 Background 1

1.2 Statement of the Problem and Objective of the Thesis 2

1.3 Structure of the Thesis 2

2 Directional Drilling **3**

2.1 The Role of Directional Drilling 3

2.2 Directional Drilling Concepts 4

2.2.1 B&H Well Profile 5

2.2.2 S-Profile 6

2.2.3 J-Profile 6

2.3 Dogleg and Dogleg Severity 6

2.4 Survey Methods 7

2.4.1 Tangential Method 7

2.4.2 Balanced Tangential Method 7

2.4.3 Average Angle Method 8

2.4.4 Radius of Curvature Method 8

2.4.5 Minimum Curvature Method 8

2.5 2D Well Profile Examples 11

2.5.1 B&H Well Profile Calculation 11

2.5.2 TVD Calculation 13

2.5.3 HD Calculation 14
2.5.4 MD Calculation 15
2.5.5 S-Profile Calculation 16
2.5.6 TVD Calculation 17
2.5.7 HD Calculation 19
2.5.8 MD Calculation 20
3 Drag Models 21
3.1 Torque and Drag Models in Well Design 21
3.2 General Concepts and Models 21
3.2.1 Buoyancy 21
3.2.2 Friction 22
3.2.3 Capstan Effect 24
3.2.4 Projected Height Principle 26
3.3 Analytical Drag Model 27
3.3.1 Drag Force for a Straight Inclined Section Without Pipe Rotation 27
3.3.2 Drag Force for a Curved Section Without Pipe Rotation 28
3.3.3 Drag Force for a Vertical Section Without Pipe Rotation 30
3.4 Numerical Drag Model 31
4 Results and Discussion 34
4.1 Case Examples 34
4.1.1 B&H Well Profile 35
4.1.2 B&H Well Profile – Tripping out Scenario 37
4.1.3 B&H Well Profile – Tripping in Scenario 39
4.1.4 B&H Well Profile – Static (Rotating off Bottom) Scenario 42
4.1.5 S-Profile 44
4.1.6 S-Profile – Tripping out Scenario 47
4.1.7 S-Profile – Tripping in Scenario 50

4.1.8 S-Profile – Static Scenario 53
4.2 Comparison of Analytical Model and Numerical Model in a Bend 56
4.2.1 Comparison of Models - Static Scenario 57
4.2.2 Comparison of Models - Tripping out Scenario 59
4.2.3 Sensitivity Analysis – Tripping out scenario 66
4.2.4 Comparison of Models for a Tripping in Scenario 69
4.3 Comparison of the Models - B&H Well Profile 75
4.4 Comparison of the Models – S-Profile 76
5 Conclusion 79
References 80
Appendix A 83
Appendix A.1 Numerical T&D Model 83
Appendix B 85
Appendix B.1 Analytical Model for B&H Well Profile – Tripping out Scenario 85
Appendix B.2 Analytical Model for B&H Well Profile – Tripping in Scenario 87
Appendix B.3 Analytical Model for B&H Well Profile – Static (Rotating off Bottom) Scenario 90
Appendix B.4 Analytical Model for S-Profile – Tripping out Scenario 91
Appendix B.5 Analytical Model for S-Profile – Tripping in Scenario 93
Appendix B.6 Analytical Model for S-Profile – Static (Rotating off Bottom) Scenario 96

List of Figures

Figure 1: Illustration of azimuth, MD, TVD, and hole inclination. Modified from [6]. 4
Figure 2: The basic 2D well profiles. Modified after [6]. 5
Figure 3: Model of the minimum curvature method [15]. 10
Figure 4: The geometry of a B&H well profile. 11
Figure 5: The geometry of an S-profile. 16
Figure 6: Forces and decomposed forces that are working on an inclined object. Modified after [5]. 23
Figure 7: Illustration of the Capstan effect. Modified after [23]. 24
Figure 8: Illustration of the projected height principle. Modified after [20]. 26
Figure 9: Geometry of a straight inclined pipe. Modified after [5] 27
Figure 10: The figure to the left illustrates the normal force resulting from weight, while the figure to the right illustrates the normal force resulting from tension. Modified after [4]. 29
Figure 11: The figure to the left illustrates the effect of gravity and the effect of tension that is acting on a curved segment of a drill string. The figure also illustrates their contribution to normal force. The figure to the right illustrates the forces during a tripping out scenario. Modified after [4]. 31
Figure 12: B&H well profile showing the drag forces for calculation. 35
Figure 13: Drag forces for the B&H well profile when μ = 0,4. 43
Figure 14: Drag forces for varying friction coefficients between 0,1 – 0,4 for a tripping out scenario, tripping in scenario and static scenario for the B&H well profile. 44
Figure 15: S-Profile showing the drag forces for calculation. 45
Figure 16: Drag forces for the S-profile when μ = 0,4. 55
Figure 17: Drag forces for varying friction coefficient between 0,1 – 0,4 for a tripping out scenario, tripping in scenario and static scenario for the S-profile. 55
Figure 18: The difference between the analytical model and the numerical model for a tripping out scenario illustrated graphically. 60
Figure 19: The distribution of friction forces for a tripping out scenario when μ = 0,4 illustrated graphically. 63
Figure 20: The difference between the numerical model and the analytical model capturing the increase in the Capstan effect further up in the bend. 66
Figure 21: The difference between the analytical model and the numerical model for a tripping in scenario illustrated graphically. 70

Figure 22: The distribution of friction forces for a tripping in scenario when μ = 0,4 illustrated graphically. 72
Figure 23: The difference between the numerical model and the analytical model capturing the decrease in the Capstan effect further up in the bend. 74
Figure 24: Comparison of the analytical model and the numerical model for a tripping out scenario and a tripping in scenario when having friction coefficients of μ = 0,1 and μ = 0,4 for the B&H well profile. 75
Figure 25: Comparison of the analytical model and the numerical model for a tripping out scenario and a tripping in scenario when having friction coefficients of μ = 0,1 and μ = 0,4 for the S-profile.....77

List of Tables

Table 1: Drill string characteristics used for drag calculations for the B&H well profile.....35
Table 2: Geometrical parameters used for drag calculations for the B&H well profile.....36
Table 3: Calculated forces at the top of the hold section for varying friction coefficients between 0,1 – 0,4 during a tripping out scenario for the B&H well profile. 38
Table 4: Calculated forces in the build-up bend section for varying friction coefficients between 0,1 – 0,4 during a tripping out scenario for the B&H well profile. 38
Table 5: Calculated forces at the top of the vertical section for varying friction coefficients between 0,1 – 0,4 during a tripping out scenario for the B&H well profile. 39
Table 6: Calculated forces at the top of the hold section for varying friction coefficients between 0,1 – 0,4 during a tripping in scenario for the B&H well profile. 40
Table 7: Calculated forces in the build-up bend section for varying friction coefficients between 0,1 – 0,4 during a tripping in scenario for the B&H well profile. 40
Table 8: Calculated forces at the top of the vertical section for varying friction coefficients between 0,1 – 0,4 during a tripping in scenario for the B&H well profile. 41
Table 9: Calculated forces at the top of the vertical section for varying friction coefficients between 0,1 – 0,4 during a tripping in scenario for the B&H well profile, including the weight force of the top drive. 41
Table 10: Calculated forces for a static scenario for the B&H well profile. 42
Table 11: Drill collar characteristics used for drag calculations of the S-profile. 45
Table 12: Geometrical parameters used for drag calculations for the S-profile. 46
Table 13: Calculated forces at the top of the inclined section for varying friction coefficients between 0,1 – 0,4 during a tripping out scenario for the S-profile. 47
Table 14: Calculated forces in the drop bend section for varying friction coefficients between 0,1 – 0,4 during a tripping out scenario for the S-profile. 48
Table 15: Calculated forces at the top of the hold section for varying friction coefficients between 0,1 – 0,4 during a tripping out scenario for the S-profile. 48
Table 16: Calculated forces in the build-up bend section for varying friction coefficients between 0,1 – 0,4 during a tripping out scenario for the S-profile. 49
Table 17: Calculated forces at the top of the vertical section for varying friction coefficients between 0,1 – 0,4 during a tripping out scenario for the S-profile. 49
Table 18: Calculated forces at the top of the inclined section for varying friction coefficients between 0,1 – 0,4 during a tripping in scenario for the S-profile. 50

Table 19: Calculated forces in the drop bend section for varying friction coefficients between 0,1 – 0,4 during a tripping in scenario for the S-profile. 51
Table 20: Calculated forces at the top of the hold section for varying friction coefficients between 0,1 – 0,4 during a tripping in scenario for the S-profile. 51
Table 21: Calculated forces in the build-up bend section for varying friction coefficients between 0,1 – 0,4 during a tripping in scenario for the S-profile. 52
Table 22: Calculated forces at the top of the vertical section for varying friction coefficients between 0,1 – 0,4 during a tripping in scenario for the S-profile. 52
Table 23: Calculated forces at the top of the vertical section for varying friction coefficients between 0,1 – 0,4 during a tripping in scenario for the S-profile, including the weight force of the top drive. 53
Table 24: Calculated forces for a static scenario for the S-profile. 54
Table 25: Comparison of the analytical model and numerical model in a bend for a static scenario. The numerical model applies a discretization of 30-meter segments. 57
Table 26: Comparison of the analytical model and numerical model in a bend for a static scenario. The numerical model applies a discretization of 10-meter segments. 58
Table 27: Comparison of the analytical model and numerical model in a bend for a tripping out scenario. The numerical model uses a discretization of 30-meter segments. 59
Table 28: The difference in percentage between the analytical model and the numerical model for a tripping out scenario. 61
Table 29: Differences in forces between the analytical model and the numerical model given in different units for the tripping out scenario. 61
Table 30: Distribution of friction forces for the tripping out scenario in the numerical model. 62
Table 31: The difference in friction forces in the numerical model when calculating the total friction force as a whole and then calculating the friction force by dividing into the friction force due to the normal force contribution caused by the weight component perpendicular to the pipe axis and friction due to the Capstan effect. 64
Table 32: The difference between the analytical model and the numerical model when only the Capstan effect is included in the numerical model for a tripping out scenario. 65
Table 33: The difference between the analytical model and the numerical model when the friction coefficient is 0,3. 67
Table 34: The difference between the analytical model and the numerical model when the friction coefficient is 0,2. 67

Table 35: The difference between the analytical model and the numerical model when the friction coefficient is 0,1. 68
Table 36: Comparison of the analytical model and numerical model in a bend for a tripping in scenario. The numerical model uses a discretization of 30-meter segments. 69
Table 37: The difference in percentage between the analytical model and the numerical model for a tripping in scenario. 70
Table 38: Differences in forces between the analytical model and the numerical model given in different units for the tripping in scenario. 71
Table 39: The distribution of friction forces for the tripping in scenario in the numerical model. 71
Table 40: The difference in friction forces in the numerical model when calculating the total friction force as a whole and then calculating the friction force by dividing it into the friction force due to the normal force contribution caused by the weight component perpendicular to the pipe axis and friction due to the Capstan effect. 73
Table 41: The difference between the analytical model and the numerical model when only the Capstan effect is included in the numerical model for a tripping in scenario. 74

Abbreviations

BHA	Bottom hole assembly
B&H	Build and Hold
DC	Drill collar
DL	Dogleg
DLS	Dogleg severity
ERD	Extended reach drilling
ERW	Extended reach well
HD	Horizontal displacement
HWDP	Heavy weight drill pipe
KOP	Kick-off point
MD	Measured depth
MW	Mud weight
POOH	Pulling out of hole
RF	Ratio factor
RIH	Running in hole
RKB	Rotary Kelly bushing
TD	Total depth
TVD	True vertical depth
T&D	Torque and drag

Symbols

A	Azimuth
F_f	Friction force
F_2	Tension force at lower end of pipe element
F_3	Tension force at upper end of pipe element
g	Gravitational constant
G_x	Axial component
G_y	Normal component
L	Length of pipe segment
N	Normal force
W	Buoyed unit mass
ΔA	Change in azimuth angle over length of element
α	Angle
$\Delta\alpha$	Change in inclination angle over length of element
$\overline{\alpha}$	Average inclination
β	Buoyancy factor
ΔL	Projected height
∅	Dogleg severity angle
ρ	Density
μ	Friction coefficient

1 Introduction

1.1 Background

Torque and drag is a limiting issue for the oil and gas industry and needs to be considered during the planning and drilling of the well. Drag is the needed force to be able to trip out, or trip into the wellbore [1]. Torque is the rotational force required to rotate the bit and drill string. Implementing torque and drag models is important to drill the well successfully and reach the target of interest [2].

Wellbore friction, especially in extended reach wells, is an issue and a critical parameter [1], [3]. This is not only important to take into consideration during drilling but also during the completion of the well and workover operations [3]. Analytical solutions have been created to calculate wellbore friction. A numerical model for calculating torque and drag was developed by Johancsik et al [4]. This was based on dividing the well path into small segments and then force balances are solved for each segment and then aggregated. The friction is modeled as a friction coefficient multiplied by the normal force. The normal force is composed of two parts. One part is the normal force contribution caused by the weight of the string. The other normal force component is caused by tension effects taking place in curved sections in the well (Capstan effect).

This numerical model must be solved using a computer. However, there has also been developed a simpler analytical model [3], [5]. Here, equations are derived for larger segments like build-up sections or hold/sail sections.

Both models are examples of so-called soft string models, but there are differences with respect to how the friction is modeled in curved sections.

1.2 Statement of the Problem and Objective of the Thesis

The objective of the thesis is to compare the analytical torque and drag model with the numerical torque and drag model. Only drag calculations will be compared. In the analytical model, the friction force related to the normal force contribution due to weight in bends is disregarded. One only considers the friction caused by the normal force due to tension effects (Capstan effect) [3]. By comparing the analytical model with the numerical model, makes it possible to see how large effect this simplification has since the numerical model both contains friction related to the normal force due to weight and normal force due to tension.

2D well profile examples such as Build and Hold (B&H) well profile and S-profile are used for calculations of axial forces (drag forces). The friction coefficient will be varied to see how the forces on top of the drill string will change for a tripping out scenario (pick-up), tripping in scenario (slack-off), and rotating off bottom scenario (static).

1.3 Structure of the Thesis

The organization of this thesis is as follows:

- Chapter 2 describes the theory of directional drilling used in this thesis. This chapter includes topics like the role of directional drilling, directional drilling concepts, well profiles, dogleg and dogleg severity, survey methods used for wellbore trajectory calculations, and well profile calculations for a B&H well profile and S-profile.
- Chapter 3 describes the drag models. Topics like torque and drag models in well design, buoyancy, friction, Capstan effect, and the projected height principle are also included here.
- Chapter 4 represents the results and discussion of the thesis.
- Chapter 5 presents the conclusion.
- The appendix covers screenshots of the analytical calculations and the MATLAB code of the simplified Johancsik torque and drag model.

2 Directional Drilling

2.1 The Role of Directional Drilling

Directional drilling is basically ``*all activities that are required to design and drill a wellbore to reach a target, or a number of targets, located at some horizontal distance from the top of the hole´´* [6]. Directional drilling has been an essential application to the oil and gas industry since the late nineteenth century [7]. According to [8], the applications of directional drilling are many. These applications can be divided into different categories:

- Side-tracking
- Drilling to avoid geological problems
- Controlling vertical boreholes
- Drilling beneath inaccessible locations
- Horizontal drilling
- Offshore development drilling

In general, the easiest accessible oil is produced first, but with new and improved technology it is possible to drain existing fields and produce new fields in a more efficient way. During the last decades, the wells have increased in both length and inclination [9]. The wells are drilled with more complexity where high inclinations are more common, making it possible to drill the so-called extended reach wells (ERW) [6].

Extended reach wells are both drilled onshore and offshore and can be between 20,000 ft (6096 m) – 40,000 ft (12 192 m) long or more [6]. The record today, as of 2021, is 15 000 m, with a step out of 14 129 m drilled within the Sakhalin-1 project [10].

For a well to be classified as an extended reach well, the depth ratio (MD/TVD) is at least at the ratio of 2:0 or having an HD/TVD ratio larger than 2.0 [11], [12]. The depth ratio is also an indication of how complex the ERD well is. The ERD well is difficult and more complex the higher the depth ratio [12].

2.2 Directional Drilling Concepts

Before representing the analytical drag models in chapter 3, some basic directional drilling concepts will be represented to ensure a better understanding of the terms and abbreviations used in further chapters of this thesis.

Definition of well trajectory concepts and terms in directional wells:

- KOP (kick-off point) is the depth where the wellbore trajectory departs from the vertical in the direction towards the target [6].
- Build-up rate is the rate at which the hole inclination angle changes along the well path [6].
- TVD (true vertical depth) is the vertical distance from the RKB to a certain point or target as shown in Figure 1 [6].
- HD (horizontal displacement) is the horizontal distance from the well center to the target of interest.
- MD (measured depth) is the distance from the RKB to a certain point or target measured along the wellbore as shown in Figure 1 [6].
- Azimuth is in the horizontal plane and is the measured angle between 0-360 degrees measured clockwise from the magnetic north as shown in Figure 1.

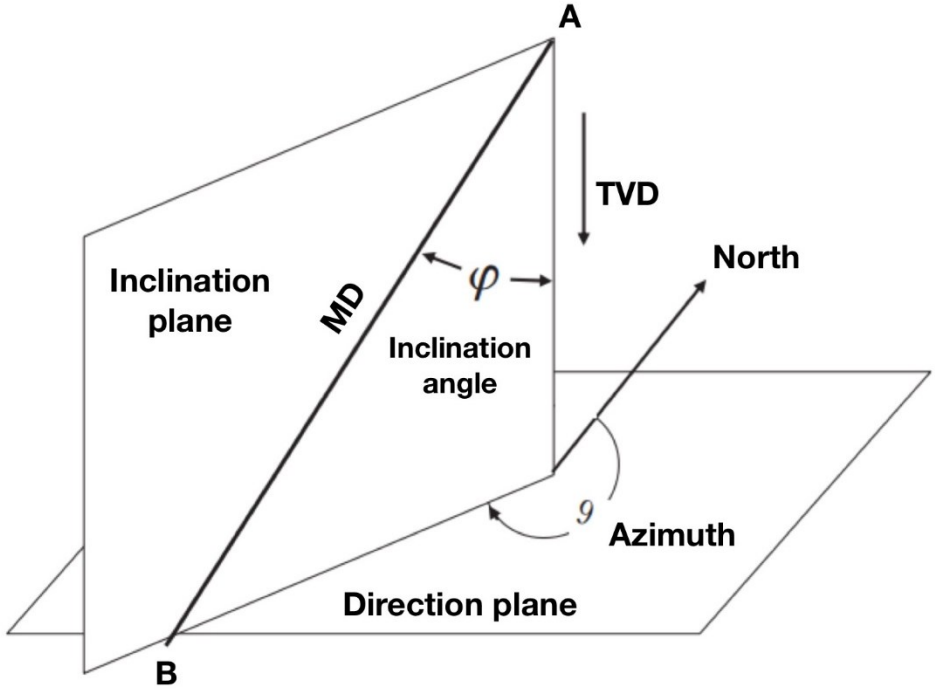

Figure 1: *Illustration of azimuth, MD, TVD, and hole inclination. Modified from [6].*

Most wells today are designed and drilled in 3D. Constructing well trajectories in 3D makes it possible to avoid obstacles like salt domes, faults, or formations that can be difficult to drill through. Wells are drilled three-dimensional offshore to avoid wells intersecting, and onshore to minimize the footprint of drilling rigs, making it more environmentally friendly [6].

In some cases, 2D wells are drilled when possible. The 2D wells are restricted to the vertical plane. The basic well trajectory profiles for 2D wells are a build and hold (B&H) well profile, an S-shaped well profile, and a J-shaped well profile as shown in Figure 2 [6].

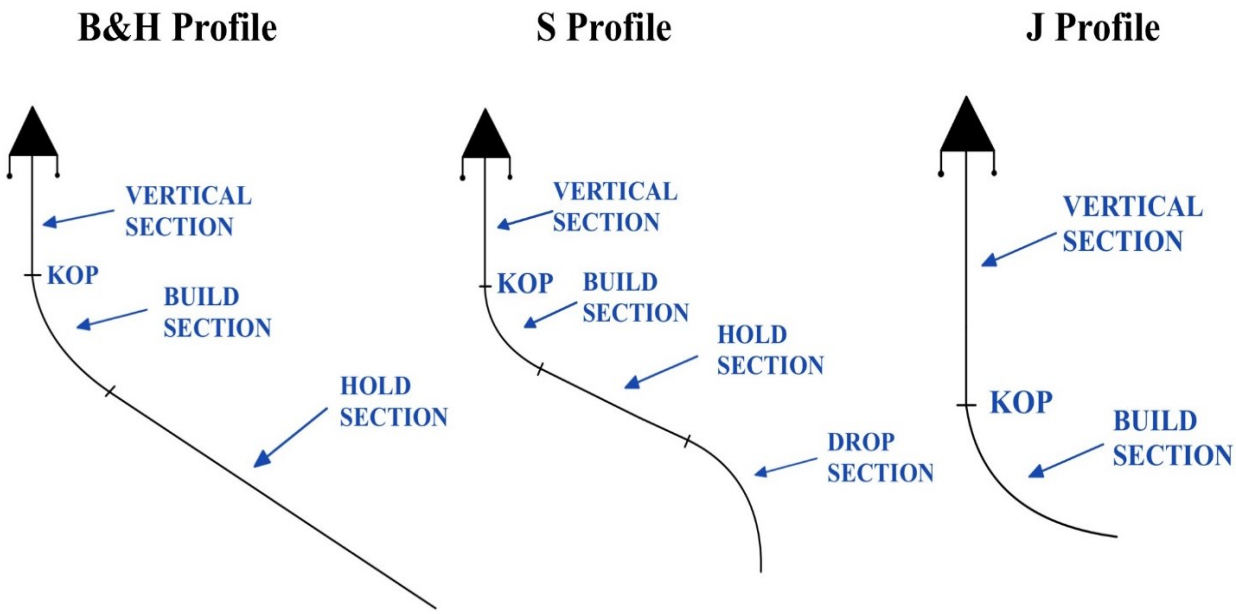

Figure 2: *The basic 2D well profiles. Modified after [6].*

2.2.1 B&H Well Profile

The B&H well profile is the simplest and most common type when it comes to directional wells [13]. For extended reach wells, the B&H well profile will be the basic build block [11]. When there is a need for large horizontal displacement, the B&H well profile is often applied. The B&H well profile can be used for both wells located at a moderate depth and for deeper wells [11].

Down to the KOP, the well is drilled vertically. The well is then deviated into the required inclination by a build-up section. The required inclination is then maintained throughout the hold section until intersecting the target [13].

There are few problems connected to this well profile. This is because, after the build-up section, there are no changes in azimuth or inclination. For a given target, the inclination angle will be reduced if the KOP is made shallower [13].

2.2.2 S-Profile

The S-shaped well profile is used when the target of interest is located deep and the horizontal displacement is small [13]. The well is drilled in a similar way as the B&H well profile down to the lower part of the hold section. After the hold section, there comes a drop section where the inclination is reduced or becomes vertical until reaching the target of interest [13].

The S-shaped well profile is more difficult to drill than the B&H well profile because of the drop section located above the target. Since this drop section is adding an additional bend, there will be expected extra torque and drag for this well profile, compared to the B&H well profile [13].

2.2.3 J-Profile

A J-shaped well profile consists of a vertical section, a deep KOP, and a continuous build section. This well profile is used in situations like exploration of stratigraphic traps, obtaining additional data on non-commercial wells, or side-tracking from existing wells [11], [13].

2.3 Dogleg and Dogleg Severity

When drilling a directional well, it is useful to determine the wellbore curvature along the well trajectory [6]. When determining the wellbore curvature, the expressions dogleg (DL) and dogleg severity (DLS) are frequently used.
``*Dogleg is the absolute change of direction, and the dogleg severity is the derivative of the dogleg´´* [14].

When there are changes in inclination and/or azimuth or direction between two points along a wellbore, the total curvature will change. This change in curvature is known as the dogleg [15]. The dogleg angle is directly used in the minimum curvature method. However, the dogleg angle does not tell directly how much the well path changes between the two points since this will also depend on the drilled distance between the points. For describing the change in well path, one uses the concept of dogleg severity.

The dogleg severity is the dogleg angle divided by the distance along the wellbore between the two points [16]. The measurements for DLS are commonly expressed as degrees per 30 meters within the oil industry [14].

2.4 Survey Methods

During drilling operations, the wellbore trajectory is required to be known at all times [16]. This is especially important during critical stages, like when kicking off near existing wells [17]. The measurements are the inclination of the borehole at a certain depth and azimuth. The measurements are usually taken every 30-40 meters, and must not exceed intervals of 100 meters [15], [16]. These measurements must then be used to find out how the well path changes in vertical (true vertical depth) direction and horizontal direction (East-West, North-South). Some wellbore trajectory calculation method is used for this.

According to [17], the most used wellbore trajectory calculation methodologies are:

- Tangential method
- Balanced tangential method
- Average angle method
- Radius of curvature method
- Minimum curvature method

2.4.1 Tangential Method

The well path is assumed to be a straight line defined by the azimuth and inclination at the lower survey point [17]. The azimuth and inclination are here assumed constant between the survey points [6].

This method is not recommended in directional wells, since the changes in azimuth and inclination can be significant, even for short intervals.

2.4.2 Balanced Tangential Method

The actual well path can be approximated by two straight lines (equal length) segments [17]. One line segment will have an inclination, I_1, and azimuth, A_1, starting at point one. The second line segments will have the inclination, I_2, and azimuth, A_2, at point two [16].

Since this method considers both sets of survey data, it is a more accurate method than the tangential method.

2.4.3 Average Angle Method

One straight line will intersect the upper survey point and the lower survey point [17]. The straight line is defined by using the average inclination and azimuth using the two survey points. These are then used in the formulas derived for the balanced tangential method [16].

This is a simple method to use and gives accurate results. In near-vertical wells, on the other hand, this method is proven to be unreliable [17].

2.4.4 Radius of Curvature Method

The well path is not a straight line but uses the inclination and azimuth values to construct circular projections [16], [17]. These circular projections of the wellbore are projected in both the vertical and the horizontal plane.

Where the well path is closer to a circular arc, this method gives better results than the average angle method [17]. This method assumes a constant radius, which in long intervals may be inaccurate. In straight hole section, where division by zero is the case, this method may experience computational problems [17].

2.4.5 Minimum Curvature Method

The minimum curvature method will be used further in the analytical model presented in this thesis, so a more detailed explanation will therefore be given.

In the minimum curvature method, the well path is replaced by a circular arc, instead of two straight line segments as used in the balanced tangential method [17]. By replacing the straight-line segments by a circular arc, a ratio factor (RF) is applied. This ratio factor is based on the dogleg angle, which is the amount of bending between the two survey points in the well path.

From Figure 3, the ratio factor, RF, can be calculated as:

$$RF = \frac{AB + BC}{AC} \tag{1}$$

Where AB:

$$AB = BC = R * \tan\left(\frac{\emptyset}{2}\right) \tag{2}$$

And AC:

$$AC = \frac{\pi * R * \emptyset}{180} \tag{3}$$

When taking this in consideration, RF can therefore be written as:

$$RF = \left(\frac{2}{\emptyset}\right) * \left(\frac{180}{\pi}\right) * \tan\left(\frac{\emptyset}{2}\right) \tag{4}$$

Where $\emptyset$ is the dogleg severity angle in degrees. This correction factor will be used in combination with the formulas derived for the balanced tangential method.

The equations for the minimum curvature method, representing the incremental distances between the survey points along the three axes are [15], [17]:

$$\Delta V = RF * \frac{1}{2} * L * (\cos I_1 + \cos I_2) \tag{5}$$

$$\Delta N = RF * \frac{1}{2} * L * (\sin I_1 * \cos A_1 + \sin I_2 * \cos A_2) \tag{6}$$

$$\Delta E = RF * \frac{1}{2} * L * (\sin I_1 * \sin A_1 + \sin I_2 * \sin A_2) \tag{7}$$

Where L is the distance between the survey points.

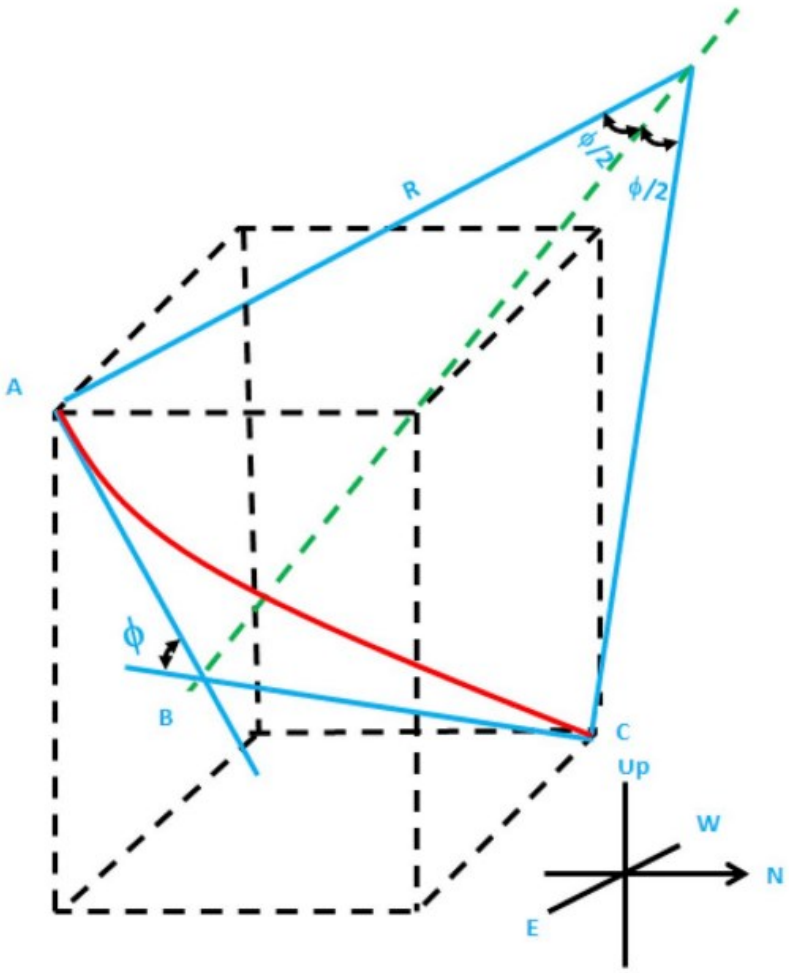

Figure 3: *Model of the minimum curvature method [15].*

When it comes to directional surveying calculations, the minimum curvature method is the most used method for this purpose. This method gives high accuracy when the survey points along the wellbore are not too far apart, and the trajectory is approximating a plane circular arc [11], [17].

2.5 2D Well Profile Examples

In this thesis, emphasis will be placed on a B&H well profile and S-profile for further calculations.

2.5.1 B&H Well Profile Calculation

By using a B&H well profile, it is possible to calculate the true vertical depth (TVD), the horizontal displacement (HD), and the measured depth (MD) by dividing the well into sections as shown in Figure 4. The well is divided into one section called AB, which will be the vertical section of the well. Section BC will be the build-up bend section, followed by the hold section CT.

Dividing the well into individual sections will also be beneficial when calculating the drag forces in later chapters.

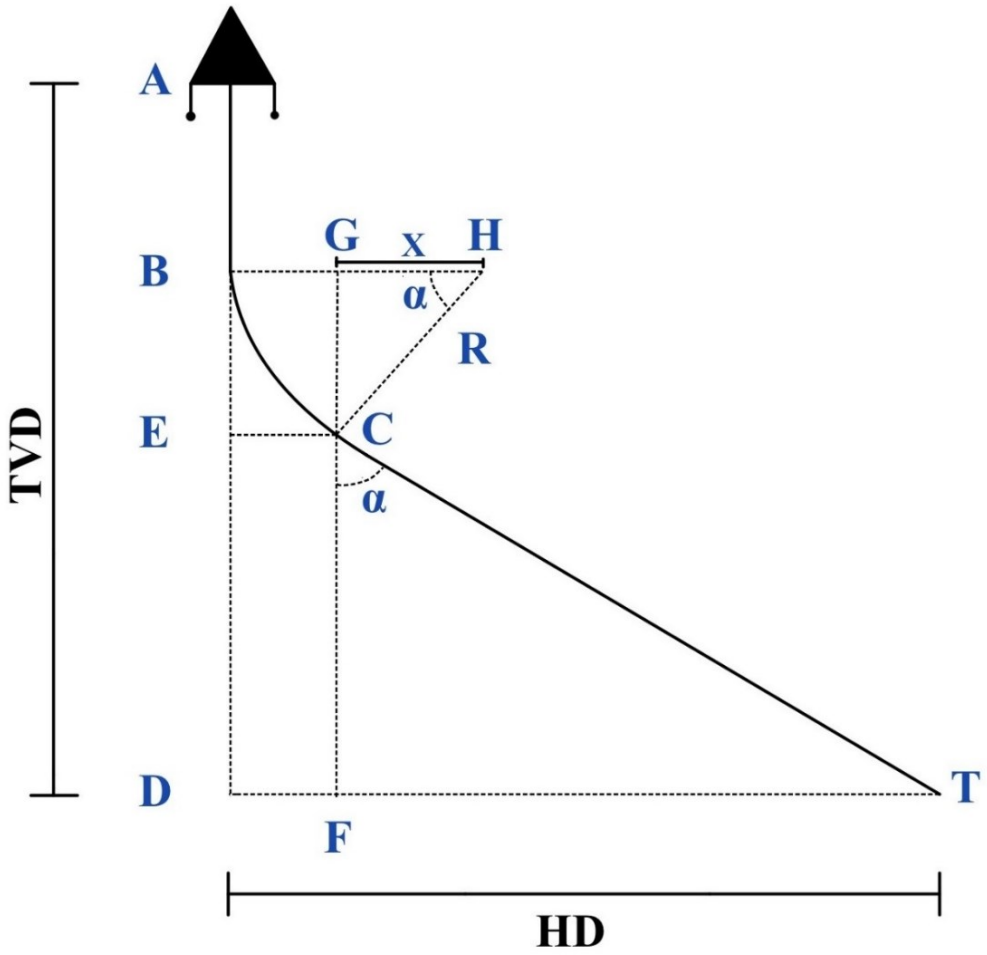

Figure 4: *The geometry of a B&H well profile.*

To be able to use the individual sections for TVD, HD, and MD calculations, some parameters must be set:

- Vertical section down to KOP = 900 m
- Hold section = 8400 m
- Build-up rate = 2°/30 m

The azimuth is fixed, so this value will be held constant at 0 degrees. The well inclination will be stopped at 80 degrees.
From the given values, the build-up rate is constant at 2 degrees per 30 meters. From this constant build-up rate, it is possible to assume the build-up bend to be an arc of a circle. This gives a radius, R, as seen in Figure 4. To find R, the following relations are needed:

$$\frac{\alpha}{BC} = \frac{\Delta i}{\Delta L}$$

Where ΔL is the change in length, and Δi is the change in angle.

By rewriting the equation above, it is possible to solve for BC:

$$BC = \frac{\Delta L}{\Delta i} * \alpha \tag{8}$$

In addition to BC, an equation for R needs to be developed:

$$\frac{BC}{2 * \pi * R} = \frac{\alpha}{360°}$$

By using the equation above, it is possible to solve for R:

$$R = \frac{BC}{2 * \pi} * \frac{360°}{\alpha} \tag{9}$$

By taking equation (8) into equation (9), R becomes:

$$R = \frac{360° * \Delta L}{2 * \pi * \Delta i} \tag{10}$$

By inserting the values given previously, the radius, R, for this B&H well profile will be:

$$R = \frac{360° * 30\ m}{2 * \pi * 2°} \approx 859{,}44\ m$$

2.5.2 TVD Calculation

To find the true vertical depth (TVD), the sections AB, BE and ED must be added together. The vertical AB section is already given. The BE and ED sections need to be solved using trigonometric relations.

In Figure 4, it is possible to solve BE by using the triangle formed by CGH. Here, the BE section will be the same as CG.

When having R, the BE section will be:

$$BE = R * \sin\alpha \tag{11}$$

By using the value for R solved from equation (10) and α, the BE section becomes:

$$BE = 859{,}44\ m * \sin(80°) \approx 846{,}4\ m$$

The ED section will be:

$$ED = CT * \cos\alpha \tag{12}$$

By inserting the given values for CT and α the ED section becomes:

$$ED = 8400\,m * \cos(80°) \approx 1458{,}6\,m$$

By adding all these sections together, it is possible to calculate the TVD of the B&H well profile:

$$TVD = AB + BE + ED = 900\,m + 846{,}4\,m + 1458{,}6\,m = 3205\,m$$

2.5.3 HD Calculation

To find the horizontal displacement (HD), the sections DF and FT must be added together. Trigonometric relations will be used to solve DF and FT here as well.

By using the triangle formed by CFT, it is possible to find FT:

$$FT = CT * \sin\alpha \tag{13}$$

$$FT = 8400\,m * \sin(80°) \approx 8272{,}4\,m$$

By using trigonometric relations, it is possible to find DF. DF will, from Figure 4, be the same as EC:

$$\cos\alpha = \frac{X}{R}$$

Solve for X:

$$X = R * \cos\alpha$$

By using the equation for X makes it now possible to solve for EC:

$$EC = R - X = R - R * \cos\alpha = R * (1 - \cos\alpha) \tag{14}$$

$$EC = 859{,}44\ m * (1 - \cos(80°)) \approx 710{,}2\ m$$

By adding the FT and EC sections together, the HD of the B&H well profile can be calculated:

$$HD = FT + EC = 8272{,}4\ m + 710{,}2\ m = 8982{,}6\ m$$

2.5.4 MD Calculation

To find the measured depth (MD), which is the depth measured along the well, the sections AB, BC, and CT must be added together.

Both AB and CT are given, while BC is found from equation (8).

$$BC = \frac{30\ m}{2°} * 80° = 1200\ m$$

MD will then be:

$$MD = AB + BC + CT = 900\ m + 1200\ m + 8400\ m = 10\ 500\ m$$

These calculations give information on where the target of interest is located. The TVD of the target of interest is located at 3205 m, the HD is at 8982,6 m, while the MD along the wellbore is 10 500 m.

To be able to connect this well to an ERD context, the depth ratio can be calculated to see if the depth ratio is at least 2:0 as mentioned earlier [11].

$$DEPTH\ RATIO = \frac{MD}{TVD} = \frac{10\ 500\ m}{3205\ m} \approx 3{,}27$$

2.5.5 S-Profile Calculation

By using an S-profile, it is possible to calculate TVD, HD, and MD by dividing the well into sections as shown in Figure 5. The well is divided into one section called AB, which will be the vertical section of the well. Section BC will be the build-up bend section, the CD will be the hold section, followed by the drop section DT and an inclined section TS down to target.

Dividing the well into individual sections will also be beneficial here when calculating the drag forces in later chapters.

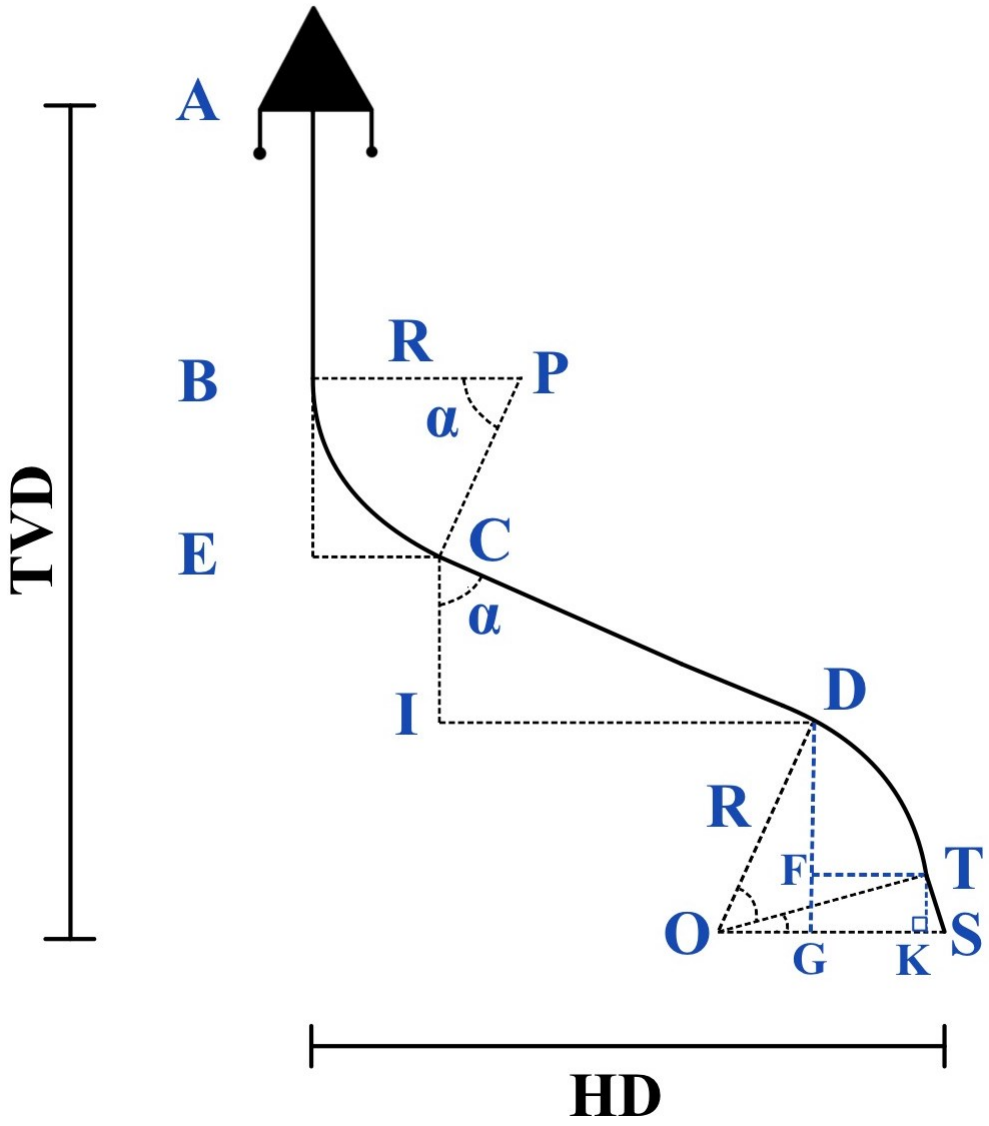

Figure 5: *The geometry of an S-profile.*

The set parameters for TVD, HD, and MD calculations are as follows:

- Vertical section down to KOP = 900 m
- Hold section = 6600 m
- Inclined section down to target = 150 m
- Inclination down to target = 10°
- Build-up rate = 2°/30 m

The azimuth is fixed as mentioned earlier, so this value will be held constant at 0 degrees. The well inclination will be stopped at 80 degrees. Both the build-up rate and drop-off rate are constant at 2 degrees per 30 meters. From this constant build-up rate, it is possible to assume the build-up bend and drop bend to be an arc of a circle here as well.

The S-profile has both a build-up bend section and a drop section, giving us a radius R_1 for the build-up section and R_2 for the drop section. Both the build-up rate and drop-off rate, are as mentioned, set constant at 2 degrees per 30 meters, giving us an equal R for both R_1 and R_2. For further calculations, equation (10) will be used for the calculation of R.

By inserting the parameters given previously into equation (10), the radius for this S-profile will be:

$$R = \frac{360° * 30\ m}{2 * \pi * 2°} \approx 859{,}44\ m$$

2.5.6 TVD Calculation

To find TVD, the sections AB, BE, IC, DF, and FG must be added together. The vertical AB section is already given. The BE, IC, DF, and FG sections need to be solved using trigonometric relations.

In Figure 5, it is possible to use equation (11) to solve for BE since BE in the S-profile is the same as BE in the B&H well profile:

$$BE = 859{,}44\ m * \sin(80°) \approx 846{,}4\ m$$

The IC section will be the same as ED in the B&H well profile, so by using equation (12) it is possible to solve for IC:

$$IC = CD * \cos\alpha$$

By inserting the given value for CD and α, the IC section becomes:

$$IC = 6600\,m * \cos(80°) \approx 1146{,}1\,m$$

To find DF, the inclination of the hold section and the angle after the drop section need to be taken into consideration when solving for DF:

$$DF = R * (\sin\alpha_1 - \sin\alpha_2) \quad \textbf{(15)}$$

$$DF = 859{,}44 * (\sin(80°) - \sin(10°)) \approx 697{,}1\,m$$

To find FG it is possible to use equation (12).

$$FG = TS * \cos\alpha$$

Here the inclination is 10°, and by inserting this angle and the given value for TS, the FG becomes:

$$FG = 150 * \cos(10°) = 147{,}7\,m$$

By adding all these sections together, it is possible to calculate the TVD of the S-profile:

$$TVD = AB + BE + IC + DF + FG$$

$$= 900\,m + 846{,}4\,m + 1146{,}1\,m + 697{,}1\,m + 147{,}7 = 3737{,}3\,m$$

2.5.7 HD Calculation

To find HD to the target, the sections EC, ID, FT, and KS must be added together.

To solve for EC, it is possible to use equation (14):

$$EC = R - X = R - R * \cos\alpha = R * (1 - \cos\alpha)$$

$$EC = R * (1 - \cos\alpha) = 859{,}44\,m * (1 - \cos(80°)) \approx 710{,}2\,m$$

When solving for ID, it is possible to use equation (13). But instead of CT we have CD:

$$ID = CD * \sin\alpha$$

$$ID = 6600\,m * \sin(80°) \approx 6499{,}7\,m$$

To be able to find FT we need to use trigonometry and take into consideration both the angle after the drop section and the inclination for the hold section:

$$FT = R * (\cos\alpha_2 - \cos\alpha_1) \quad \textbf{(16)}$$

$$FT = 859{,}44\,m * (\cos(10°) - \cos(80°)) \approx 697{,}1\,m$$

When solving for KS it is possible to use equation (13). But here one needs to use TS and an angle of 10°:

$$KS = TS * \sin\alpha$$

$$KS = 150\,m * \sin(10°) \approx 26\,m$$

By adding the EC, ID, FT, and KS sections together, the HD of the S-profile can be calculated:

$$HD = EC + ID + FT + KS$$

$$= 710{,}2\ m + 6499{,}7\ m + 697{,}1\ m\ + 26\ m\ = 7933\ m$$

2.5.8 MD Calculation

To find MD, the sections AB, BC, CD, DT, and TK must be added together. AB, CD, and TK are given, while BC and DT must be solved using trigonometric relations.

When solving for BC, one can use equation (8):

$$BC = \frac{30\ m}{2°} * 80° = 1200\ m$$

When solving for DT, the inclination after the drop section must be considered, so the DT section becomes:

$$DT = \frac{\Delta L}{\Delta i} * (\alpha_1 - \alpha_2) \tag{17}$$

$$DT = \frac{30\ m}{2°} * (80° - 10°) = \frac{30\ m}{2°} * 70° = 1050\ m$$

MD will then become:

$$MD = AB + BC + CD + DT + TK$$

$$= 900\ m + 1200\ m + 6600\ m\ + 1050\ m + 150\ m\ = 9900\ m$$

The TVD of the target of interest is located at 3737,3 m, the HD is at 7933 m, while the MD along the wellbore is 9900 m.

The depth ratio can be calculated to see if the (MD/TVD) ratio is at least 2:0 [11]:

$$DEPTH\ RATIO = \frac{MD}{TVD} = \frac{9900\ m}{3737{,}3\ m} \approx 2{,}65$$

3 Drag Models

3.1 Torque and Drag Models in Well Design

Torque and drag (T&D) models are beneficial diagnostic tools that can be applied during the well planning phase, drilling phase, and post-analysis phase (after finishing the well) [9]. In ERD wells, high torque and drag may prevent the driller to reach the target of interest [2]. The T&D models give insight into the frictional behavior within the well and are therefore applied to predict and prevent problems that may occur [3]. According to [4], the problems that may create high drag forces and excessive torque are tight hole conditions, cuttings build-up due to poor hole cleaning, differential sticking, sloughing hole, key seats, and sliding wellbore friction. By taking use of these models already at the well planning phase, the trajectory design may be optimized and the risk of getting stuck pipe is minimized [9].

Stuck pipe is possible to predict by using real-time T&D data, creating roadmaps that provide information about the downhole conditions [18], [19]. Roadmaps are simulated drag curves for different friction coefficients for different depths used under operation. By using these roadmaps, the data will fit one of these curves, and the result is useful if the data follows this curve by one of the friction coefficients that were assumed. If the trend suddenly changes and no longer follows the original curve, then this is a sign that the friction has changed severely, creating an early sign of stuck pipe.

3.2 General Concepts and Models

3.2.1 Buoyancy

During a drilling operation, the well is filled with drilling fluid. This drilling fluid is designed to meet certain criteria to ease the drilling operation. During drilling, the drill string is submerged in drilling fluid. The weight of the drill string needs therefore to be corrected for buoyancy effects [5].

In a well, there is always buoyancy. ``*Buoyancy is a surface force acting on a body in the opposite direction of the gravitational force*´´ [20]. The buoyancy factor for both inclined and vertical wellbores are identical [21].

If a drill string is submerged in a drilling fluid, having the same density both inside and outside of the string, and if the string is also having a uniform circumference (not composed of many pipe sizes), the buoyancy factor can in this case be defined as [20]:

$$\beta = 1 - \frac{\rho_{fluid}}{\rho_{steel}} \quad \textbf{(18)}$$

And the buoyed unit mass of drill string is [20]:

$$W = \beta * W_{Drillpipe} \quad \textbf{(19)}$$

Where:

- β is the buoyancy factor
- ρ_{fluid} is the density of drilling fluid [kg/m^3]
- ρ_{steel} is the density of drill pipe [kg/m^3]
- $W_{Drillpipe}$ is the unit weight of the drill pipe in air [kg/m]

3.2.2 Friction

Basic well friction principles will be defined in this chapter using the Coulomb friction model. The Coulomb friction model is also known as sliding friction forces.

Friction between the drill string and wellbore results in torque and drag [2]. Having the presence of torque and drag in a well will affect the success. This applies especially to deep and complex wells. For ERD wells, the presence of torque and drag may prevent the driller from reaching the target of interest [2].

When a body has a force acting on it, the body will start to move when the maximum friction force is reached [2]. Figure 6 defines the forces acting on a drill string on an inclined plane according to the Coulomb friction model.

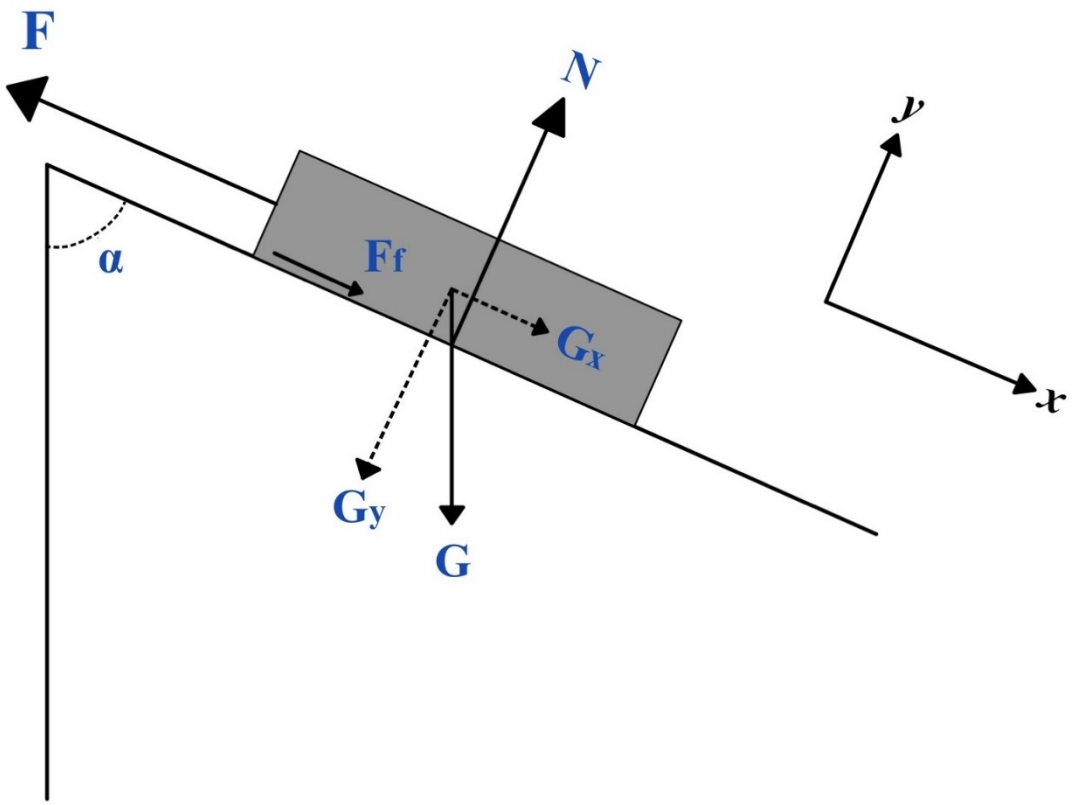

Figure 6: *Forces and decomposed forces that are working on an inclined object. Modified after [5].*

The force G in Figure 6 will be the weight of the drill pipe, including buoyancy:

$$G = W * g \tag{20}$$

The G component is decomposed into an axial component, G_x, and a normal component, G_y, as shown:

$$G_x = G * \cos\alpha \tag{21}$$

$$G_y = N = G * \sin\alpha \tag{22}$$

The friction force, F_f, takes into consideration the friction coefficient, μ, between an object and a surface, and the normal force, N, acting on the object from the surface [2]:

$$F_f = \pm\mu * G_y = \pm\mu * G * \sin\alpha \tag{23}$$

The friction will always work in the opposite direction of motion [5].

3.2.3 Capstan Effect

The Capstan effect, also known as belt friction, is the friction force acting between a belt and a surface [22]. If a belt is wrapped around a curved surface and one applies tension to one end of the belt, the frictional forces between the belt and surface increase with the number of rounds of wrapping around the curved surface. Only a small part of the force will be transmitted to the other end of the belt.

Figure 7 represents a belt wrapped around a curved surface. By dividing this belt into a small segment and assuming that this is a weightless belt in equilibrium, it is possible to derive the Capstan equation [23].

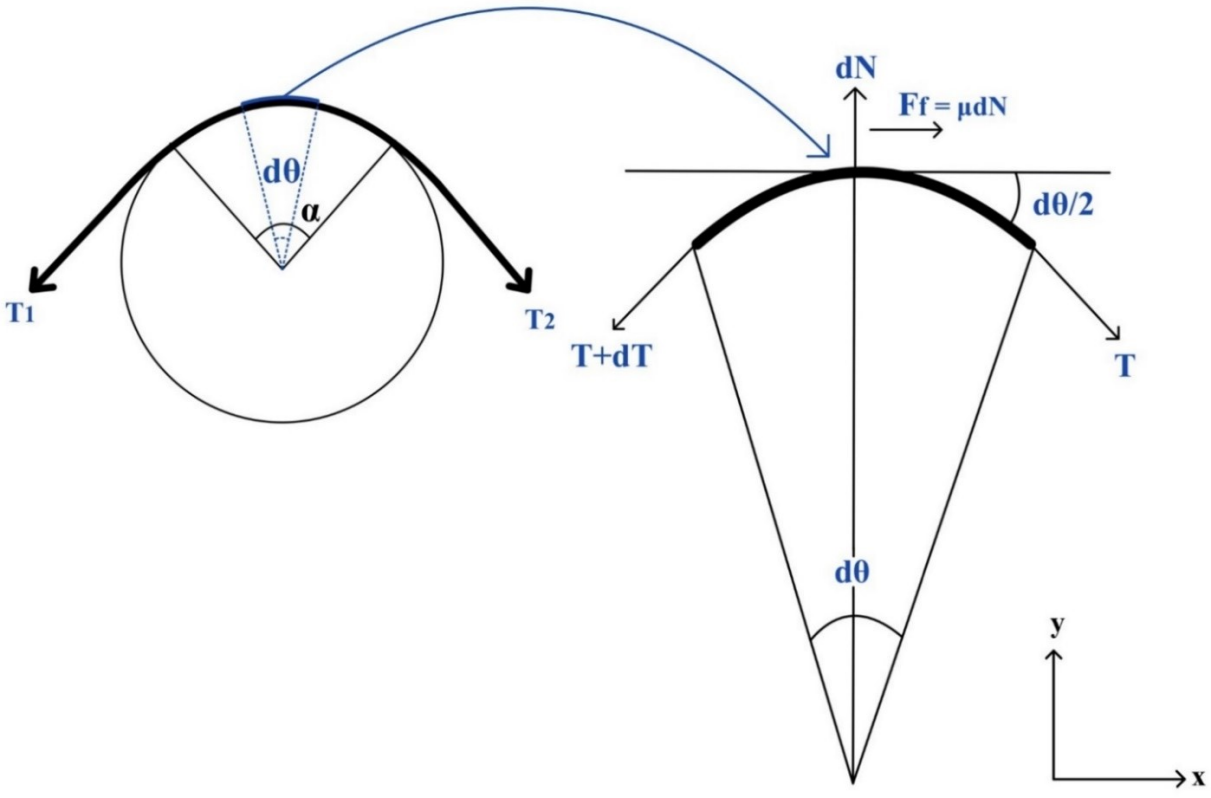

Figure 7: *Illustration of the Capstan effect. Modified after [23].*

By using force balance, the forces in the X-direction and Y-direction become:

$$\text{X-direction: } -dT\cos\left(\frac{d\theta}{2}\right) + \mu * dN = 0 \tag{24}$$

$$\text{Y-direction: } dN - 2 * T * \sin\left(\frac{d\theta}{2}\right) - dT * \sin\left(\frac{d\theta}{2}\right) = 0 \tag{25}$$

By solving for dN in equation (25) and then inserting dN into equation (24), one will get:

$$-dT * \cos\left(\frac{d\theta}{2}\right) + \mu * 2 * T * \sin\left(\frac{d\theta}{2}\right) + \mu * dT * \sin\left(\frac{d\theta}{2}\right) = 0 \tag{26}$$

By assuming that the segment of the belt is small, the expressions $\sin\left(\frac{d\theta}{2}\right) \approx \frac{d\theta}{2}$ and $\cos\left(\frac{d\theta}{2}\right) \approx 1$. The last term in equation (26) will also be neglected since the two small values are multiplied. By using these approximations, the equations for dT and $\frac{dT}{T}$ become:

$$dT = \mu * T * d\theta \tag{27}$$

$$\frac{dT}{T} = \mu * d\theta \tag{28}$$

By integrating equation (28), the expression becomes:

$$\int_{T_1}^{T_2} \frac{dT}{T} = \int_{\theta=0}^{\theta=\alpha} \mu * d\theta \tag{29}$$

Solving the integrals in equation (29):

$$\ln\frac{T_2}{T_1} = \mu * \alpha \tag{30}$$

By solving for T_2 in equation (30), the Capstan equation becomes:

$$T_2 = T_1 * e^{\mu * \alpha} \tag{31}$$

3.2.4 Projected Height Principle

In this chapter, a closer explanation of the projected height principle will be given.

The projected height principle is used to find the axial weight of a pipe [21]. By dividing the weight of the pipe into an axial component, G_x, and a normal component, G_y, as illustrated in Figure 8, it is possible to find the axial weight, G_x, of the pipe within the well as the product of the buoyed unit weight (N/m) multiplied by the projected height [5], [20]. The projected height, ΔL, is defined as:

$$\Delta L = L * \cos \alpha \tag{32}$$

This is valid for any type of buoyed well path, and by using this concept it is possible to calculate the hook load by using the pipe unit weight and the projected height [20].

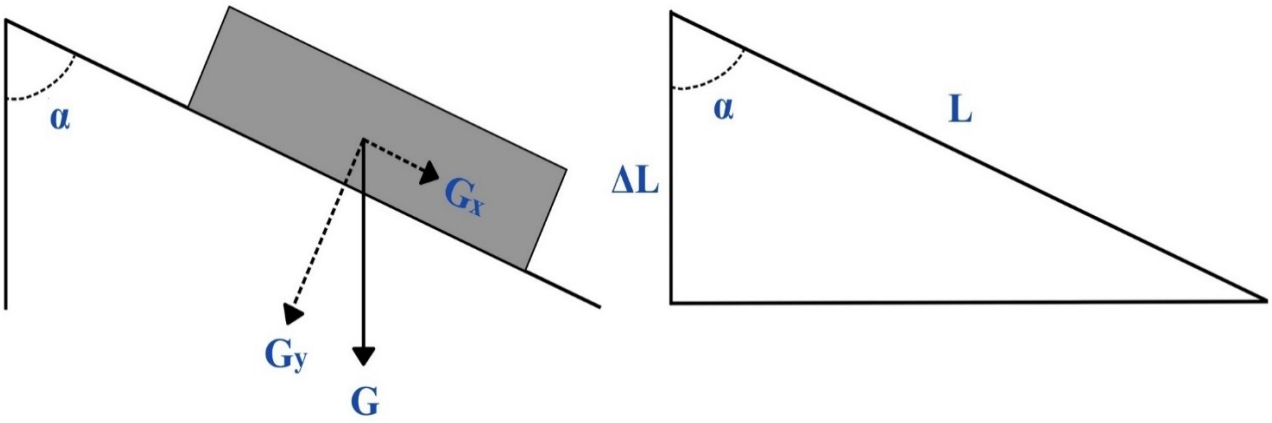

Figure 8: *Illustration of the projected height principle. Modified after [20].*

3.3 Analytical Drag Model

The analytical drag model calculates on larger segments, where the segments are divided into vertical, straight inclined, and curved segments. The calculations start from the bottom of the well and are calculated upwards [5]. The analytical model is developed for 3D well paths, where inclination and azimuth vary. In this thesis, only the model for varying inclination will be presented, and the analytical model will address the concepts and models already discussed in earlier chapters.

The analytical model will be used for a tripping out scenario, a tripping in scenario, and a static (rotating off bottom) scenario. For the models in this thesis, the friction in the axial direction disappears completely for the static (rotating off bottom) scenario.
This is because the pipe will be under high rotation which removes the friction in the axial direction [3].

3.3.1 Drag Force for a Straight Inclined Section Without Pipe Rotation

In straight inclined sections, the mechanical friction is only dependent on weight. The tension in the drill string is not contributing to the normal force acting perpendicular on the pipe. Hence, friction is only dependent on the weight component that is balancing the normal force as shown in Figure 6 and Figure 9 [3].

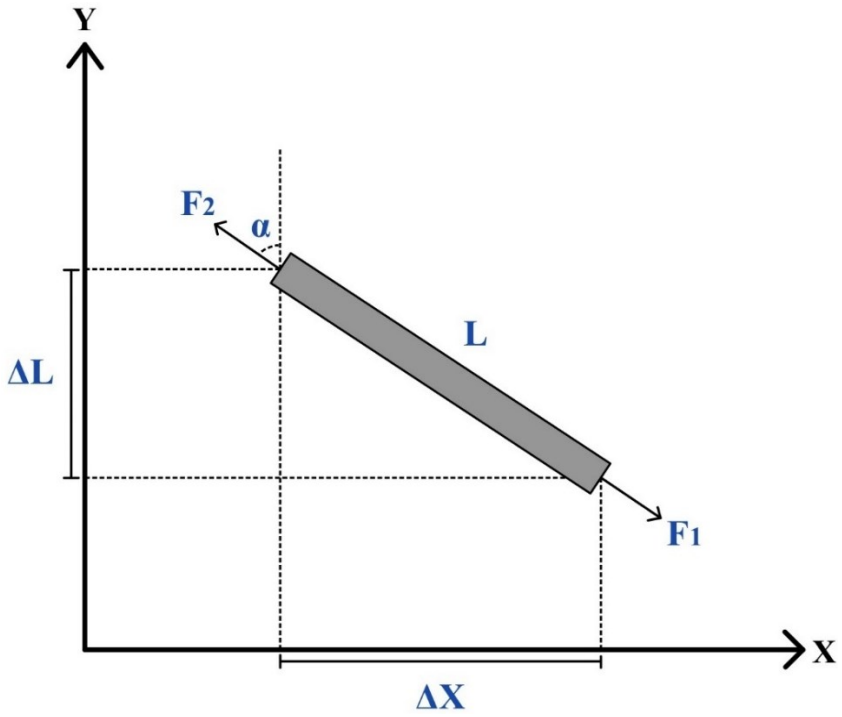

Figure 9: *Geometry of a straight inclined pipe. Modified after [5].*

The bottom force, F_1, will be the contact force between the drill bit and formation. This contact force will be set as a boundary force equal to zero:

$$F_1 = 0 \tag{33}$$

During tripping in and out of the well, there will be no contact between the bit and the formation. In this case, F_1 is set to zero.

The top force, F_2, will then become:

$$F_2 = F_1 + W * g * L * (\cos\alpha \pm \mu * \sin\alpha) \tag{34}$$

Where:

- W is buoyed mass per meter of pipe in drilling fluid [kg/m]
- L is the pipe length [m]
- g is the gravitational constant [m/s^2]
- μ is the friction coefficient
- ± is tripping in (-) and tripping out (+)
- W*g*L*cos(α) is the axial weight term including buoyancy
- W*g*L*μ*sin(α) is the mechanical friction

From Figure 9 and equation (34) it is possible to see that the pipe will be in a vertical position when α = 0 degrees. The friction will then be zero. When α = 90 degrees, the pipe will be in a horizontal position and the axial weight will become zero [1].

3.3.2 Drag Force for a Curved Section Without Pipe Rotation

For curved sections, there will be two contributions to the normal force. One part is the normal force contribution caused by the weight component of the string acting perpendicular to the pipe axis. The other normal force component is caused by tension effects taking place in curved sections in the well (Capstan effect) as illustrated in Figure 10 [4].

In the analytical model, it will be assumed that the mechanical friction is dominated by tension effects (Capstan effect). The normal force will only have a contribution from the axial pipe loading. This means that the normal force contribution from the weight component perpendicular to the string is neglected [3].

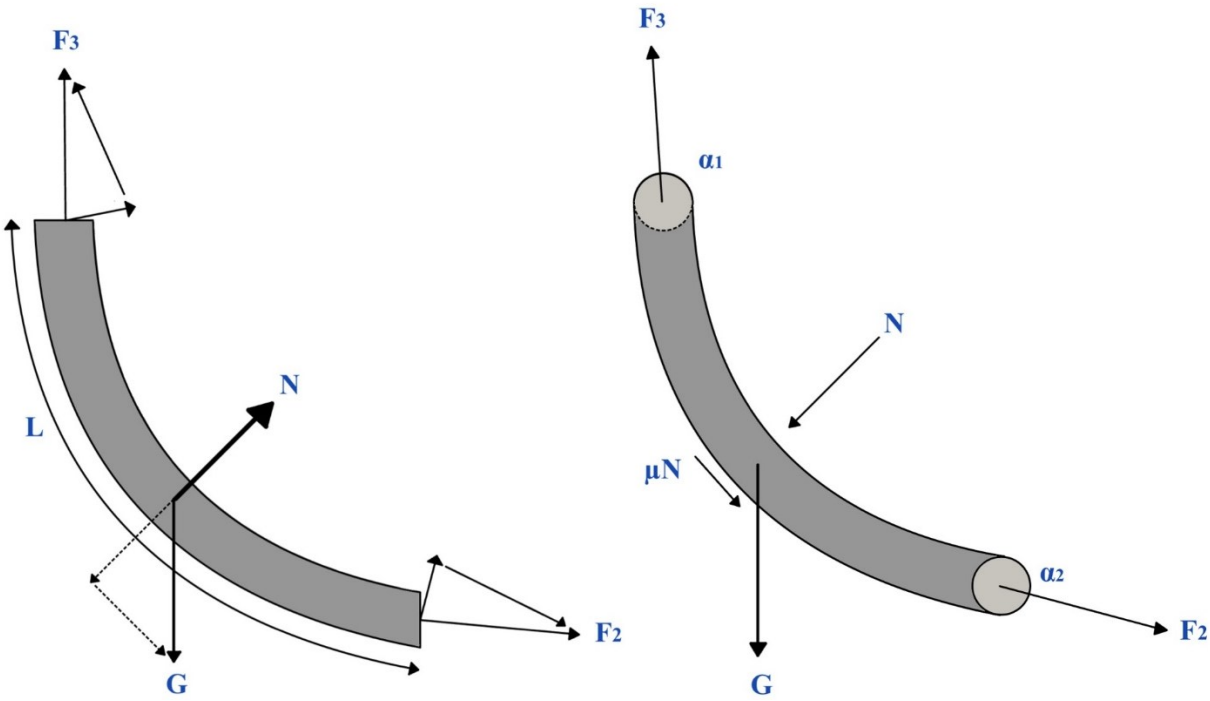

Figure 10: *The figure to the left illustrates the normal force resulting from weight, while the figure to the right illustrates the normal force resulting from tension. Modified after [4].*

When defining the drag force along a curved section, it is useful to make an assumption that the drill pipe is weightless when computing the friction, and afterwards add the weight at the end of the bend [3]. When defining the vertical projected height for curved sections, the minimum curvature method is here applied in this model, but other approaches are also possible [16]. For instance, in [3], the radius of curvature method was used. However, the minimum curvature is used in this thesis, since this method gives exact vertical displacement for curved sections.

The F3 force will then become:

$$F_3 = F_2 * \left(e^{\pm\mu * \left(|\alpha_2 - \alpha_1| * \left(\frac{\pi}{180}\right)\right)} - 1 \right) + F_2 + W * g * \frac{1}{2} * L * (\cos\alpha_1 + \cos\alpha_2) * RF \quad \textbf{(35)}$$

Where the first term represents the friction due to the Capstan effect (tension effect), and the third term represents the weight. The + sign in the exponential function will correspond to upward movement while the minus sign will be used for downward movement.

The ratio factor, RF, is defined by equation (4):

$$RF = \frac{2}{\emptyset} * \left(\frac{180}{\pi}\right) * \tan\left(\frac{\emptyset}{2}\right)$$

(Ø is the dogleg angle in degrees, and $\alpha_1 = 0°$ and $\alpha_2 = 80°$ for the curved section in Figure 10.) In this case, the dogleg is $\alpha_2 - \alpha_1 = 80°$.

Where:

- W is buoyed mass per meter of pipe in drilling fluid [kg/m]
- L is the pipe length [m]
- g is the gravitational constant [m/s^2]
- μ is the friction coefficient
- ± is tripping in (-) and tripping out (+)
- $|\alpha_2 - \alpha_1|$ is the change in angle

3.3.3 Drag Force for a Vertical Section Without Pipe Rotation

Drag forces along a vertical section will be the buoyed drill pipe multiplied by the vertical height of the well [3]. When a well is vertical, the friction will be zero since there is no contact force (no normal force between formation and string). When the inclination is zero, the term related to friction, μ*sin α, becomes zero. This will make the term (cos α ± μ*sin α) become equal to 1. The force, F_4, then becomes:

$$F_4 = F_3 + W * g * L \quad \textbf{(36)}$$

3.4 Numerical Drag Model

The numerical model will be based on the T&D model by Johancsik et al [4].

The T&D model based on Johancsik et al [4] takes into consideration that the sliding friction, also known as the Coulomb friction model, is the primary cause of torque and drag in directional wellbores [4]. This T&D model considers the effect of gravity on pipe and tension through curvatures as contributions to the normal force as shown in Figure 11. It was developed for well profiles where both inclination and azimuth changes. It is based on dividing the well path into a certain number of small segments and the force balances shown below are for such a segment.

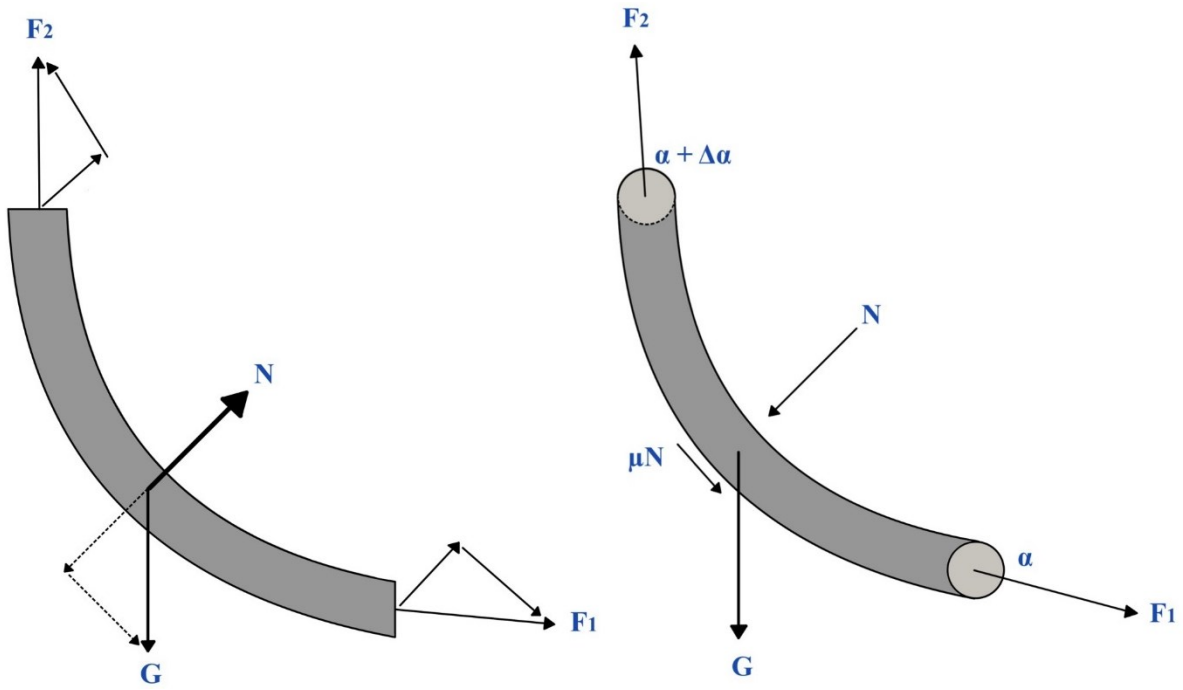

Figure 11: *The figure to the left illustrates the effect of gravity and the effect of tension that is acting on a curved segment of a drill string. The figure also illustrates their contribution to normal force. The figure to the right illustrates the forces during a tripping out scenario. Modified after [4].*

The friction calculations in this T&D model require only the magnitude of the normal force. The direction is not necessary. The magnitude of the normal force according to [4] is:

$$N = [(F_1 * \Delta A * \sin\overline{\alpha})^2 + (F_1 * \Delta\alpha + G * \sin\overline{\alpha})^2]^{1/2} \quad \textbf{(37)}$$

Since the well profiles and calculations to be considered in this thesis are kept in 2D, the azimuth component in equation (37) is therefore neglected. The normal force then becomes:

$$N = [(F_1 * \Delta\alpha + G * \sin\overline{\alpha})^2]^{1/2} \quad \textit{(38)}$$

The first term in equation (38) gives the normal force contribution due to tension in the string across the element. This will correspond to the Capstan effect. The second term is the contribution from the weight component acting perpendicular to the axis of the pipe.

The force, F_2, on top of the element will then be:

$$F_2 = F_1 + G * \cos\overline{\alpha} \pm \mu * N \quad \textit{(39)}$$

Where:

- N is the normal force acting on element [N]
- F_1 is the tension force at bottom of element [N]
- F_2 the tension force at the top of element [N]
- ΔA is the change in azimuth angle over length of element [rad]
- $\overline{\alpha}$ is the average inclination of the element [rad]
- $\Delta\alpha$ is the change in inclination angle over length of element [rad]
- G is the buoyed weight of drill string element [N]
- μ is the friction coefficient between the wellbore and drill string

The term G*cos $\overline{\alpha}$ in equation (39) is the contribution of the weight working in the axial direction. This has similarities with the analytical model and by further inspection, one can be convinced that the projected height principle is used also here, where the projected height is calculated using the same principles as in the average angle survey calculation method. The third term is the mechanical friction and from previous formulas, one can see that the normal force has two contributions.

To be able to get an exact numerical model, the equations (38) and (39) must be applied to infinitesimal elements of the drill string [4]. Errors will appear if the model is applied to larger elements.

The friction coefficient in this thesis will be represented as a single characteristic friction coefficient [4]. This is because the friction coefficient is not a known parameter but usually depends on other effects within the wellbore [4], [12]. For the calculations in this thesis, the friction coefficient will take the conditions in a wellbore and act as a friction coefficient, representing the average conditions [4].

All the calculations to be presented in the thesis for this numerical T&D model are made by dividing the drill string into 30-meter elements. One will also here start the calculation process from the bottom and calculate for each segment/element or cell upwards.

The numerical model is implemented in MATLAB, and for further details of the code developed in the thesis work, see Appendix A.

4 Results and Discussion

4.1 Case Examples

In the following, the data to be used in the drag calculations for the well profiles will be represented. These data will be used when comparing the two models. The analytical model will be used for a tripping out scenario, tripping in scenario, and a static (rotating off bottom) scenario for both well profiles. One will first start calculating drag forces for these three cases for a B&H well profile, followed by the S-profile. The drag calculations will be calculated using a friction coefficient from 0,1 to 0,4.

The analytical model starts its calculations at the bottom with $F_1 = 0$ as stated in equation (33). Then one calculates on the hold section to find F_2 by using equation (34). After finding the value for F_2, one moves onto the curved section calculating F_3 from equation (35). After having the value for F_3, one calculates the vertical section until reaching the top of the well by using equation (36).

The analytical model has been implemented in spreadsheets and some screenshots of the Excel sheet are presented in Appendix B.

4.1.1 B&H Well Profile

Calculation of drag forces starts at the bottom of the drill string and continues upwards section by section as shown in Figure 12. The same approach will be used for both hold section and curved section [1].

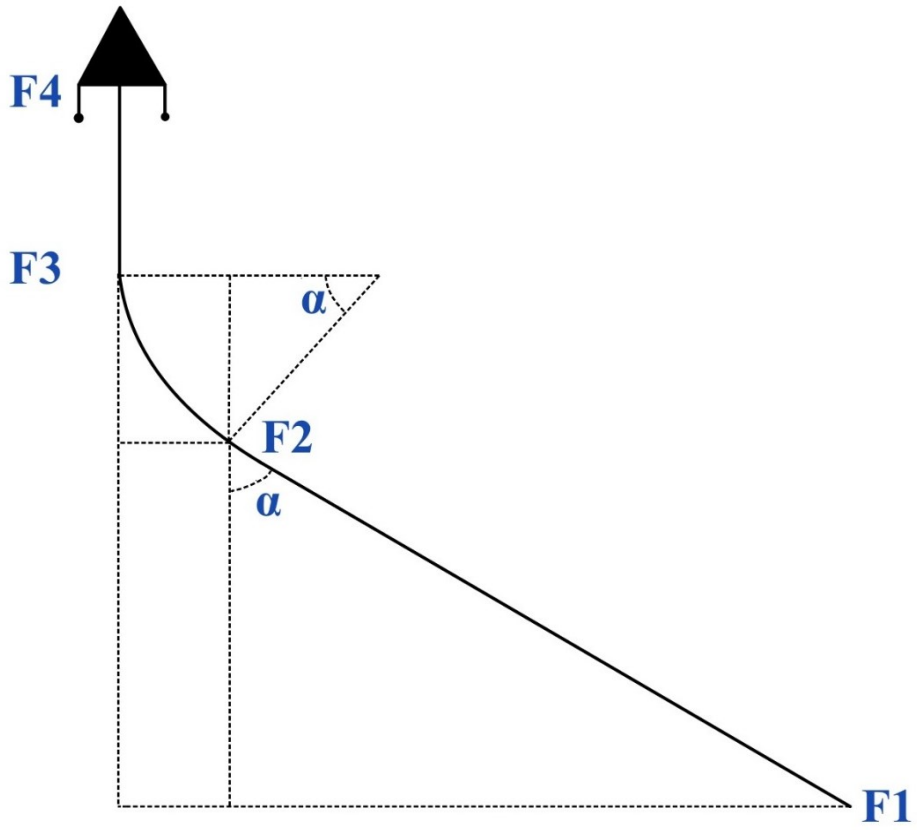

Figure 12: *B&H well profile showing the drag forces for calculation.*

Some parameters must be set before being able to calculate drag forces for the B&H well profile. The drill string characteristics are represented in Table 1:

Table 1: *Drill string characteristics used for drag calculations for the B&H well profile.*

Nominal Diameter of Drill pipe	**Nominal Unit Mass of Drill pipe**	**Grade**	**Type of Tool joint**	**Appr. Unit Mass incl. Tool Joint**	**Nominal Diameter of HWDP**	**Connection HWDP**	**Nominal Unit Mass HWDP**
(inch)	(lb/ft)	S-135	5 ½ FH	(kg/m)	(inch)	NC50 (4 ½ IF)	(kg/m)
5	25,6			43,73	5		73,4

The mud weight (MW) is set to 1700 kg/m^3, and the density of steel (ρ_{steel}) is set to 7850 kg/m^3. The length of the heavy weight drill pipe (HWDP) is 100 m and will be the bottom hole assembly (BHA) in this case.

The geometrical parameters stated in chapter 2.5.1 are repeated in Table 2. These parameters are useful when calculating the forces using the analytical model.

Table 2: *Geometrical parameters used for drag calculations for the B&H well profile.*

Geometrical Parameters		
DLS	2/30	°/*m*
R	859,44	*m*
Vertical down to KOP (AB)	900	*m*
Build-up bend (BC)	1200	*m*
Hold section (CT)	8400	*m*
Vertical depth of build-up bend (BE)	846,4	*m*
Vertical depth of hold section (ED)	1458,6	*m*

By assuming premium class on the stated drill string, the tensile yield strength will be 331,8 * 10^3 daN = 3318 kN [24]. This tensile yield strength must be greater than the worst load case, which will be the tripping out scenario with high friction coefficient. If the force on top of the drill string exceeds this tensile yield strength, one may risk deformed pipe, and in the worst case, tearing of the pipe. Hence it is important to be able to quantify which load situations that can occur with an appropriate torque/drag model.

When the parameters are set, one should start the calculations by calculating the buoyancy factor from equation (18):

$$\beta = 1 - \frac{\rho_{fluid}}{\rho_{steel}} = 1 - \frac{1700\,\frac{kg}{m^3}}{7850\,\frac{kg}{m^3}} \approx 0{,}783$$

After the buoyancy factor is calculated, one wants to calculate the buoyed unit masses for the BHA and drill pipe from equation (19):

$$W_{Drillpipe} = 0{,}783 * 43{,}73 \frac{kg}{m} \approx 34{,}3 \frac{kg}{m^3}$$

$$W_{BHA} = 0{,}783 * 73{,}4 \frac{kg}{m} \approx 57{,}5 \frac{kg}{m^3}$$

When having all the necessary values for calculating drag forces, one can now continue by calculating the drag forces for a tripping out scenario, tripping in scenario, and a static (rotating off bottom) scenario for the B&H well profile.

4.1.2 B&H Well Profile – Tripping out Scenario

The results of the drag force calculations for a tripping out scenario using the analytical model for the B&H well profile will be presented in this chapter.

The boundary force is equal to zero as mentioned in chapter 3.3.1. This bottom force, F_1, is therefore zero when calculating the upcoming drag forces. When moving into the calculation of the top force of the hold section, one must take into consideration that both the BHA and the drill pipe are located here. The buoyed weights of the BHA and drill pipe needs therefore to be differentiated. Using equation (34) the formula for F_2 can be written as:

$$F_2 = F_1 + (W_{Drillpipe} * (L_{Hold\ section} - L_{BHA}) + W_{BHA} * L_{BHA}) * g * (\cos\alpha + \mu * \sin\alpha)$$

By the above equation for F_2 and varying the friction coefficient from 0,1 – 0,4 the result of the force at the top of the hold section is represented in Table 3.

Table 3: *Calculated forces at the top of the hold section for varying friction coefficients between 0,1 – 0,4 during a tripping out scenario for the B&H well profile.*

F_2			
		(N)	(kN)
μ = 0,1	F_2	774464,9	774,465
μ = 0,15	F_2	914600,5	914,601
μ = 0,2	F_2	1054736,1	1054,736
μ = 0,25	F_2	1194871,7	1194,872
μ = 0,3	F_2	1335007,3	1335,007
μ = 0,35	F_2	1475142,9	1475,143
μ = 0,4	F_2	1615278,5	1615,279

Calculation of the force in the build-up bend, F_3, is next. The force in the build-up bend is calculated from equation (35). The results of the forces, F_3, are represented in Table 4.

Table 4: *Calculated forces in the build-up bend section for varying friction coefficients between 0,1 – 0,4 during a tripping out scenario for the B&H well profile.*

F_3			
		(N)	(kN)
μ = 0,1	F_3	1174972,7	1174,973
μ = 0,15	F_3	1412149,1	1412,149
μ = 0,2	F_3	1678969,0	1678,969
μ = 0,25	F_3	1978479,2	1978,479
μ = 0,3	F_3	2314012,2	2314,012
μ = 0,35	F_3	2689211,4	2689,211
μ = 0,4	F_3	3108059,0	3108,059

The force in the top of the vertical section (top of the well), F_4, is the last thing that needs to be calculated. The F_4 is calculated using equation (36), and the results for various friction coefficients are represented in Table 5.

Table 5: *Calculated forces at the top of the vertical section for varying friction coefficients between 0,1 – 0,4 during a tripping out scenario for the B&H well profile.*

F_4			
		(N)	(kN)
μ = 0,1	F_4	1477452,5	1477,453
μ = 0,15	F_4	1714629,0	1714,629
μ = 0,2	F_4	1981448,9	1981,449
μ = 0,25	F_4	2280959,1	2280,959
μ = 0,3	F_4	2616492,1	2616,492
μ = 0,35	F_4	2991691,3	2991,691
μ = 0,4	F_4	3410538,9	3410,539

4.1.3 B&H Well Profile – Tripping in Scenario

The results of a tripping in scenario using the analytical model for the B&H well profile will be presented in this chapter.

The calculation for a tripping in scenario is the same as for the tripping out scenario, but for the calculation of F_2, the friction is negative. The BHA and drill pipe are still located in the hold section, and the parameters are still the same as stated in previous chapters.
When now taking into consideration that the friction is negative, the formula for F_2 can be written as:

$$F_2 = F_1 + (W_{Drillpipe} * (L_{Hold\ section} - L_{BHA}) + W_{BHA} * L_{BHA}) * g \\ * (\cos\alpha - \mu * \sin\alpha)$$

The results of the force on top of the hold section during a tripping in scenario are represented in Table 6.

Table 6: *Calculated forces at the top of the hold section for varying friction coefficients between 0,1 – 0,4 during a tripping in scenario for the B&H well profile.*

F_2			
		(N)	(kN)
μ = 0,1	F_2	213922,5	213,923
μ = 0,15	F_2	73786,9	73,787
μ = 0,2	F_2	-66348,7	-66,349
μ = 0,25	F_2	-206484,3	-206,484
μ = 0,3	F_2	-346619,8	-346,620
μ = 0,35	F_2	-486755,4	-486,755
μ = 0,4	F_2	-626891,0	-626,891

The forces in the build-up bend section, F_3, are represented in Table 7. The force in the build-up bend is calculated from equation (35).

Table 7: *Calculated forces in the build-up bend section for varying friction coefficients between 0,1 – 0,4 during a tripping in scenario for the B&H well profile.*

F_3			
		(N)	(kN)
μ = 0,1	F_3	470503,6	470,504
μ = 0,15	F_3	344302,8	344,303
μ = 0,2	F_3	234276,0	234,276
μ = 0,25	F_3	138815,8	138,816
μ = 0,3	F_3	56457,8	56,458
μ = 0,35	F_3	-14130,7	-14,131
μ = 0,4	F_3	-74162,7	-74,163

The forces on top of the vertical section (top of the well), F_4, are represented in Table 8. The results in Table 8 do not take into consideration the weight of the top drive.

Table 8: *Calculated forces at the top of the vertical section for varying friction coefficients between 0,1 – 0,4 during a tripping in scenario for the B&H well profile.*

F_4			
		(N)	(kN)
μ = 0,1	F_4	772983,4	772,983
μ = 0,15	F_4	646782,7	646,783
μ = 0,2	F_4	536755,9	536,756
μ = 0,25	F_4	441295,6	441,296
μ = 0,3	F_4	358937,7	358,938
μ = 0,35	F_4	288349,1	288,349
μ = 0,4	F_4	228317,1	228,317

The results after adding the weight of the 25 000 kg top drive are represented in Table 9. In cases where we are concerned about if we are able to enter the well, one needs to add the additional weight that can be provided by the top drive. However, in the comparison of forces along the string for the three scenarios, this will not be shown since only the forces along the string vs measured depth are shown.

Table 9: *Calculated forces at the top of the vertical section for varying friction coefficients between 0,1 – 0,4 during a tripping in scenario for the B&H well profile, including the weight force of the top drive.*

F_5			
		(N)	(kN)
μ = 0,1	F_5	1018233,4	1018,233
μ = 0,15	F_5	892032,7	892,033
μ = 0,2	F_5	782005,9	782,006
μ = 0,25	F_5	686545,6	686,546
μ = 0,3	F_5	604187,7	604,188
μ = 0,35	F_5	533599,1	533,599
μ = 0,4	F_5	473567,1	473,567

4.1.4 B&H Well Profile – Static (Rotating off Bottom) Scenario

The results of a static scenario using the analytical model for the B&H well profile will be presented in this chapter. It is assumed that one is rotating off bottom which effectively will remove the axial static friction.

For a static scenario, there is no friction in the analytical model, only weight. So, when calculating the forces for varying friction coefficients, the forces will be the same since the friction term is neglected. The forces for a static scenario are represented in Table 10.

Table 10: *Calculated forces for a static scenario for the B&H well profile.*

Forces		
	(N)	(kN)
F_1	0	0
F_2	494193,7	494,1937
F_3	778652,5	778,6525
F_4	1081132,3	1081,1323

In Figure 13, the forces along the string are shown from total depth (TD) to just beneath the top drive for the three scenarios. From Figure 13 it is possible to observe that the build-up bend has a dominating effect on the well friction. From equation (35), the friction due to the Capstan effect increases as the angle of bend increases for a tripping out scenario. For a tripping in scenario, the friction becomes negative, which will lead to a decrease in drag force.

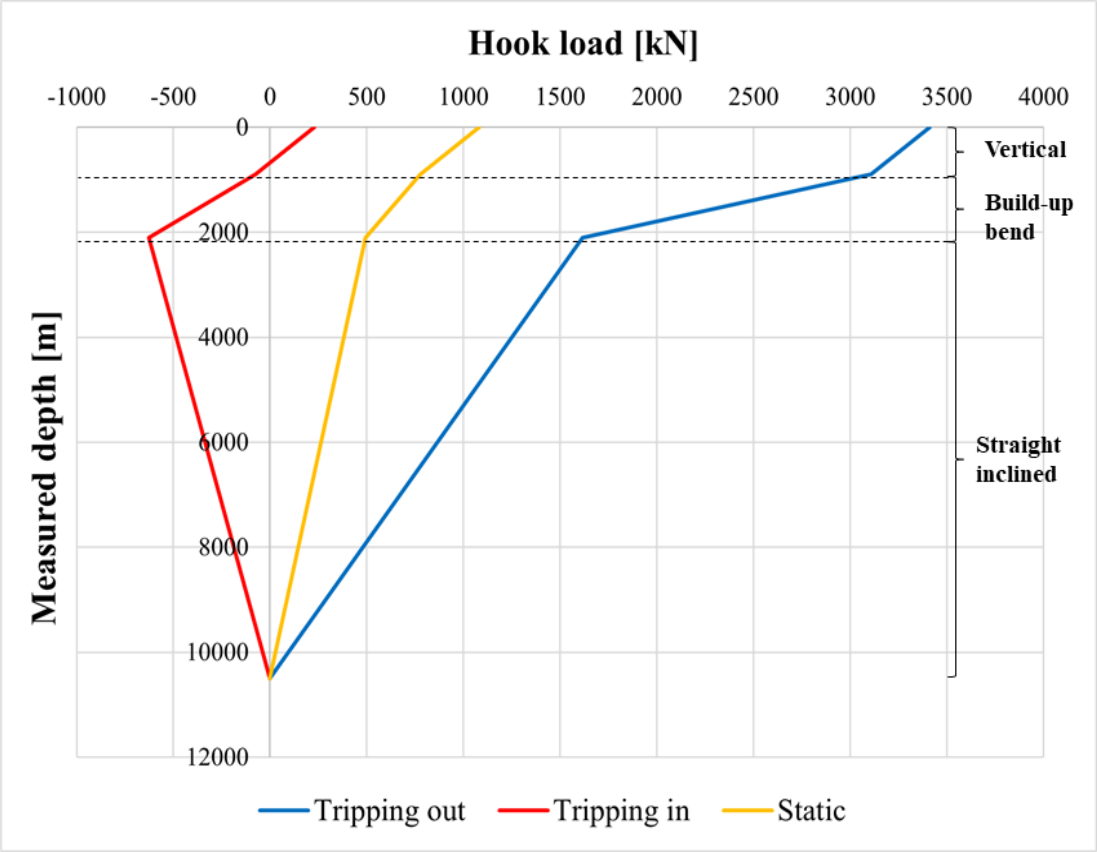

Figure 13: *Drag forces for the B&H well profile when μ = 0,4.*

In the analytical model, the friction coefficients are varied from 0,1 to 0,4 as mentioned. Figure 14 shows a comparison of the calculated drag forces for varying friction coefficients. Both the data for a tripping out scenario and a tripping in scenario are compared to the static scenario, which is the weight of the drill string when no friction is present.

For a tripping out scenario, the drag calculations should be higher than the static weight which is the case here. This is because friction between the wellbore and drill string plays a significant role. For the tripping out scenario in Figure 14, the drag forces increase as the friction coefficient increases. This is evident from equations (34) and (35) where the friction is positive when POOH. A higher friction coefficient produces more friction, and since the friction is acting in the direction of motion, this will be the case for a tripping out scenario.

For a tripping in scenario, the friction is acting in the opposite direction of motion, meaning that the friction becomes negative when RIH. This is the opposite as for a tripping out scenario.

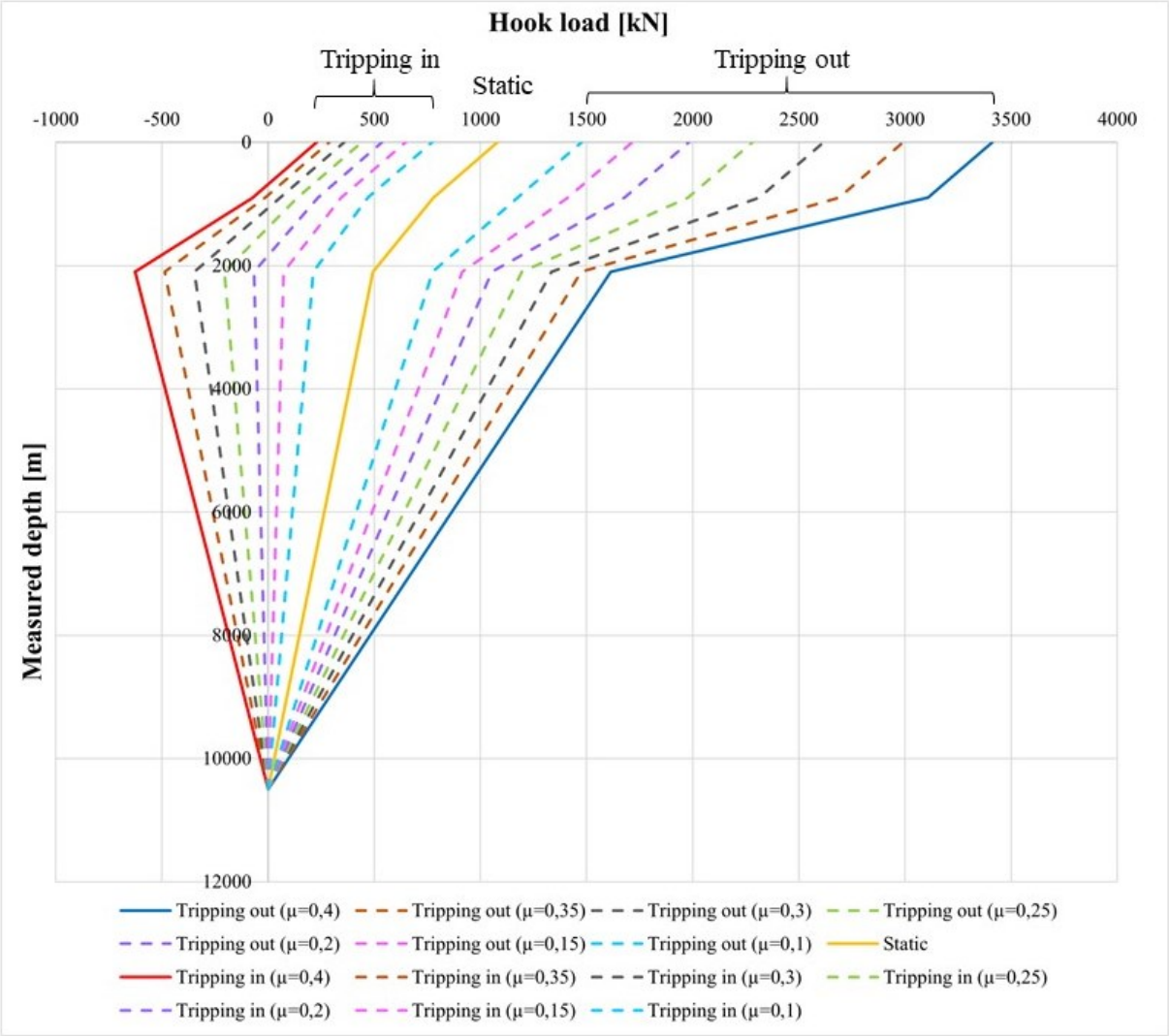

Figure 14: *Drag forces for varying friction coefficients between 0,1 – 0,4 for a tripping out scenario, tripping in scenario and static scenario for the B&H well profile.*

4.1.5 S-Profile

Calculations of drag forces for an S-profile will have the same approach as for the B&H well profile, where the calculations start at the bottom of the drill string and continues upwards section by section as shown in Figure 15. In addition, unlike the B&H well profile, a drop section and an inclined section after the drop section are added for the S-profile drag calculations.

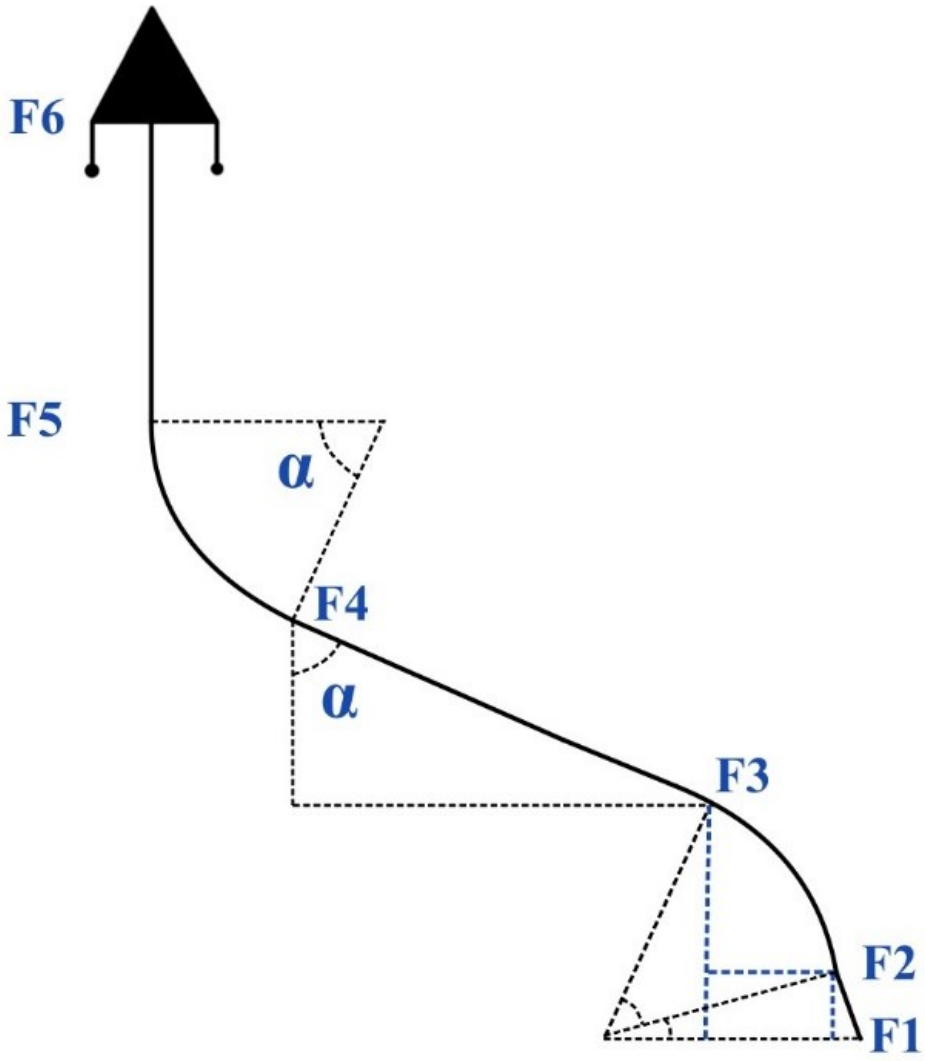

Figure 15: *S-Profile showing the drag forces for calculation.*

Before moving into drag calculations for the S-profile, some parameters must be set. The drill string characteristics are the same as found in Table 1, but in addition, there is also used drill collar (DC) in this profile having the characteristics stated in Table 11.

Table 11: *Drill collar characteristics used for drag calculations of the S-profile.*

Drill Collar (OD & ID)	**Nominal Unit Mass of Drill Collar**
(inch)	(kg/m)
8 x 3	218,77

The geometrical parameters stated in chapter 2.5.5 are repeated in Table 12. The presented data will be used for drag calculations for the S-profile.

Table 12: *Geometrical parameters used for drag calculations for the S-profile.*

Geometrical Parameters		
DLS	2/30	°/*m*
R	859,44	*m*
Vertical down to KOP (AB)	900	*m*
Build-up bend (BC)	1200	*m*
Hold section (CD)	6600	*m*
Drop bend (DT)	1050	*m*
Inclined section to target (TK)	150	*m*
Inclination down to target	10	°
Vertical depth of build-up bend (BE)	846,4	*m*
Vertical depth of hold section (IC)	1146,1	*m*
Vertical depth of drop bend (DF)	697,1	*m*
Vertical depth of inclined section (FG)	147,7	*m*

When the parameters are set, one should start by calculating the buoyancy factor. Since the MW and the steel density are the same as for the B&H well profile, the buoyancy factor will be the same as before. The length of the HWDP is 90 m and the length of the DC is 30 m.

The buoyed unit mass for the drill pipe, HWDP and DC are calculated from equation (19):

$$W_{Drillpipe} = 0{,}783 * 43{,}73 \frac{kg}{m} \approx 34{,}3 \frac{kg}{m}$$

$$W_{HWDP} = 0{,}783 * 73{,}4 \frac{kg}{m} \approx 57{,}5 \frac{kg}{m}$$

$$W_{DC} = 0{,}783 * 218{,}77 \frac{kg}{m} \approx 171{,}3 \frac{kg}{m}$$

When having all the necessary values for calculating drag forces, one can now continue by calculating the drag forces for a tripping out scenario, tripping in scenario, and a static (rotating off bottom) scenario for the S-profile.

4.1.6 S-Profile – Tripping out Scenario

The results of the drag force calculations for a tripping out scenario using the analytical model for the S-profile will be presented in this chapter.

For the drag calculations of this S-profile, the HWDP and DC are located right below the drop section. When knowing this, the force at the bottom of the drop section/top of the inclined section, F_2, can be calculated using equation (34):

$$F_2 = F_1 + \Big(W_{Drillpipe} * \big(L_{Inclined\ section} - (L_{HWDP} + L_{DC})\big) + (W_{HWDP} * L_{HWDP}) + (W_{DC} * L_{DC})\Big) * g * (\cos\alpha + \mu * \sin\alpha)$$

By using the equation for F_2 and varying the friction coefficient from 0,1 – 0,4 the result of the force at the bottom of the drop section/top of the inclined section is represented in Table 13.

Table 13: *Calculated forces at the top of the inclined section for varying friction coefficients between 0,1 – 0,4 during a tripping out scenario for the S-profile.*

F_2			
		(N)	(kN)
μ = 0,1	F_2	111536,1	111,536
μ = 0,15	F_2	112502,4	112,502
μ = 0,2	F_2	113468,7	113,469
μ = 0,25	F_2	114435,0	114,435
μ = 0,3	F_2	115401,3	115,401
μ = 0,35	F_2	116367,6	116,368
μ = 0,4	F_2	117333,9	117,334

Calculation of the force in the drop bend, F_3, is next. The force on the drop bend is calculated from equation (35). The results of the forces, F_3, are represented in Table 14.

Table 14: *Calculated forces in the drop bend section for varying friction coefficients between 0,1 – 0,4 during a tripping out scenario for the S-profile.*

F_3			
		(N)	(kN)
$\mu = 0,1$	F_3	360331,2	360,331
$\mu = 0,15$	F_3	369430,6	369,431
$\mu = 0,2$	F_3	379176,3	379,176
$\mu = 0,25$	F_3	389613,6	389,614
$\mu = 0,3$	F_3	400791,0	400,791
$\mu = 0,35$	F_3	412760,2	412,760
$\mu = 0,4$	F_3	425576,8	425,577

The force at the top of the hold section of the S-profile, F_4, is represented in Table 15. The force, F_4, is calculated using equation (34).

Table 15: *Calculated forces at the top of the hold section for varying friction coefficients between 0,1 – 0,4 during a tripping out scenario for the S-profile.*

F_4			
		(N)	(kN)
$\mu = 0,1$	F_4	963963,7	963,964
$\mu = 0,15$	F_4	1082287,4	1082,287
$\mu = 0,2$	F_4	1201257,5	1201,257
$\mu = 0,25$	F_4	1320919,1	1320,919
$\mu = 0,3$	F_4	1441320,8	1441,321
$\mu = 0,35$	F_4	1562514,3	1562,514
$\mu = 0,4$	F_4	1684555,2	1684,555

Calculation of the force in the build-up bend, F_5, is next. The force in the build-up bend is calculated from equation (35). The results of the forces, F_5, are represented in Table 16.

Table 16: *Calculated forces in the build-up bend section for varying friction coefficients between 0,1 – 0,4 during a tripping out scenario for the S-profile.*

F_5			
		(N)	(kN)
$\mu = 0,1$	F_5	1392866,7	1392,867
$\mu = 0,15$	F_5	1618904,9	1618,905
$\mu = 0,2$	F_5	1872690,9	1872,691
$\mu = 0,25$	F_5	2157181,9	2157,182
$\mu = 0,3$	F_5	2475635,9	2475,636
$\mu = 0,35$	F_5	2831642,8	2831,643
$\mu = 0,4$	F_5	3229158,7	3229,159

The force at the top of the vertical section (top of the well), F_6, is the last thing that needs to be calculated. The F_6 is calculated using equation (36), and the results are represented in Table 17.

Table 17: *Calculated forces at the top of the vertical section for varying friction coefficients between 0,1 – 0,4 during a tripping out scenario for the S-profile.*

F_6			
		(N)	(kN)
$\mu = 0,1$	F_6	1695346,6	1695,347
$\mu = 0,15$	F_6	1921384,7	1921,385
$\mu = 0,2$	F_6	2175170,8	2175,171
$\mu = 0,25$	F_6	2459661,8	2459,662
$\mu = 0,3$	F_6	2778115,7	2778,116
$\mu = 0,35$	F_6	3134122,7	3134,123
$\mu = 0,4$	F_6	3531638,5	3531,639

4.1.7 S-Profile – Tripping in Scenario

The results of a tripping in scenario using the analytical model for the S-profile will be presented in this chapter.

The drag force calculations will be the same as for the tripping out scenario, but when RIH the friction will be negative for a tripping in scenario. The formula for F_2 can therefore be written as:

$$F_2 = F_1 + \Big(W_{Drillpipe} * \big(L_{Inclined\ section} - (L_{HWDP} + L_{DC})\big) + (W_{HWDP} * L_{HWDP}) + (W_{DC} * L_{DC})\Big) * g * (\cos\alpha - \mu * \sin\alpha)$$

The results of the force on the bottom of the drop section/top inclined section during a tripping in scenario is represented in Table 18.

Table 18: *Calculated forces at the top of the inclined section for varying friction coefficients between 0,1 – 0,4 during a tripping in scenario for the S-profile.*

F_2			
		(N)	(kN)
μ = 0,1	F_2	107670,9	107,671
μ = 0,15	F_2	106704,6	106,705
μ = 0,2	F_2	105738,3	105,738
μ = 0,25	F_2	104772,0	104,772
μ = 0,3	F_2	103805,7	103,806
μ = 0,35	F_2	102839,4	102,839
μ = 0,4	F_2	101873,1	101,873

Calculation of the force in the drop bend, F_3, is next. The force on the drop bend is calculated from equation (35). The results of the forces, F_3, are represented in Table 19.

Table 19: *Calculated forces in the drop bend section for varying friction coefficients between 0,1 – 0,4 during a tripping in scenario for the S-profile.*

F_3			
		(N)	(kN)
μ = 0,1	F_3	329589,2	329,589
μ = 0,15	F_3	323138,1	323,138
μ = 0,2	F_3	317117,0	317,117
μ = 0,25	F_3	311497,5	311,497
μ = 0,3	F_3	306253,2	306,253
μ = 0,35	F_3	301359,3	301,359
μ = 0,4	F_3	296792,8	296,793

The force at the top of the hold section, F_4, is represented in Table 20. The force, F_4, is calculated using equation (34).

Table 20: *Calculated forces at the top of the hold section for varying friction coefficients between 0,1 – 0,4 during a tripping in scenario for the S-profile.*

F_4			
		(N)	(kN)
μ = 0,1	F_4	496324,5	496,324
μ = 0,15	F_4	380649,1	380,649
μ = 0,2	F_4	265403,6	265,404
μ = 0,25	F_4	150559,8	150,560
μ = 0,3	F_4	36091,2	36,091
μ = 0,35	F_4	-78027,0	-78,027
μ = 0,4	F_4	-191817,8	-191,818

Calculation of the force in the build-up bend, F_5, is next. The force in the build-up bend is calculated from equation (35). The results of the forces, F_5, are represented in Table 21.

Table 21: *Calculated forces in the build-up bend section for varying friction coefficients between 0,1 – 0,4 during a tripping in scenario for the S-profile.*

F_5			
		(N)	(kN)
μ = 0,1	F_5	716103,8	716,104
μ = 0,15	F_5	593179,9	593,180
μ = 0,2	F_5	485196,4	485,196
μ = 0,25	F_5	390655,6	390,656
μ = 0,3	F_5	308198,9	308,199
μ = 0,35	F_5	236594,8	236,595
μ = 0,4	F_5	174726,8	174,727

The force at the top of the vertical section (top of the well), F_6, is the last thing that needs to be calculated. The F_6 is calculated using equation (36), and the results are represented in Table 22. The results in Table 22 do not take into consideration the weight of the top drive.

Table 22: *Calculated forces at the top of the vertical section for varying friction coefficients between 0,1 – 0,4 during a tripping in scenario for the S-profile.*

F_6			
		(N)	(kN)
μ = 0,1	F_6	1018583,6	1018,584
μ = 0,15	F_6	895659,7	895,660
μ = 0,2	F_6	787676,3	787,676
μ = 0,25	F_6	693135,4	693,135
μ = 0,3	F_6	610678,8	610,679
μ = 0,35	F_6	539074,6	539,075
μ = 0,4	F_6	477206,6	477,207

The results after adding the weight of the 25 000 kg top drive are represented in Table 23.

Table 23: *Calculated forces at the top of the vertical section for varying friction coefficients between 0,1 – 0,4 during a tripping in scenario for the S-profile, including the weight force of the top drive.*

F_7			
		(N)	(kN)
μ = 0,1	F_7	1263833,6	1263,834
μ = 0,15	F_7	1140909,7	1140,910
μ = 0,2	F_7	1032926,3	1032,926
μ = 0,25	F_7	938385,4	938,385
μ = 0,3	F_7	855928,8	855,929
μ = 0,35	F_7	784324,6	784,325
μ = 0,4	F_7	722456,6	722,457

4.1.8 S-Profile – Static Scenario

The results of a static scenario using the analytical model for the S-profile will be presented in this chapter.

As mentioned earlier, the static scenario does not take friction into consideration in the analytical model. Only the weight. The forces for a static scenario are represented in Table 24.

Table 24: *Calculated forces for a static scenario for the S-profile.*

Forces		
	(N)	(kN)
F_1	0	0
F_2	109603,5	109,604
F_3	343904,5	343,905
F_4	729088,4	729,088
F_5	1013547,1	1013,547
F_6	1316027,0	1316,027

From Figure 16, it is possible to see that in this well profile, as well as for the B&H well profile, the force increase is bigger in the bend sections (build-up bend and drop bend). This is a result of the Capstan effect, where the friction coefficient, μ, increases the force in a bend.

For the tripping out scenario, the drag calculations are higher than the static weight as seen in Figure 17. For the tripping in scenario, the drag calculations will be less than the static weight, which is correct. By varying the friction coefficient for this S-profile, it is observed here as well for the B&H well profile that the drag forces increase when the friction coefficient increases.

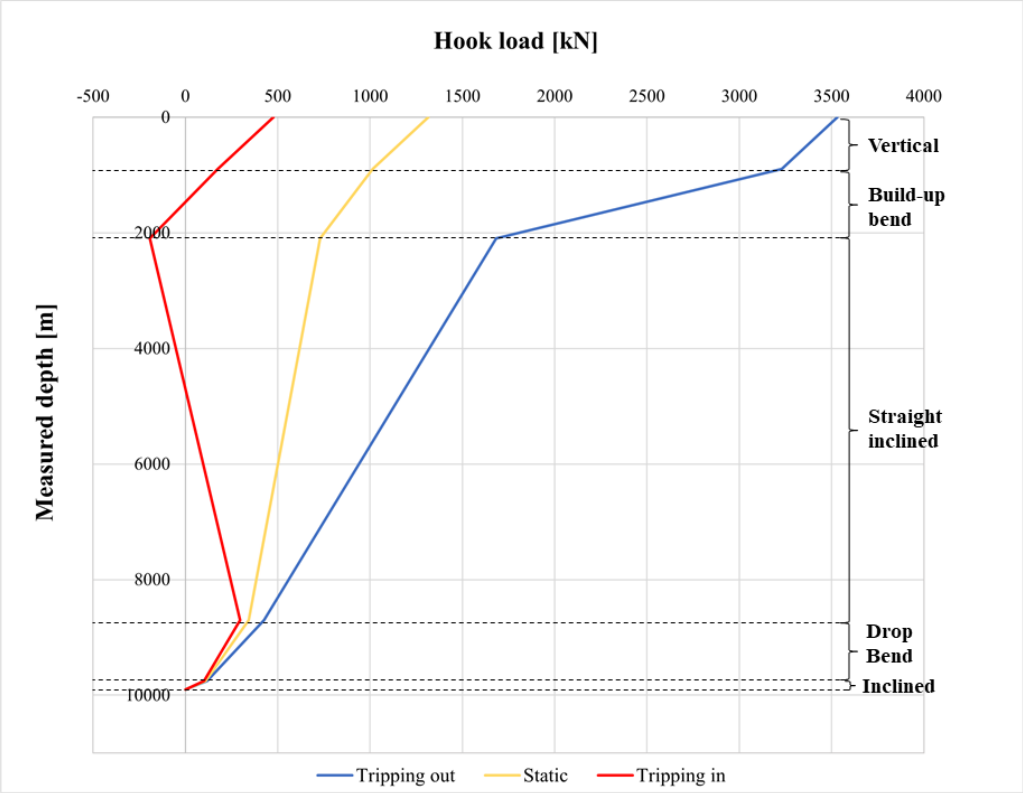

Figure 16: *Drag forces for the S-profile when μ = 0,4.*

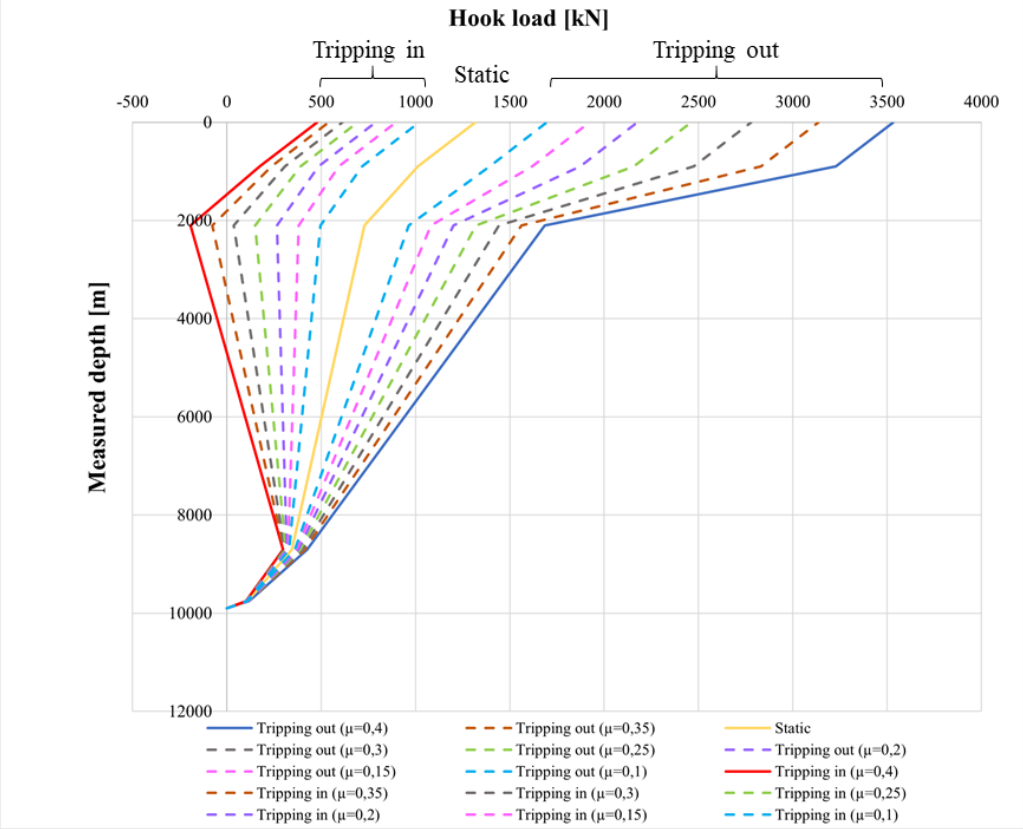

Figure 17: *Drag forces for varying friction coefficient between 0,1 – 0,4 for a tripping out scenario, tripping in scenario and static scenario for the S-profile.*

4.2 Comparison of Analytical Model and Numerical Model in a Bend

The comparison between the analytical model and the numerical model is made by analyzing the build-up bend of the B&H well profile. The reason why a bend is chosen is because this is where the models will differ. The models are basically equal for the straight sections. When analyzing the bend, only the weight of the drill pipe will be used, and there is no HWDP, or DC involved in the calculations. The friction coefficient is set to be 0,4.

When comparing the two models, the highest bottom force, F_2, will be calculated for a static scenario, tripping out scenario, and tripping in scenario from given parameters. This bottom force then gets divided into an interval of five until reaching zero. This is done to study the impact of variations in the bottom force on the friction in the bend.

For the case where F_2 is equal to zero, the force at KOP, F_3, in Figure 4 and Figure 12, will be a result of the axial weight in the analytical model. This is observed from equation (35) where the expression of friction is removed. This will not be the case for the numerical model.

As mentioned earlier, the normal force contribution due to the weight component perpendicular to the pipe axis is not taken into consideration in the analytical model as in the numerical model. In the analytical model, one only calculates the Capstan effect through the bend.

4.2.1 Comparison of Models - Static Scenario

The results of comparing the analytical model and the numerical model for a static scenario are represented in Table 25.

Table 25: *Comparison of the analytical model and numerical model in a bend for a static scenario. The numerical model applies a discretization of 30-meter segments.*

F_2	**Analytical (F_3)**	**Force due to friction**	**Numerical (F_3)**	**Force due to friction**	**Difference between models**
(kN)	(kN)	(kN)	(kN)	(kN)	(kN)
0	284,459	0	284,473	0	0,014
98,047	382,506	0	382,520	0	0,014
196,094	480,552	0	480,567	0	0,014
294,140	578,599	0	578,614	0	0,014
392,187	676,646	0	676,660	0	0,014
490,234	774,693	0	774,707	0	0,014

For a static scenario, the force in a bend will only be a result of the axial weight in both the analytical model and the numerical model. This is because there is no friction acting in the bend when the drill pipe is not moving up or down in the wellbore.

By discretizing the well into 10-meter segments instead of 30-meter segments in the numerical model as in Table 25, one can check if the results between the two models become more identical to each other. The results are represented in Table 26.

Table 26: *Comparison of the analytical model and numerical model in a bend for a static scenario. The numerical model applies a discretization of 10-meter segments.*

F_2	**Analytical (F_3)**	**Force due to friction**	**Numerical (F_3)**	**Force due to friction**	**Difference between models**
(kN)	(kN)	(kN)	(kN)	(kN)	(kN)
0	284,459	0	284,460	0	0,002
98,047	382,506	0	382,507	0	0,002
196,094	480,552	0	480,554	0	0,002
294,140	578,599	0	578,601	0	0,002
392,187	676,646	0	676,648	0	0,002
490,234	774,693	0	774,694	0	0,002

When discretizing the numerical model into 10-meter segments instead of 30-meter segments, the difference between the two models decreases. This is also stated in chapter 3.4 where the equation (38) and (39) must be applied to infinitesimal elements of the drill string to accomplish exact calculations.

4.2.2 Comparison of Models - Tripping out Scenario

The comparison of the analytical model and the numerical model for a tripping out scenario is represented in Table 27. The friction coefficient is set to be 0,4 and the numerical model is discretized into 30-meter segments.

Table 27: *Comparison of the analytical model and numerical model in a bend for a tripping out scenario. The numerical model uses a discretization of 30-meter segments.*

F_2	**Analytical (F_3)**	**Force due to friction**	**Numerical (F_3)**	**Force due to friction**	**Difference between models**
(kN)	(kN)	(kN)	(kN)	(kN)	(kN)
0	284,459	0	492,885	208	208,426
320,467	844,654	240	1050,900	446	206,246
640,934	1404,849	479	1609,000	684	204,151
961,402	1965,045	719	2167,000	921	201,955
1281,869	2525,240	959	2725,000	1159	199,760
1602,336	3085,435	1199	3283,100	1396	197,665

A graphical comparison of Table 27 is illustrated in Figure 18.

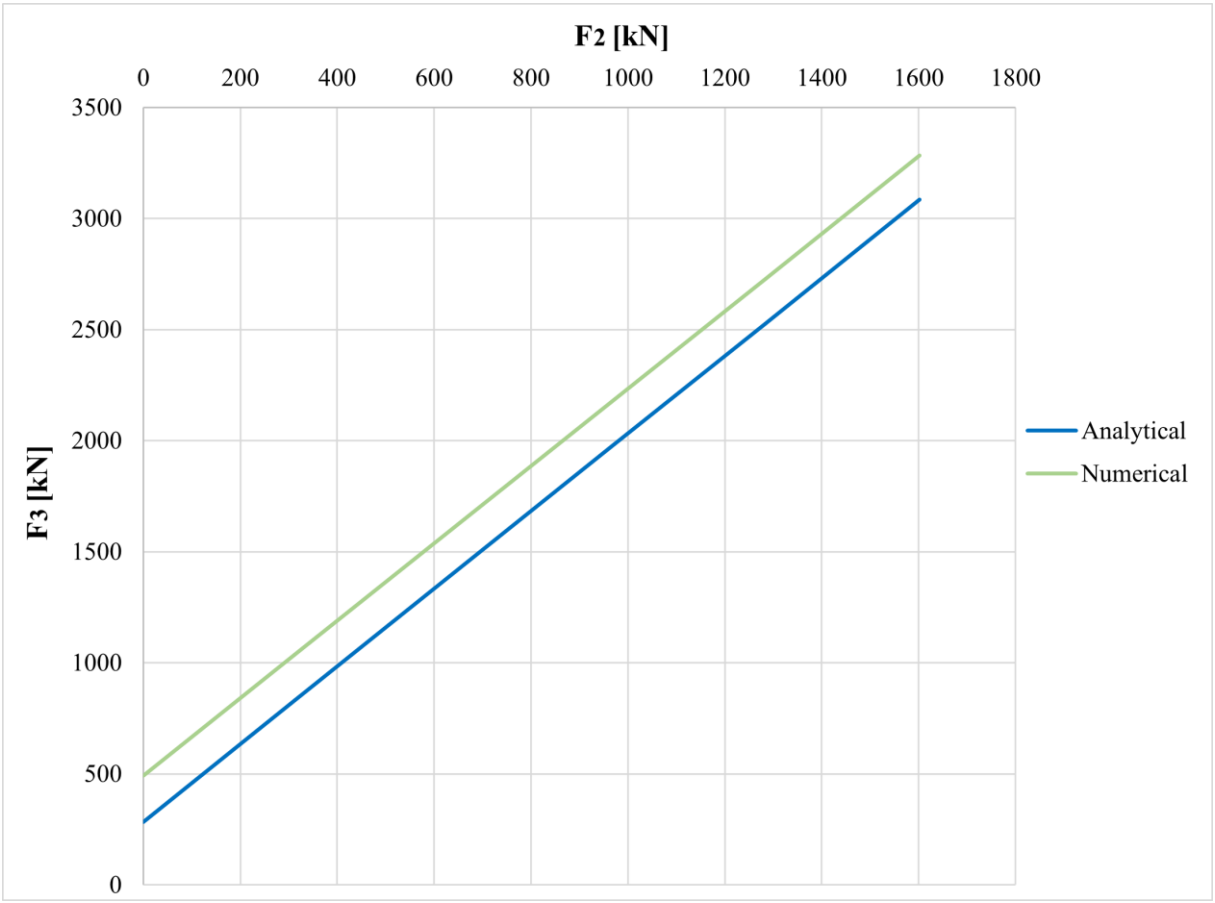

Figure 18: *The difference between the analytical model and the numerical model for a tripping out scenario illustrated graphically.*

From Table 27 and Figure 18, the difference in absolute value between the models does not decrease much. This is because the friction associated with the normal force component due to the weight component perpendicular to the pipe axis is disregarded in the analytical model. The only thing one calculates is the Capstan effect. The difference in Table 27 is an indication of how much this simplification in the analytical model is compared to the numerical model where the normal force contribution due to the weight component perpendicular to the pipe axis is taken into consideration.

This almost constant difference in friction between the models will be present even though the F_2 force is increased, and the normal force starts to get dominated by tension effects. However, as shown in Table 28, when the difference between the models is measured in terms of percentage, one can notice that the difference between the models gets reduced when the F_2 force is increased, and the tension becomes the dominating contributor to the normal force.

Table 28: *The difference in percentage between the analytical model and the numerical model for a tripping out scenario.*

F_2	**Analytical (F_3)**	**Numerical (F_3)**	**Difference between models**
(kN)	(kN)	(kN)	(%)
0	284,459	492,885	73,27
320,467	844,654	1050,900	24,42
640,934	1404,849	1609,000	14,53
961,402	1965,045	2167,000	10,28
1281,869	2525,240	2725,000	7,91
1602,336	3085,435	3283,100	6,41

Table 28 represents the difference between the models as a percentage. The overall difference between the models decreases when the bottom force, F_2, increases. The difference between the models is represented as tons in Table 29.

Table 29: *Differences in forces between the analytical model and the numerical model given in different units for the tripping out scenario.*

(kN)	**(daN)**	**(kg)**	**(Ton)**
208,426	20842,6	21246,3	21,246
206,246	20624,6	21024,1	21,024
204,151	20415,1	20810,5	20,810
201,955	20195,5	20586,7	20,587
199,760	19976,0	20362,9	20,363
197,665	19766,5	20149,3	20,149

From Table 29, the difference between the models is around 20 tons. This difference in tons is when having a friction coefficient, $\mu = 0,4$. This friction coefficient is not a known parameter. By varying this friction coefficient will possibly give other differences than the 20 tons calculated here.

By using the B&H well profile as an example, the top force, F_4, is 3410,539 kN when having a friction coefficient $\mu = 0,4$. This top force of 3410,539 kN equals 347,8 tons. When the friction coefficient is $\mu = 0,1$, the top force equals 150,7 tons. This is quite a difference in top force, indicating that the friction coefficient plays a significant role in drag calculations.

The friction forces divided into friction due to weight and the friction due to the Capstan effect are represented in Table 30. A graphical illustration of Table 30 is given in Figure 19.

Table 30: *Distribution of friction forces for the tripping out scenario in the numerical model.*

F_2	**Numerical (F_3)**	**Force due to total friction**	**Friction due to weight**	**Capstan friction**
(kN)	(kN)	(kN)	(kN)	(kN)
0	492,885	208	95,481	71,767
320,467	1050,900	446	95,481	309,335
640,934	1609,000	684	95,493	546,893
961,402	2167,000	921	95,525	784,425
1281,869	2725,000	1159	95,458	1022,058
1602,336	3283,100	1396	95,491	1259,591

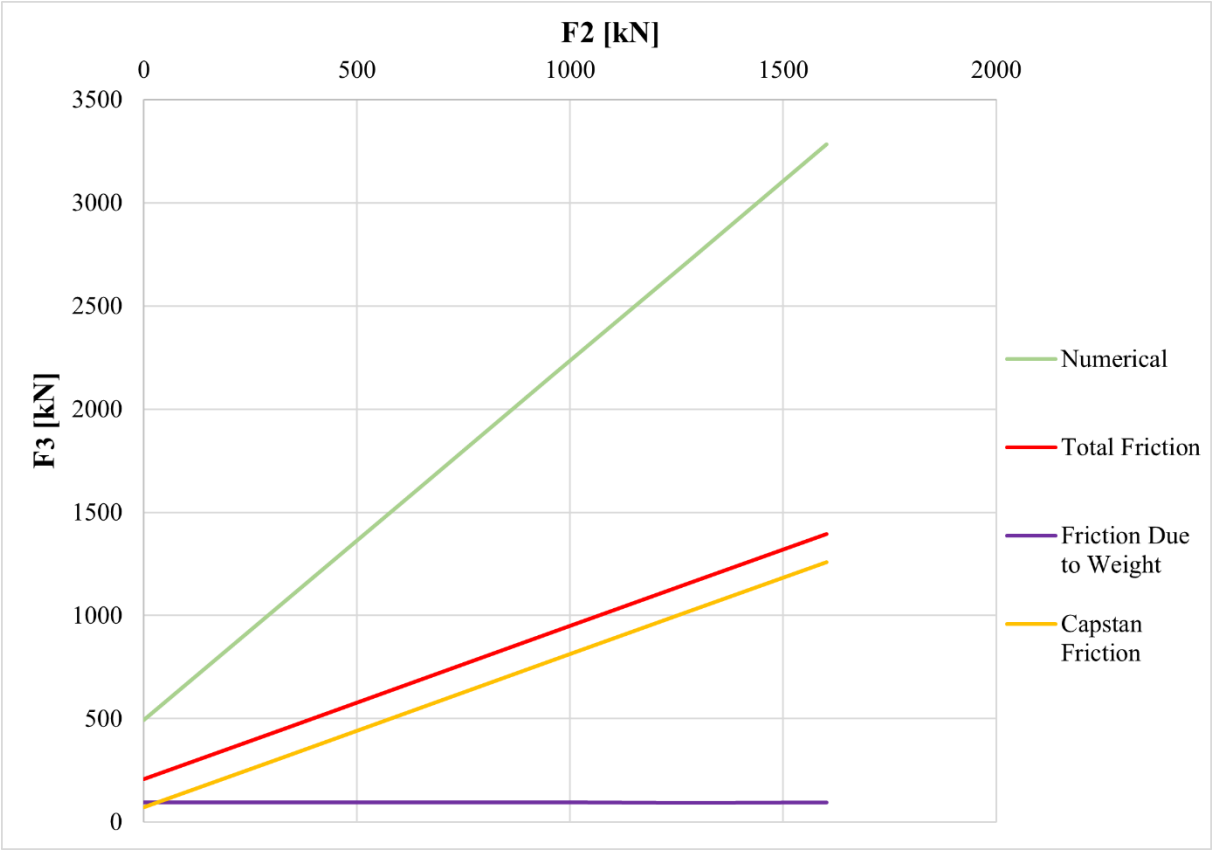

Figure 19: *The distribution of friction forces for a tripping out scenario when μ = 0,4 illustrated graphically.*

From Table 30, the total friction forces are divided into friction due to the normal force contribution caused by the weight component perpendicular to the pipe axis and the friction due to tension effects (Capstan effect). This was tested by playing with equation (38) in the numerical model by setting the first and then later the second term to zero. By keeping both terms, the overall friction was calculated.

As one can see, the friction due to the normal force contribution caused by the weight component perpendicular to the pipe axis is kept constant while the friction forces due to the Capstan effect is increasing as the bottom force, F_2, increases.

By adding the friction due to the normal force contribution caused by the weight component perpendicular to the pipe axis and the friction force due to the Capstan effect together, it is possible to check if these values are adding up equally to the total friction force. The result of this is represented in Table 31.

Table 31: *The difference in friction forces in the numerical model when calculating the total friction force as a whole and then calculating the friction force by dividing into the friction force due to the normal force contribution caused by the weight component perpendicular to the pipe axis and friction due to the Capstan effect.*

Force due to total friction	**Friction due to weight + Capstan friction**	**Difference**
(kN)	(kN)	(kN)
208	167,248	41,165
446	404,816	41,144
684	642,385	41,207
921	879,951	41,175
1159	1117,516	41,142
1396	1355,082	41,209

From Table 31 it is possible to see that the result of adding the friction due to the normal force contribution caused by the weight component perpendicular to the pipe axis and the friction force due to tension effects (Capstan effect) together creates a value less than the total friction force. The deviation is around 41 kN.

This difference is probably caused by the fact that when the normal force contribution related to the gravitational force is neglected in equation (38), it will change the tension in the string slightly, which again will have an impact on the Capstan effect. The two effects are to some extent interlinked. From Table 30 it is possible to see that the Capstan effect becomes more dominant with an increasing F_2.

By only including the Capstan effect in the numerical model makes it possible to see if the two models give identical results or if there is still a certain difference. The results are represented in Table 32:

Table 32: *The difference between the analytical model and the numerical model when only the Capstan effect is included in the numerical model for a tripping out scenario.*

F_2	**Analytical (F_3)**	**Numerical (F_3) (Only including Capstan effect)**	**Difference**
(kN)	(kN)	(kN)	(kN)
0	284,459	356,240	71,781
320,467	844,654	914,275	69,621
640,934	1404,849	1472,300	67,451
961,402	1965,045	2030,300	65,255
1281,869	2525,240	2588,400	63,160
1602,336	3085,435	3146,400	60,965

From Table 32, the difference between the analytical model and the numerical model decreases as the bottom force, F_2, increases. It can be noticed that there is some difference in the way the Capstan friction is calculated, and this can probably be explained by the discretization process taking place in the numerical model. The difference seems to be around 6-7 tons. The analytical model will give a straight line for the changes in the axial force across the bend, while in the numerical model it is not a straight line. The numerical model will capture that the Capstan effect gets stronger the further up in the bend as shown in Figure 20.

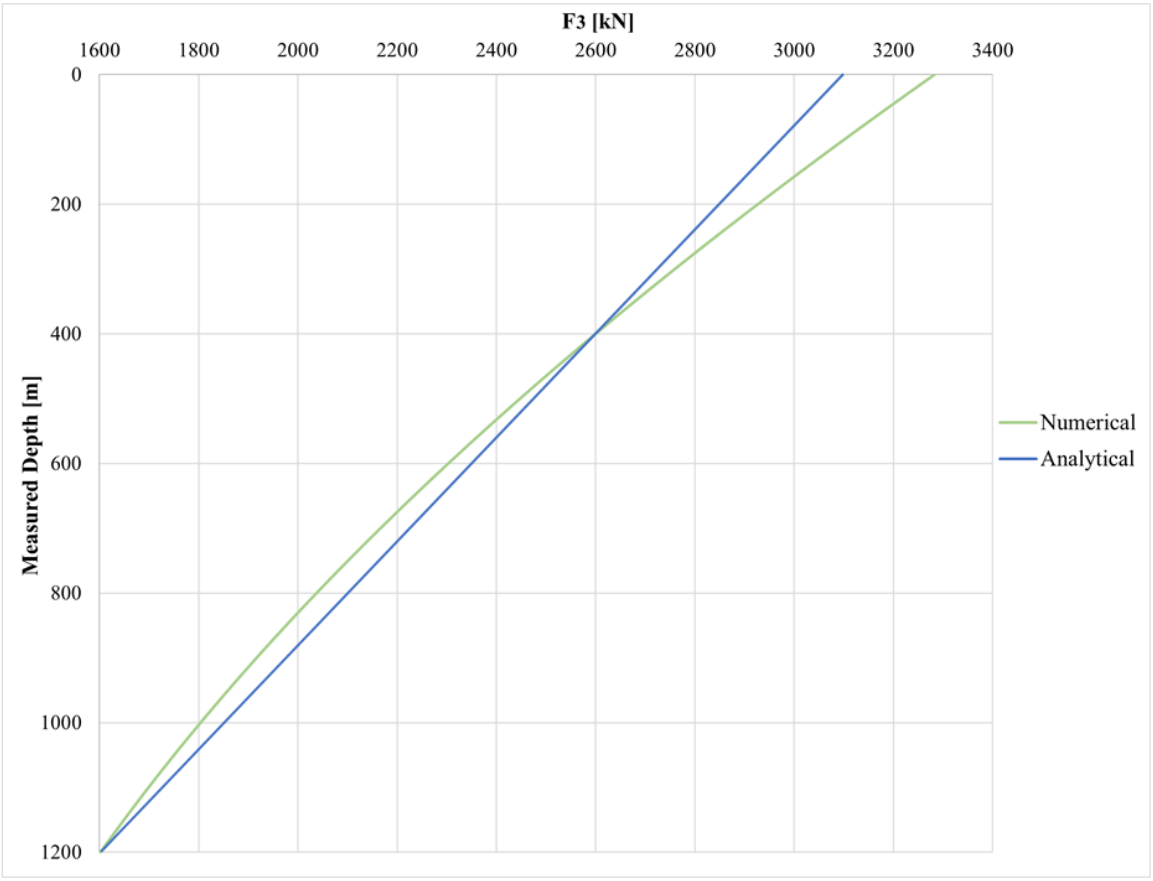

Figure 20: *The difference between the numerical model and the analytical model capturing the increase in the Capstan effect further up in the bend.*

4.2.3 Sensitivity Analysis – Tripping out scenario

A sensitivity analysis is performed on the bend of the B&H well profile for a tripping out scenario to be able to see if the difference between the analytical model and numerical model decreases as the friction coefficient decreases.

The sensitivity analysis is performed on the bend within the B&H well profile, having the same parameters as before. The friction coefficient will be varied between 0,1-0,4, while all other parameters are kept constant.

The results of the sensitivity analysis are represented below. The difference between the analytical model and numerical model when the friction coefficient, $\mu = 0{,}4$, is represented in Table 27 and Table 28. The difference between the models when the friction coefficient is $\mu = 0{,}3$ is represented in Table 33:

Table 33: *The difference between the analytical model and the numerical model when the friction coefficient is 0,3.*

μ = 0,3				
F_2	**Analytical (F_3)**	**Numerical (F_3)**	**Difference between models**	**Difference between models**
(kN)	(kN)	(kN)	(kN)	(%)
0	284,459	429,781	145,322	51,09
320,467	771,651	915,913	144,262	18,70
640,934	1258,843	1402,000	143,157	11,37
961,402	1746,036	1888,200	142,164	8,14
1281,869	2233,228	2374,300	141,072	6,32
1602,336	2720,421	2860,400	139,979	5,15

The difference between the analytical model and the numerical model when μ = 0,2 is represented in Table 34:

Table 34: *The difference between the analytical model and the numerical model when the friction coefficient is 0,2.*

μ = 0,2				
F_2	**Analytical (F_3)**	**Numerical (F_3)**	**Difference between models**	**Difference between models**
(kN)	(kN)	(kN)	(kN)	(%)
0	284,459	374,646	90,187	31,70
320,467	708,162	797,938	89,776	12,68
640,934	1131,865	1221,200	89,335	7,89
961,402	1555,568	1644,500	88,932	5,72
1281,869	1979,271	2067,800	88,529	4,47
1602,336	2402,974	2491,100	88,126	3,67

The difference between the analytical model and the numerical model when μ = 0,1 is represented in Table 35:

Table 35: *The difference between the analytical model and the numerical model when the friction coefficient is 0,1.*

μ = 0,1				
F_2	**Analytical (F_3)**	**Numerical (F_3)**	**Difference between models**	**Difference between models**
(kN)	(kN)	(kN)	(kN)	(%)
0	284,459	326,499	42,040	14,78
320,467	652,946	694,896	41,950	6,42
640,934	1021,433	1063,300	41,867	4,10
961,402	1389,921	1431,700	41,779	3,01
1281,869	1758,408	1800,100	41,692	2,37
1602,336	2126,896	2168,500	41,604	1,96

From the results in the tables above, the two models become more equal, and the difference decreases when the friction coefficient becomes small. When μ = 0,1 the difference between the analytical model and the numerical model is at around 42 kN, while for μ = 0,4 the difference is at around 200 – 208 kN.

This difference in values is due to the normal force contribution due to the weight component perpendicular to the pipe axis in the numerical model. This friction component will have a smaller significance the more the friction coefficient decreases in value.

4.2.4 Comparison of Models for a Tripping in Scenario

The comparison of the analytical model and the numerical model for a tripping in scenario is represented in Table 36. The friction coefficient is set to be 0,4 and the same bottom force, F_2, is used as for the tripping out scenario.

Table 36: *Comparison of the analytical model and numerical model in a bend for a tripping in scenario. The numerical model uses a discretization of 30-meter segments.*

F_2	**Analytical (F_3)**	**Force due to friction**	**Numerical (F_3)**	**Force due to friction**	**Difference between models**
(kN)	(kN)	(kN)	(kN)	(kN)	(kN)
0	284,459	0	163,705	-121	-120,753
320,467	467,786	-137	346,313	-259	-121,474
640,934	651,114	-274	528,920	-396	-122,194
961,402	834,442	-411	711,527	-534	-122,914
1281,869	1017,769	-549	894,135	-672	-123,634
1602,336	1201,097	-686	1076,700	-810	-124,397

The minus sign in Table 36, the rightmost column, shows that the numerical method gives lower values on top of the bend. This is because the friction associated with the normal force due to gravity is disregarded in the analytical model. The only thing one calculates is, as mentioned, the Capstan effect. The difference between the models is smaller in absolute value for this tripping in scenario compared to the tripping out scenario. A graphical representation of Table 36 is illustrated in Figure 21.

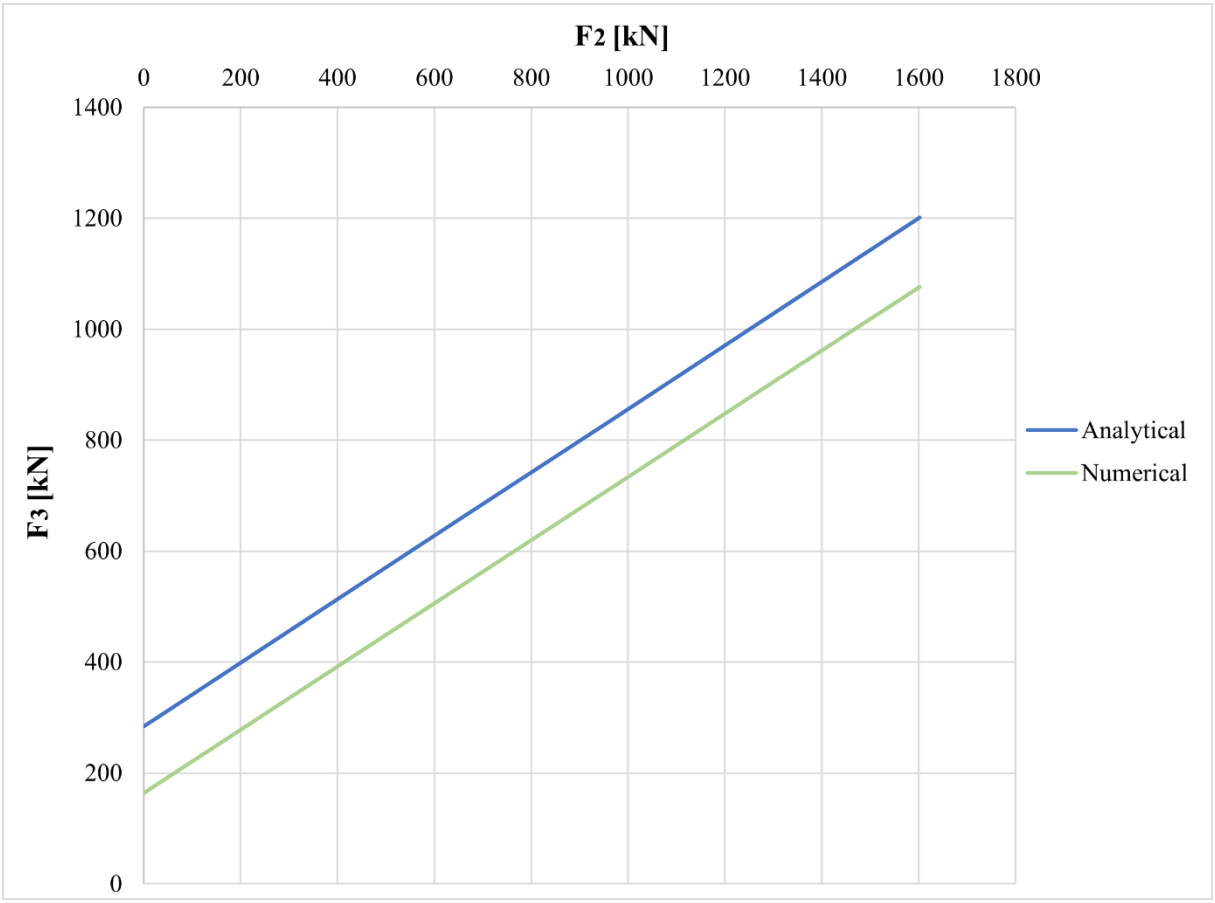

Figure 21: *The difference between the analytical model and the numerical model for a tripping in scenario illustrated graphically.*

Table 37: *The difference in percentage between the analytical model and the numerical model for a tripping in scenario.*

F_2	**Analytical (F_3)**	**Numerical (F_3)**	**Difference between models**
(kN)	(kN)	(kN)	(%)
0	284,459	163,705	42,45
320,467	467,786	346,313	25,97
640,934	651,114	528,920	18,77
961,402	834,442	711,527	14,73
1281,869	1017,769	894,135	12,15
1602,336	1201,097	1076,700	10,36

Table 37 represents the difference between the models as a percentage for the tripping in scenario. The overall difference between the models decreases when the bottom force, F_2, increases.

Table 38: *Differences in forces between the analytical model and the numerical model given in different units for the tripping in scenario.*

(kN)	(daN)	(kg)	(Ton)
-120,753	-12075,3	-12309,2	-12,309
-121,474	-12147,4	-12382,6	-12,383
-122,194	-12219,4	-12456,1	-12,456
-122,914	-12291,4	-12529,5	-12,529
-123,634	-12363,4	-12602,9	-12,603
-124,397	-12439,7	-12680,6	-12,681

The difference between the models is around 12 tons for the tripping in scenario. This is less than for the tripping out scenario, illustrating that the friction creates less of a difference for the tripping in scenario than for the tripping out scenario.

Table 39: *The distribution of friction forces for the tripping in scenario in the numerical model.*

F_2	Numerical (F_3)	Force due to total friction	Friction due to normal force	Capstan friction
(kN)	(kN)	(kN)	(kN)	(kN)
0	163,705	-121	-95,480	-53,186
320,467	346,313	-259	-95,480	-191,046
640,934	528,920	-396	-95,480	-328,906
961,402	711,527	-534	-95,475	-466,766
1281,869	894,135	-672	-95,442	-604,625
1602,336	1076,700	-810	-95,509	-742,509

The friction forces divided into friction due to weight and the friction due to the Capstan effect are represented in Table 39. A graphical illustration of Table 39 is given in Figure 22.

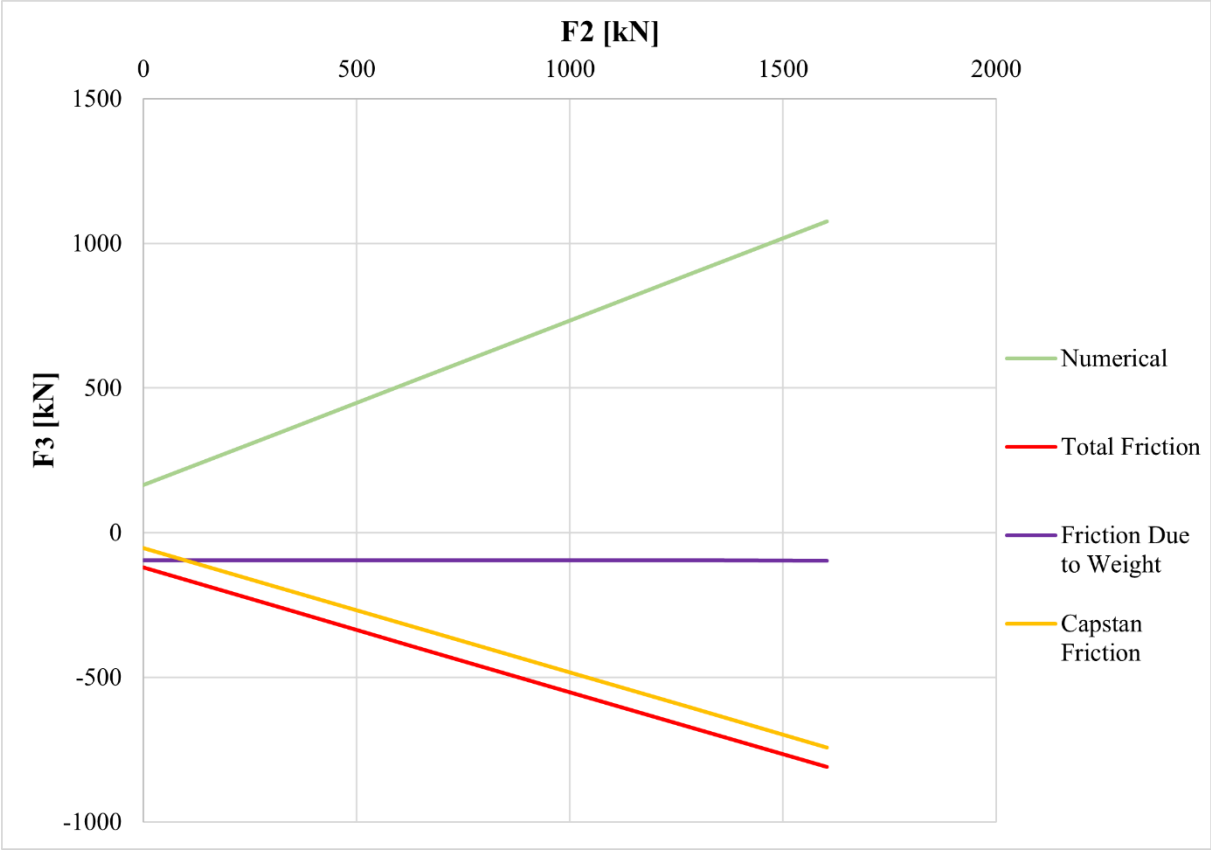

Figure 22: *The distribution of friction forces for a tripping in scenario when μ = 0,4 illustrated graphically.*

Table 40: *The difference in friction forces in the numerical model when calculating the total friction force as a whole and then calculating the friction force by dividing it into the friction force due to the normal force contribution caused by the weight component perpendicular to the pipe axis and friction due to the Capstan effect.*

Force due to total friction	**Friction due to normal force + Capstan friction**	**Difference**
(kN)	(kN)	(kN)
-121	-148,667	27,899
-259	-286,526	27,899
-396	-424,386	27,899
-534	-562,240	27,893
-672	-700,067	27,860
-810	-838,018	27,909

When dividing the total friction forces into friction due to the normal force contribution caused by the weight component perpendicular to the pipe axis and the friction force due to tension effects (Capstan effect), one sees from Table 40 that the difference is around 27 kN. This is a difference of around 2,8 tons. When adding the two independent friction terms together, the result is a higher value than the total friction force. This is the opposite as for the tripping out scenario.

From Table 41 and Figure 23 it is possible to see that the Capstan effect gets weaker the further up in the bend. This is the opposite as for the tripping out scenario. The difference in the way the Capstan effect is calculated is explained by the discretization process as stated previously. The difference for the tripping in scenario is around 5,5 tons.

Table 41: *The difference between the analytical model and the numerical model when only the Capstan effect is included in the numerical model for a tripping in scenario.*

F2	Analytical (F3)	Numerical (F_3) (Only including Capstan effect)	Difference
(kN)	(kN)	(kN)	(kN)
0	284,459	231,287	-53,172
320,467	467,786	413,894	-53,892
640,934	651,114	596,502	-54,612
961,402	834,442	779,109	-55,332
1281,869	1017,769	961,717	-56,052
1602,336	1201,097	1144,300	-56,797

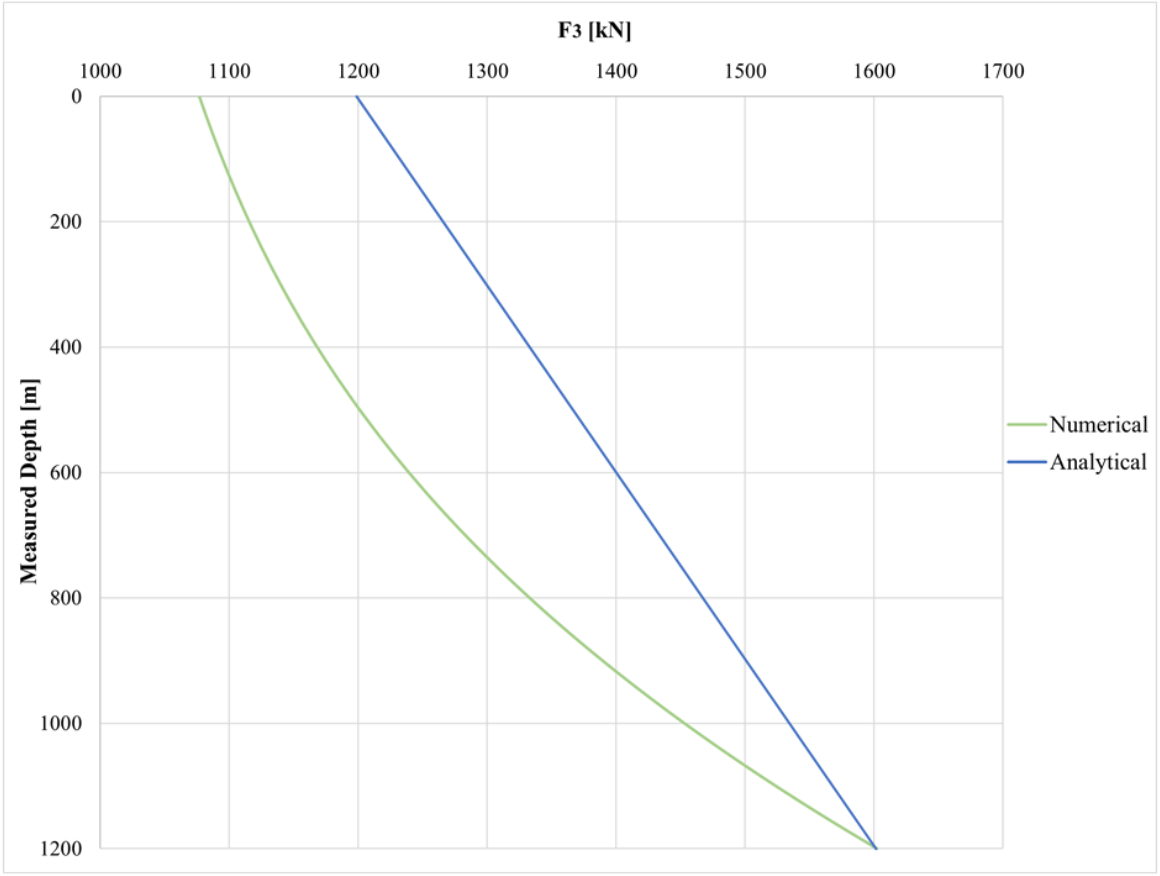

Figure 23: *The difference between the numerical model and the analytical model capturing the decrease in the Capstan effect further up in the bend.*

4.3 Comparison of the Models - B&H Well Profile

A comparison of the analytical model and the numerical model for the B&H well profile will be presented in this chapter. The friction coefficients of 0,1 and 0,4 are used for a tripping out scenario and a tripping in scenario, and the only weight included in the calculations is the drill pipe.

The results of the comparison between the two models are illustrated in Figure 24. As one can see from Figure 24, the only place where the models start to differ from each other is within the bend section.

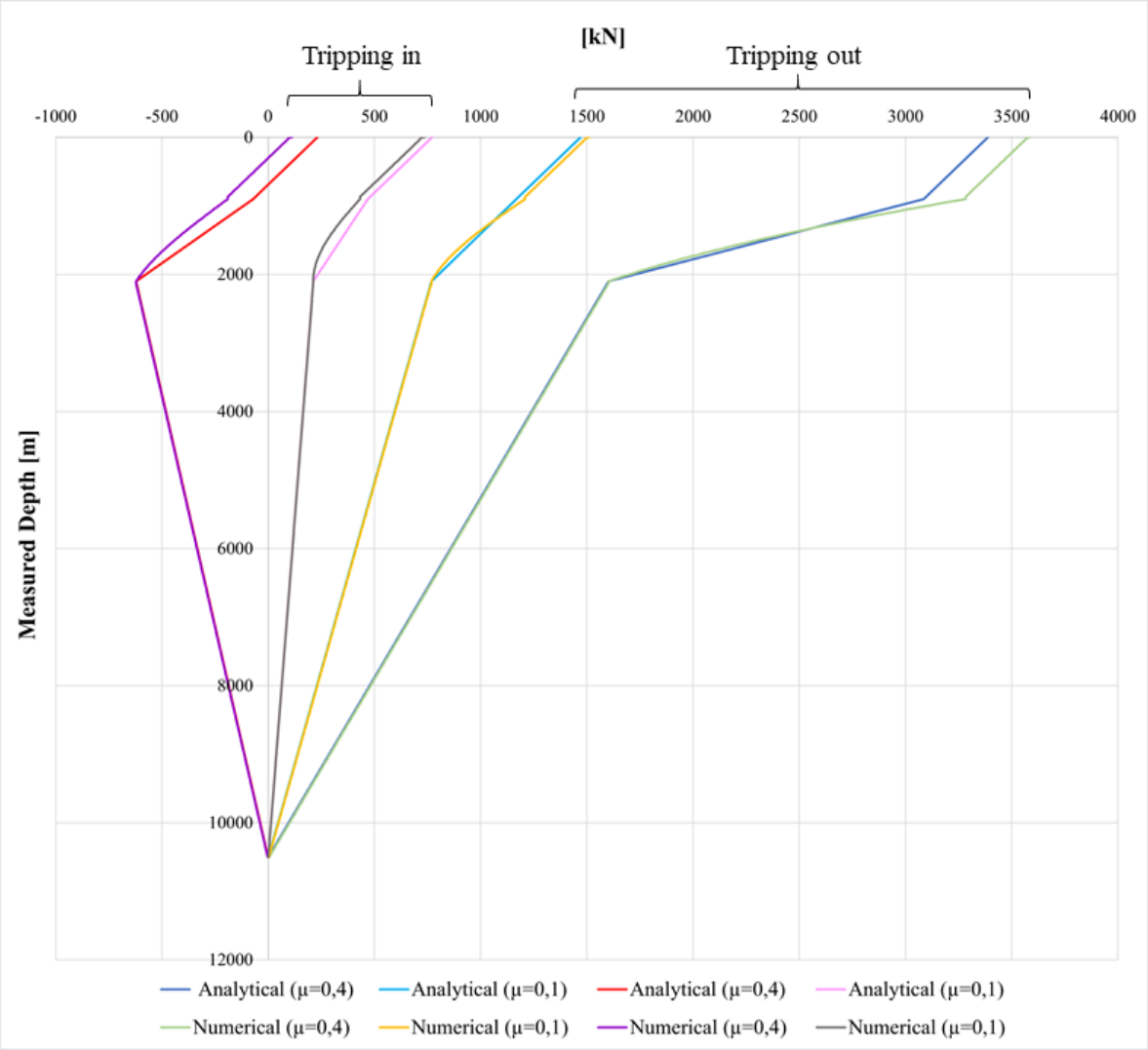

Figure 24: *Comparison of the analytical model and the numerical model for a tripping out scenario and a tripping in scenario when having friction coefficients of μ = 0,1 and μ = 0,4 for the B&H well profile.*

For the tripping out scenario the difference in top force between the analytical model and the numerical model is 4,3 tons when having a friction coefficient of $\mu = 0,1$. This is a difference of 2,8 %. For a tripping out scenario when the friction coefficient is $\mu = 0,4$ makes up a difference between the models of 20,2 tons. This is a difference of 5,8 %.
For the tripping in scenario the difference in top force between the models are 3,7 tons when the friction coefficient is $\mu = 0,1$. This is a difference of 4,8 %. When the friction coefficient is $\mu = 0,4$, the difference between the models for a tripping in scenario is 12,2 tons. This makes a difference of 51,6 %.

4.4 Comparison of the Models – S-Profile

A comparison of the analytical model and the numerical model for the S-profile will be presented in this chapter. The friction coefficients of 0,1 and 0,4 and only the weight of the drill pipe is used for a tripping out scenario and a tripping in scenario.

The results of the two models are illustrated in Figure 25. From Figure 25 it is possible to see that the models start to differ from each other at the drop section. This discrepancy between the models starting in the drop section affects the overall top force. The top force will be especially affected in this well profile since there are two bends.

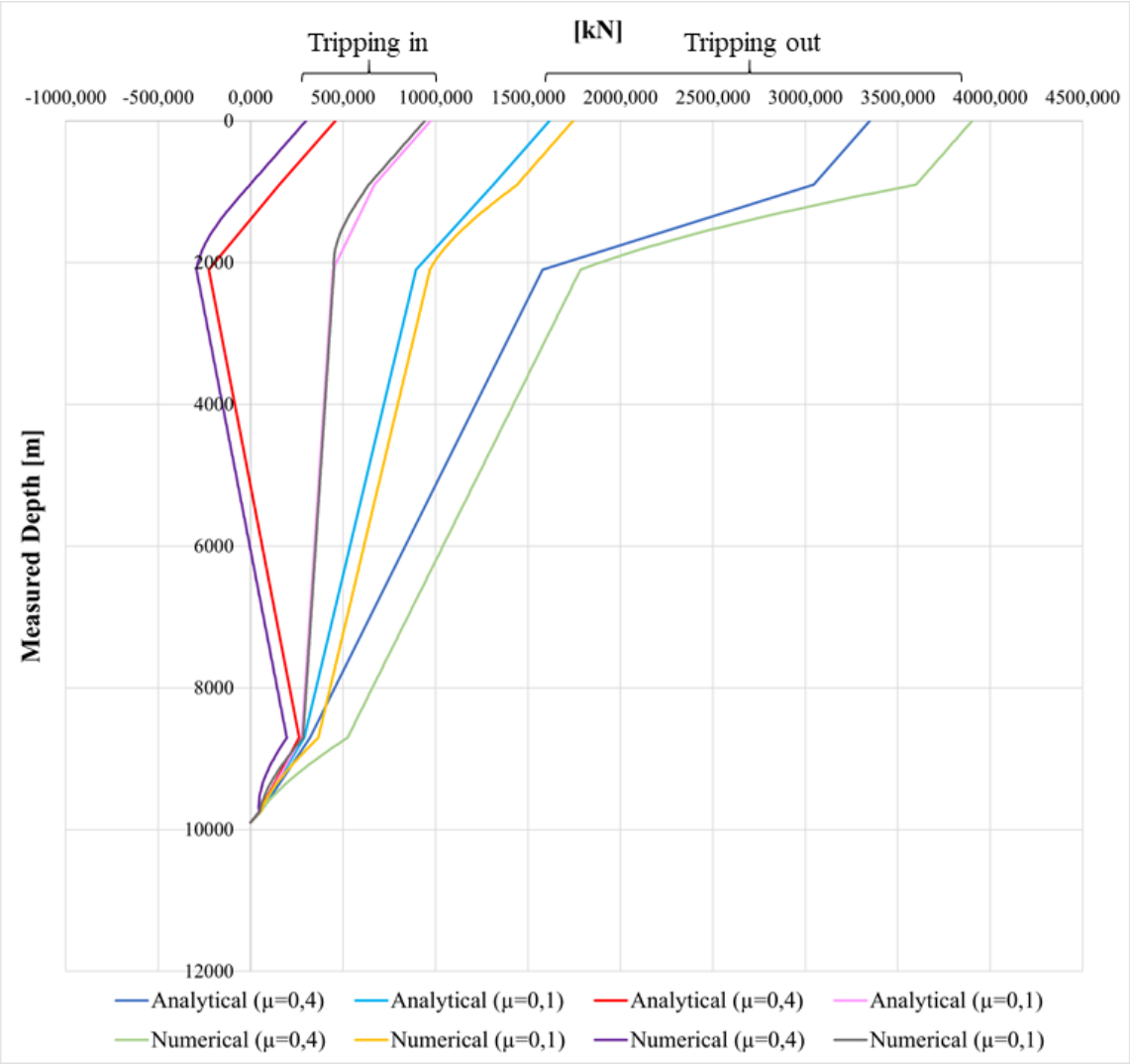

Figure 25: *Comparison of the analytical model and the numerical model for a tripping out scenario and a tripping in scenario when having friction coefficients of μ = 0,1 and μ = 0,4 for the S-profile.*

For the tripping out scenario, the difference in top force between the two models is 13 tons when having a friction coefficient of μ = 0,1. This is a difference between the models of 7,9 %. For a tripping out scenario when the friction coefficient is μ = 0,4, the difference in top force is 56,4 tons. This is a difference of 16,5 %.

For the tripping in scenario the difference in top force between the models is 3,2 tons when the friction coefficient is μ = 0,1. This is a difference of 3,2 %. When the friction coefficient is μ = 0,4, the difference in top force between the models is around 16,2 tons. This is a difference of 34,6 %.

The S-profile will have more well friction than the B&H well profile as the S-profile has two bends (drop bend and build-up bend). The difference between the models is much smaller than what the changes in friction coefficients will constitute. The friction coefficient is, as mentioned before, not a known parameter. The friction coefficient is uncertain and is a typical calibration factor.

5 Conclusion

In this thesis, an analytical model has been compared with a numerical model for drag prediction, where the focus has been on the bend section by looking at varying friction coefficients. For the analytical model, the minimum curvature method is recommended since this method is the most used in the industry today due to its high accuracy.

The analytical model and the numerical model calculate equally on straight inclined sections and vertical sections. The main difference between the models is that both models include the Capstan effect in a bend section, but it is only the numerical model that considers the friction caused by the weight component acting perpendicular to the pipe axis. The Capstan effect impacts the top force as the Capstan effect increases further up in the bend as the bottom force increases. The differences between the analytical model and the numerical model increase as the friction coefficient increases, since a higher friction coefficient increases the friction force.

The friction coefficient is a calibration factor and not a known parameter. The differences between the models are higher when having a higher friction coefficient. The friction term will be less important the smaller the coefficient of friction. In terms of well planning, the quality of the model will count, but it is probably the chosen friction coefficient that matters the most.

The numerical model gives a slightly more conservative result than the analytical model. This is especially for the tripping out scenario, which is the worst case in terms of tearing of pipe. Safety factors are added to find a strong enough drill string. So, the question is whether these differences in the models mean so much when one looks at the safety measures that are in the picture.

The analytical model is easier to use and can be easily set up in a spreadsheet. The numerical model is more complicated and requires programming competence.

References

[1] M. Fazaelizadeh, G. Hareland, and B. Aadnoy, 'Application of New 3-D Analytical Model for Directional Wellbore Friction', *MAS*, vol. 4, no. 2, Jan. 2010, doi: 10.5539/mas.v4n2p2.

[2] A. A. Elgibaly, M. S. Farhat, E. W. Trant, and M. Kelany, 'A study of friction factor model for directional wells', *Egyptian Journal of Petroleum*, vol. 26, no. 2, pp. 489–504, Jun. 2017, doi: 10.1016/j.ejpe.2016.07.004.

[3] B. S. Aadnoy, M. Fazaelizadeh, and G. Hareland, 'A 3D Analytical Model for Wellbore Friction', *Journal of Canadian Petroleum Technology*, vol. 49, no. 10, pp. 25–36, Oct. 2010, doi: 10.2118/141515-PA.

[4] C. A. Johancsik, D. B. Friesen, and R. Dawson, 'Torque and Drag in Directional Wells-Prediction and Measurement', *Journal of Petroleum Technology*, vol. 36, no. 06, pp. 987–992, Jun. 1984, doi: 10.2118/11380-PA.

[5] B. S. Aadnoy and K. Andersen, 'Design of oil wells using analytical friction models', *Journal of Petroleum Science and Engineering*, vol. 32, no. 1, pp. 53–71, Dec. 2001, doi: 10.1016/S0920-4105(01)00147-4.

[6] R. F. Mitchell and S. Z. Miska, Eds., 'Directional Drilling', in *Fundamentals of Drilling Engineering*, vol. 12, Richardson, UNITED STATES: Society of Petroleum Engineers, 2010, pp. 449–584. [Online]. Available: http://ebookcentral.proquest.com/lib/uisbib/detail.action?docID=3404993

[7] T. A. Inglis, 'Introduction', in *Directional Drilling*, vol. 2, Dordrecht: Springer Netherlands, 1987, pp. 1–4. doi: 10.1007/978-94-017-1270-5_1.

[8] T. A. Inglis, 'Applications of Directional Drilling', in *Directional Drilling*, vol. 2, Dordrecht: Springer Netherlands, 1987, pp. 5–12. doi: 10.1007/978-94-017-1270-5_2.

[9] S. A. Mirhaj, M. Fazaelizadeh, E. Kaarstad, and B. S. Aadnoy, 'New Aspects of Torque-and-Drag Modeling in Extended-Reach Wells', presented at the SPE Annual Technical Conference and Exhibition, Florence, Italy, Sep. 2010. doi: 10.2118/135719-MS.

[10] P. D. Szymczak, 'Extended-Reach Drilling Hits Mainstream To Squeeze Difficult Reservoirs', *JPT*, Aug. 01, 2021. https://jpt.spe.org/extended-reach-drilling-hits-mainstream-to-squeeze-difficult-reservoirs (accessed Jan. 20, 2022).

[11] R. F. Mitchell, Ed., 'Directional Drilling', in *Petroleum Engineering Handbook: Drilling Engineering*, Richardson, UNITED STATES: Society of Petroleum Engineers, 2006,

pp. 274–295. [Online]. Available: https://ebookcentral-proquest-com.ezproxy.uis.no/lib/uisbib/detail.action?docID=3405012

[12] M. Mims and T. Krepp, 'What is extended reach drilling', in *Drilling Design and Implementation for Extended Reach and Complex Wells*, 3rd ed., Houston, Texas: K & M Technology Group, 2002, pp. 14–17. [Online]. Available: https://dokumen.tips/documents/km-erd-textbook-3rd-edition.html

[13] T. A. Inglis, 'Directional Well Planning', in *Directional Drilling*, Dordrecht: Springer Netherlands, 1987, pp. 40–62. doi: 10.1007/978-94-017-1270-5_4.

[14] B. S. Aadnoy, 'Drilling operations and well', in *Modern Well Design: Second Edition*, Boca Raton, UNITED KINGDOM: Taylor & Francis Group, 2010, pp. 235–270. Accessed: Feb. 07, 2022. [Online]. Available: http://ebookcentral.proquest.com/lib/uisbib/detail.action?docID=1446872

[15] T. Eren and V. S. Suicmez, 'Directional drilling positioning calculations', *Journal of Natural Gas Science and Engineering*, vol. 73, p. 103081, Jan. 2020, doi: 10.1016/j.jngse.2019.103081.

[16] E. L. Eriksen, 'The Well Bore Trajectory - Position Calculations', in *Høgskolesenteret i Rogaland*, 1993, p. 16.

[17] T. A. Inglis, 'Survey Calculations', in *Directional Drilling*, Dordrecht: Springer Netherlands, 1987, pp. 155–171. doi: 10.1007/978-94-017-1270-5_9.

[18] K. Salminen, C. Cheatham, M. Smith, and K. Valiullin, 'Stuck-Pipe Prediction by Use of Automated Real-Time Modeling and Data Analysis', *SPE Drilling & Completion*, vol. 32, no. 03, pp. 184–193, Sep. 2017, doi: 10.2118/178888-PA.

[19] B. Foster, '"Roadmaps" improve extended reach well performance and decision making.', *World Oil*, vol. 225, no. 6, pp. 41–45, Jun. 2004. URL: https://search.ebscohost.com/login.aspx?direct=true&db=bth&AN=13505068&scope=site

[20] B. S. Aadnoy and E. Kaarstad, 'Theory and Application of Buoyancy in Wells', presented at the IADC/SPE Asia Pacific Drilling Technology Conference and Exhibition, Bangkok, Thailand, Nov. 2006, p. 10. doi: 10.2118/101795-MS.

[21] B. S. Aadnoy, K. Larsen, and P. C. Berg, 'Analysis of stuck pipe in deviated boreholes', *Journal of Petroleum Science and Engineering*, vol. 37, no. 3–4, pp. 195–212, Mar. 2003, doi: 10.1016/S0920-4105(02)00353-4.

[22] J. Moore and Contributors, 'Belt Friction', *Engineering-LibreTexts*, Jul. 28, 2021. https://eng.libretexts.org/@go/page/53833 (accessed Mar. 15, 2022).

[23] V. A. Lubarda, ‘The Mechanics of Belt Friction Revisited’, *International Journal of Mechanical Engineering Education*, vol. 42, no. 2, pp. 97–112, Apr. 2014, doi: 10.7227/IJMEE.0002.

[24] G. Gabolde and J. P. Nguyen, ‘Drill String Standards’, in *DDH: Drilling data handbook*, 9th edition., Paris: Editions TECHNIP, 2014, pp. B1–B67.

Appendix A

Appendix A.1 Numerical T&D Model

```
clear
clc

%%% T&D Numerical model based on Johancsik 1984 %%%

%%% This is an attempt to use the model proposed by Johansick et al
%%% to calculate the force on top of a bend. The bend cover 0 to 80 degrees.

% Define variables: %

MW = 1700;                                  % Density of mud [kg/m^3]
Rho_steel = 7850;                           % Density of drill pipe [kg/m^3]
W_drillstring = 43.73;                      % Weight of drill string, including
tooljoint [kg/m]
g = 9.81;                                   % Gravitational constant [m/s^2]
Cell_length = 30;                           % Cell length in discretization [m]
DLS = 2/30;                                 % Dogleg severity [degree/m]
Dogleg = 80;                                % Degrees of bend [degree]
KOP = 900;                                  % Length of vertical section down to
KOP [m]
EOB = Dogleg/DLS;                           % Length of build-up bend section [m]
Total_MD = EOB;                             % Total measured depth of bend section
[m]
Mu = 0.4;                                   % Friction coefficient

% Calculate Buoyancy factor: %
BF = 1 - (MW/Rho_steel);                    % Buoyancy factor

% Divide the well into cells: %
Number_cells = Total_MD/Cell_length;        % Number of cells
Number_points = Number_cells+1;             % Number of survey points


% Fill up tables with inclination and measured depth: %
Inclination(1) = 0;
MD(1) = 0;

for i = 2:Number_points
  Inclination_increase = Cell_length*DLS;                   % Inclination increase
  Inclination(i) = Inclination(i-1) + Inclination_increase; % Inclination
  MD(i)= MD(i-1) + Cell_length;                             % Measured depth from
1 to top, increasing with one cell length at a time
end


% Calculation of axial forces from bottom and upwards: %
% Tripping out (F1), Tripping in (F2) and static (F3) %

F1(Number_points) = 0;
F2(Number_points) = 0;
F3(Number_points) = 0;

for j = Number_points-1:-1:1
```

```
% Use cosd and sind because they work with input in degrees
   Average_inclination =0.5*(Inclination(j+1)+Inclination(j));
   Weight = W_drillstring*BF*g*Cell_length*cosd(Average_inclination);
   % Average angle method is used for TVD of the segment

   F_normal_1 =
W_drillstring*BF*g*Cell_length*sind(Average_inclination)+F1(j+1)*Inclination_incre
ase*pi/180;
   F_normal_2 =
W_drillstring*BF*g*Cell_length*sind(Average_inclination)+F2(j+1)*Inclination_incre
ase*pi/180;
   F_normal_3 =
W_drillstring*BF*g*Cell_length*sind(Average_inclination)+F3(j+1)*Inclination_incre
ase*pi/180;
   % The normal force has two components.
   % First term is due to weight and second due to tension effect (Capstan effect)

   F1(j) = Weight + F1(j+1) + Mu*F_normal_1;    % Tripping out (+)
   F2(j) = Weight + F2(j+1) - Mu*F_normal_2;    % Tripping in (-)
   F3(j) = Weight + F3(j+1);                    % Static (Rotating off bottom)

end


% Plot graph of the result: Tension (kN) VS Measured Depth %

plot(F1/1000,MD,F2/1000,MD,F3/1000,MD)
set(gca,'ydir','reverse');
title('Johancsik Torque & Drag Model','color','#0072BD')
subtitle('Force on top off bend','color','#0072BD')
xlabel('Hook load [kN]','FontWeight','bold')
ylabel('Depth [m]','FontWeight','bold')
legend('Tripping Out','Tripping In','Rotating off
Bottom/Static','location','best')
grid on

% The top Force in kN is: %

Top_Force_Tripping_out = F1(1)/1000
Top_Force_Tripping_in = F2(1)/1000
Top_Force_Static = F3(1)/1000
```

Appendix B

Appendix B.1 Analytical Model for B&H Well Profile – Tripping out Scenario

DRILLSTRING CHARACTERISTICS:							
Nominal Diameter of Drillpipe	Nominal Unit Mass of Drillpipe	Grade	Type of Tooljoint	Appr. Unit Mass incl. Tooljoint	Nominal Diameter of HWDP	Connection HWDP	Nominal Unit Mass HWDP
(inch)	(lb/ft)	S-135	5 1/2 FH	(kg/m)	(inch)	NC50 (4 1/2 IF)	(kg/m)
5	25,6			43,73	5		73,4
	in air			*in air*			*in air*

Additional										
MW	ρ(steel)	g	Inclination	Build-up angle	Vertical length down to KOP	Build-up bend (ΔBC)	Lenght of Hold/sail section	Total length (MD)	Radius (R)	Length of HWDP
(kg/m^3)	(kg/m^3)	(m/s^2)	(degree)	(degree/m)	(m)	(m)	(m)	(m)	(m)	(m)
1700	7850	9,81	80	2/30	900	1200	8400	10 500	859,44	100
					MD & TVD	*MD*	*MD*			

Buoyancy Factor		
β	1 - (ρmud / ρsteel)	0,783

Buoyed Weight			
W(HWDP)	β * W(HWDP)	57,5	(kg/m)
W(drillpipe)	β * W(app.incl.tolljoint)	34,26	(kg/m)

Angles in Radians:	
0*(π/180) =	0
80*(π/180) =	1,3963

Ratio Factor:	
RF =	1,202

	Drag force calculations (Tripping out)				
$\mu = 0,1$	**Bottom hold section (F1)**	F1 =	0		N
	Top hold section (F2)	F2 = F1 + (W*L)*g*(cos α ± μ*sin α)			
		F2 = F1 + (W(drillpipe)*(L Hold-L HWDP)+W(HWDP)*L HWDP)*g*(cos(80)+0,1*sin(80))			
		F2 =	774464,9		N
	Top build-up section (F3)	F3 = F2*(e^(±0,1*(80*(π/180))-1)+F2+W*g*0,5*L*(cos(α1)+cos(α2))*RF			
		F3 = F2*(e^(+0,1*(80*(π/180))-1)+F2+W(drillpipe)*g*0,5*ΔBC*(cos(0)+cos(80))*RF			
		F3 =	1174972,7		N
	Top Well (F4)	F4 = F3 + W*L*g			
		F4 = F3 + (W(drillpipe)*L vertical)*g			
		F4 =	1477452,5		N
$\mu = 0,15$	**Bottom hold section (F1)**	F1 =	0		N
	Top hold section (F2)	F2 = F1 + (W*L)*g*(cos α ± μ*sin α)			
		F2 = F1 + (W(drillpipe)*(L Hold-L HWDP)+W(HWDP)*L HWDP)*g*(cos(80)+0,15*sin(80))			
		F2 =	914600,5		N
	Top build-up section (F3)	F3 = F2*(e^(±0,15*(80*(π/180))-1)+F2+W*g*0,5*L*(cos(α1)+cos(α2))*RF			
		F3 = F2*(e^(+0,15*(80*(π/180))-1)+F2+W(drillpipe)*g*0,5*ΔBC*(cos(0)+cos(80))*RF			
		F3 =	1412149,1		N
	Top Well (F4)	F4 = F3 + W*L*g			
		F4 = F3 + (W(drillpipe)*L vertical)*g			
		F4 =	1714629,0		N
$\mu = 0,2$	**Bottom hold section (F1)**	F1 =	0		N
	Top hold section (F2)	F2 = F1 + (W*L)*g*(cos α ± μ*sin α)			
		F2 = F1 + (W(drillpipe)*(L Hold-L HWDP)+W(HWDP)*L HWDP)*g*(cos(80)+0,2*sin(80))			
		F2 =	1054736,1		N
	Top build-up section (F3)	F3 = F2*(e^(±0,2*(80*(π/180))-1)+F2+W*g*0,5*L*(cos(α1)+cos(α2))*RF			
		F3 = F2*(e^(+0,2*(80*(π/180))-1)+F2+W(drillpipe)*g*0,5*ΔBC*(cos(0)+cos(80))*RF			
		F3 =	1678969,0		N
	Top Well (F4)	F4 = F3 + W*L*g			
		F4 = F3 + (W(drillpipe)*L vertical)*g			
		F4 =	1981448,9		N
$\mu = 0,25$	**Bottom hold section (F1)**	F1 =	0		N
	Top hold section (F2)	F2 = F1 + (W*L)*g*(cos α ± μ*sin α)			
		F2 = F1 + (W(drillpipe)*(L Hold-L HWDP)+W(HWDP)*L HWDP)*g*(cos(80)+0,25*sin(80))			
		F2 =	1194871,7		N
	Top build-up section (F3)	F3 = F2*(e^(±0,25*(80*(π/180))-1)+F2+W*g*0,5*L*(cos(α1)+cos(α2))*RF			
		F3 = F2*(e^(+0,25*(80*(π/180))-1)+F2+W(drillpipe)*g*0,5*ΔBC*(cos(0)+cos(80))*RF			
		F3 =	1978479,2		N
	Top Well (F4)	F4 = F3 + W*L*g			
		F4 = F3 + (W(drillpipe)*L vertical)*g			
		F4 =	2280959,1		N
$\mu = 0,3$	**Bottom hold section (F1)**	F1 =	0		N
	Top hold section (F2)	F2 = F1 + (W*L)*g*(cos α ± μ*sin α)			
		F2 = F1 + (W(drillpipe)*(L Hold-L HWDP)+W(HWDP)*L HWDP)*g*(cos(80)+0,3*sin(80))			
		F2 =	1335007,3		N
	Top build-up section (F3)	F3 = F2*(e^(±0,3*(80*(π/180))-1)+F2+W*g*0,5*L*(cos(α1)+cos(α2))*RF			
		F3 = F2*(e^(+0,3*(80*(π/180))-1)+F2+W(drillpipe)*g*0,5*ΔBC*(cos(0)+cos(80))*RF			
		F3 =	2314012,2		N
	Top Well (F4)	F4 = F3 + W*L*g			
		F4 = F3 + (W(drillpipe)*L vertical)*g			
		F4 =	2616492,1		N

μ = 0,35	**Bottom hold section (F1)**	F1 =	0		N
	Top hold section (F2)	F2 = F1 + (W*L)*g*(cos α ± μ*sin α)			
		F2 = F1 + (W(drillpipe)*(L Hold-L HWDP)+W(HWDP)*L HWDP)*g*(cos(80)+0,35*sin(80))			
		F2 =	1475142,9		N
	Top build-up section (F3)	F3 = F2*(e^(±0,35*(80*(π/180))-1)+F2+W*g*0,5*L*(cos(α1)+cos(α2))*RF			
		F3 = F2*(e^(+0,35*(80*(π/180))-1)+F2+W(drillpipe)*g*0,5*ΔBC*(cos(0)+cos(80))*RF			
		F3 =	2689211,4		N
	Top Well (F4)	F4 = F3 + W*L*g			
		F4 = F3 + (W(drillpipe)*L vertical)*g			
		F4 =	2991691,3		N
μ = 0,4	**Bottom hold section (F1)**	F1 =	0		N
	Top hold section (F2)	F2 = F1 + (W*L)*g*(cos α ± μ*sin α)			
		F2 = F1 + (W(drillpipe)*(L Hold-L HWDP)+W(HWDP)*L HWDP)*g*(cos(80)+0,4*sin(80))			
		F2 =	1615278,5		N
	Top build-up section (F3)	F3 = F2*(e^(±0,4*(80*(π/180))-1)+F2+W*g*0,5*L*(cos(α1)+cos(α2))*RF			
		F3 = F2*(e^(+0,4*(80*(π/180))-1)+F2+W(drillpipe)*g*0,5*ΔBC*(cos(0)+cos(80))*RF			
		F3 =	3108059,0		N
	Top Well (F4)	F4 = F3 + W*L*g			
		F4 = F3 + (W(drillpipe)*L vertical)*g			
		F4 =	3410538,9		N

Appendix B.2 Analytical Model for B&H Well Profile – Tripping in Scenario

DRILLSTRING CHARACTERISTICS:							
Nominal Diameter of Drillpipe	Nominal Unit Mass of Drillpipe	Grade	Type of Tooljoint	Appr. Unit Mass incl. Tooljoint	Nominal Diameter of HWDP	Connection HWDP	Nominal Unit Mass HWDP
(inch)	(lb/ft)	S-135	5 1/2 FH	(kg/m)	(inch)	NC50 (4 1/2 IF)	(kg/m)
5	25,6			43,73	5		73,4
	in air			*in air*			*in air*

Additional										
MW	ρ(steel)	g	Inclination	Build-up angle	Vertical length down to KOP	Build-up bend (ΔBC)	Lenght of Hold/sail section	Total length (MD)	Radius (R)	Length of HWDP
(kg/m^3)	(kg/m^3)	(m/s^2)	(degree)	(degree/m)	(m)	(m)	(m)	(m)	(m)	(m)
1700	7850	9,81	80	2/30	900	1200	8400	10 500	859,44	100
					MD & TVD	*MD*	*MD*			

Buoyancy Factor		
β	1 - (ρmud / ρsteel)	0,783

Buoyed Weight			
W(HWDP)	β * W(HWDP)	57,5	(kg/m)
W(drillpipe)	β * W(app.incl.tolljoint)	34,26	(kg/m)

Angles in Radians:	
0*(π/180) =	0
80*(π/180) =	1,3963

Weight of Topdrive		
W(Top Drive)	25	tons
	25000	kg
	245250	N

Ratio Factor:	
RF =	1,202

	Drag force calculations (Tripping in)				
μ = 0,1	**Bottom hold section (F1)**	F1 =	0		N
	Top hold section (F2)	F2 = F1 + (W*L)*g*(cos α ± μ*sin α)			
		F2 = F1 + (W(drillpipe)*(L Hold-L HWDP)+W(HWDP)*L HWDP)*g*(cos(80)-0,1*sin(80))			
		F2 =	213922,5		N
	Top build-up section (F3)	F3 = F2*(e^(±0,1∗(80*(π/180))-1)+F2+W*g*0,5*L*(cos(α1)+cos(α2))*RF			
		F3 = F2*(e^(-0,1∗(80*(π/180))-1)+F2+W(drillpipe)*g*0,5*ΔBC*(cos(0)+cos(80))*RF			
		F3 =	470503,6		N
	Top Well (F4)	F4 = F3 + W*L*g			
		F4 = F3 + (W(drillpipe)*L vertical)*g			
		F4 =	772983,4		N
μ = 0,15	**Bottom hold section (F1)**	F1 =	0		N
	Top hold section (F2)	F2 = F1 + (W*L)*g*(cos α ± μ*sin α)			
		F2 = F1 + (W(drillpipe)*(L Hold-L HWDP)+W(HWDP))*L HWDP)*g*(cos(80)-0,15*sin(80))			
		F2 =	73786,9		N
	Top build-up section (F3)	F3 = F2*(e^(±0,15∗(80*(π/180))-1)+F2+W*g*0,5*L*(cos(α1)+cos(α2))*RF			
		F3 = F2*(e^(-0,15∗(80*(π/180))-1)+F2+W(drillpipe)*g*0,5*ΔBC*(cos(0)+cos(80))*RF			
		F3 =	344302,8		N
	Top Well (F4)	F4 = F3 + W*L*g			
		F4 = F3 + (W(drillpipe)*L vertical)*g			
		F4 =	646782,7		N
μ = 0,2	**Bottom hold section (F1)**	F1 =	0		N
	Top hold section (F2)	F2 = F1 + (W*L)*g*(cos α ± μ*sin α)			
		F2 = F1 + (W(drillpipe)*(L Hold-L HWDP)+W(HWDP)*L HWDP)*g*(cos(80)-0,2*sin(80))			
		F2 =	-66348,7		N
	Top build-up section (F3)	F3 = F2*(e^(±0,2∗(80*(π/180))-1)+F2+W*g*0,5*L*(cos(α1)+cos(α2))*RF			
		F3 = F2*(e^(-0,2∗(80*(π/180))-1)+F2+W(drillpipe)*g*0,5*ΔBC*(cos(0)+cos(80))*RF			
		F3 =	234276,0		N
	Top Well (F4)	F4 = F3 + W*L*g			
		F4 = F3 + (W(drillpipe)*L vertical)*g			
		F4 =	536755,9		N
μ = 0,25	**Bottom hold section (F1)**	F1 =	0		N
	Top hold section (F2)	F2 = F1 + (W*L)*g*(cos α ± μ*sin α)			
		F2 = F1 + (W(drillpipe)*(L Hold-L HWDP)+W(HWDP)*L HWDP)*g*(cos(80)-0,25*sin(80))			
		F2 =	-206484,3		N
	Top build-up section (F3)	F3 = F2*(e^(±0,25∗(80*(π/180))-1)+F2+W*g*0,5*L*(cos(α1)+cos(α2))*RF			
		F3 = F2*(e^(-0,25∗(80*(π/180))-1)+F2+W(drillpipe)*g*0,5*ΔBC*(cos(0)+cos(80))*RF			
		F3 =	138815,8		N
	Top Well (F4)	F4 = F3 + W*L*g			
		F4 = F3 + (W(drillpipe)*L vertical)*g			
		F4 =	441295,6		N
μ = 0,3	**Bottom hold section (F1)**	F1 =	0		N
	Top hold section (F2)	F2 = F1 + (W*L)*g*(cos α ± μ*sin α)			
		F2 = F1 + (W(drillpipe)*(L Hold-L HWDP)+W(HWDP)*L HWDP)*g*(cos(80)-0,3*sin(80))			
		F2 =	-346619,8		N
	Top build-up section (F3)	F3 = F2*(e^(±0,3∗(80*(π/180))-1)+F2+W*g*0,5*L*(cos(α1)+cos(α2))*RF			
		F3 = F2*(e^(-0,3∗(80*(π/180))-1)+F2+W(drillpipe)*g*0,5*ΔBC*(cos(0)+cos(80))*RF			
		F3 =	56457,8		N
	Top Well (F4)	F4 = F3 + W*L*g			
		F4 = F3 + (W(drillpipe)*L vertical)*g			
		F4 =	358937,7		N

μ = 0,35	**Bottom hold section (F1)**	F1 =	0		N
	Top hold section (F2)	F2 = F1 + (W*L)*g*(cos α ± μ*sin α)			
		F2 = F1 + (W(drillpipe)*(L Hold-L HWDP)+W(HWDP)*L HWDP)*g*(cos(80)-0,35*sin(80))			
		F2 =	-486755,4		N
	Top build-up section (F3)	F3 = F2*(e^(±0,35∗(80*(π/180))-1)+F2+W*g*0,5*L*(cos(α1)+cos(α2))*RF			
		F3 = F2*(e^(-0,35∗(80*(π/180))-1)+F2+W(drillpipe)*g*0,5*ΔBC*(cos(0)+cos(80))*RF			
		F3 =	-14130,7		N
	Top Well (F4)	F4 = F3 + W*L*g			
		F4 = F3 + (W(drillpipe)*L vertical)*g			
		F4 =	288349,1		N
μ = 0,4	**Bottom hold section (F1)**	F1 =	0		N
	Top hold section (F2)	F2 = F1 + (W*L)*g*(cos α ± μ*sin α)			
		F2 = F1 + (W(drillpipe)*(L Hold-L HWDP)+W(HWDP)*L HWDP)*g*(cos(80)-0,4*sin(80))			
		F2 =	-626891,0		N
	Top build-up section (F3)	F3 = F2*(e^(±0,4∗(80*(π/180))-1)+F2+W*g*0,5*L*(cos(α1)+cos(α2))*RF			
		F3 = F2*(e^(-0,4∗(80*(π/180))-1)+F2+W(drillpipe)*g*0,5*ΔBC*(cos(0)+cos(80))*RF			
		F3 =	-74162,7		N
	Top Well (F4)	F4 = F3 + W*L*g			
		F4 = F3 + (W(drillpipe)*L vertical)*g			
		F4 =	228317,1		N

Drag Forces inluding Topdrive

μ = 0,1	**Top Vertical section incl. Topdrive**	F5 = F4 + W(topdrive)		
		F5 =	1018233,4	kN
μ = 0,15	**Top Vertical section incl. Topdrive**	F5 = F4 + W(topdrive)		
		F5 =	892032,7	kN
μ = 0,2	**Top Vertical section incl. Topdrive**	F5 = F4 + W(topdrive)		
		F5 =	782005,9	kN
μ = 0,25	**Top Vertical section incl. Topdrive**	F5 = F4 + W(topdrive)		
		F5 =	686545,6	kN
μ = 0,3	**Top Vertical section incl. Topdrive**	F5 = F4 + W(topdrive)		
		F5 =	604187,7	kN
μ = 0,35	**Top Vertical section incl. Topdrive**	F5 = F4 + W(topdrive)		
		F5 =	533599,1	kN
μ = 0,4	**Top Vertical section incl. Topdrive**	F5 = F4 + W(topdrive)		
		F5 =	473567,1	kN

Appendix B.3 Analytical Model for B&H Well Profile – Static (Rotating off Bottom) Scenario

DRILLSTRING CHARACTERISTICS:							
Nominal Diameter of Drillpipe	Nominal Unit Mass of Drillpipe	Grade	Type of Tooljoint	Appr. Unit Mass incl. Tooljoint	Nominal Diameter of HWDP	Connection HWDP	Nominal Unit Mass HWDP
(inch)	(lb/ft)	S-135	5 1/2 FH	(kg/m)	(inch)	NC50 (4 1/2 IF)	(kg/m)
5	25,6			43,73	5		73,4
	in air			*in air*			*in air*

Additional										
MW	ρ(steel)	g	Inclination	Build-up angle	Vertical length down to KOP	Build-up bend (ΔBC)	Lenght of Hold/sail section	Total length (MD)	Radius (R)	Length of HWDP
(kg/m^3)	(kg/m^3)	(m/s^2)	(degree)	(degree/m)	(m)	(m)	(m)	(m)	(m)	(m)
1700	7850	9,81	80	2/30	900	1200	8400	10 500	859,44	100
					MD & TVD	*MD*	*MD*			

Additional		
ΔL Build section	ΔL Hold section	ΔL HWDP
(m)	(m)	(m)
846,4	1458,6	17,4
TVD	*TVD*	*TVD*

Buoyancy Factor		
β	1 - (ρmud / ρsteel)	0,783

Buoyed Weight			
W(HWDP)	β * W(HWDP)	57,5	(kg/m)
W(drillpipe)	β * W(app.incl.tolljoint)	34,26	(kg/m)

Angles in Radians:	
0*(π/180) =	0
80*(π/180) =	1,3963

Ratio Factor:	
RF =	1,202

	Drag force calculations (Static (rotating off bottom))				
μ = 0,1-0,4	**Bottom hold section (F1)**	F1 =	0		N
	Top hold section (F2)	F2 = F1 + (W*L)*g			
		F2 = F1 + (W(drillpipe)*(ΔL Hold-ΔL HWDP)+W(HWDP)*ΔL HWDP)*g			
		F2 =	494193,7		N
	Top build-up section (F3)	F3 = F2 + (W*L)*g			
		F3 = F2 + (W(drillpipe)*ΔL build)*g			
		F3 =	778652,5		N
	Top Well (F4)	F4 = F3 + (W*L)*g			
		F4 = F3 + (W(drillpipe)*L)*g			
		F4 =	1081132,3		N

Appendix B.4 Analytical Model for S-Profile – Tripping out Scenario

DRILLSTRING CHARACTERISTICS:									
Nominal Diameter of Drillpipe	Nominal Unit Mass of Drillpipe	Grade	Type of Tooljoint	Appr. Unit Mass incl. Tooljoint	Nominal Diameter of HWDP	Connection HWDP	Nominal Unit Mass HWDP	Drill Collar (OD & ID)	Nominal unit mass of Drill Collar
(inch)	(lb/ft)	S-135	5 1/2 FH	(kg/m)	(inch)	NC50 (4 1/2 IF)	(kg/m)	(inch)	(kg/m)
5	25,6			43,73	5		73,4	8 x 3	218,77
	in air			*in air*			*in air*		*in air*

Additional														
MW	ρ(steel)	g	Inclination 1	Build-up angle	Vertical length down to KOP	Build-up bend (ΔBC)	Lenght of Hold/sail section	Drop bend (ΔDT)	Inclined section to target	Total length (MD)	Radius (R)	Length of HWDP	Length of DC	Inclination 2
(kg/m^3)	(kg/m^3)	(m/s^2)	(degree)	(degree/m)	(m)	(m)	(m)	(m)	(m)	(m)	(m)	(m)	(m)	(degree)
1700	7850	9,81	80	2/30	900	1200	6600	1050	150	9 900	859,44	90	30	70
					MD & TVD	*MD*	*MD*							

Buoyancy Factor		
β	1 - (ρmud / ρsteel)	0,783

Buoyed Weight			
W(HWDP)	β * W(HWDP)	57,5	(kg/m)
W(drillpipe)	β * W(app.incl.tolljoint)	34,26	(kg/m)
W(DC)	β * W(DC)	171,4	(kg/m)

Angles in Radians:	
0*(π/180) =	0
10*(π/180) =	0,1745
70*(π/180) =	1,2217
80*(π/180) =	1,3963

Ratio Factor:	
RF = (80°)	1,202
RF = (70°)	1,146

	Drag force calculations (Tripping out)				
μ = 0,1	**Bottom inclined section (F1)**	F1 =	0		N
	Top inclined section (F2)	F2 = F1 + (W*L)*g*(cos α ± μ*sin α)			
		F2 = F1 + (W(drillpipe)*(L Inc-(L HWDP+L DC))+(W(HWDP)*L HWDP)+(W(DC)*L DC))*g*(cos(10)+0,1*sin(10)			
		F2 =	111536,1		N
	Top drop section (F3)	F3 = F2*(e^(±0,1*(70*(π/180))-1)+F2+W*g*0,5*L*(cos(α1)+cos(α2))*RF			
		F3 = F2*(e^(+0,1*(70*(π/180))-1)+F2+W(drillpipe)*g*0,5*ΔDT*(cos(80)+cos(10))*RF			
		F3 =	360331,2		N
	Top hold section (F4)	F4 = F3 + (W*L)*g*(cos α ± μ*sin α)			
		F4 = F3 + (W(drillpipe)*L hold)*g*(cos(80)+0,1*sin(80))			
		F4 =	963963,7		N
	Top build-up section (F5)	F5 = F4*(e^(±0,1*(80*(π/180))-1)+F4+W*g*0,5*L*(cos(α1)+cos(α2))*RF			
		F5 = F4*(e^(+0,1*(80*(π/180))-1)+F4+W(drillpipe)*g*0,5*ΔBC*(cos(80)+cos(0))*RF			
		F5 =	1392866,7		N
	Top Well (F6)	F6 = F5 + W*L*g			
		F6 = F5 + (W(drillpipe)*L vertical)*g			
		F6 =	1695346,6		N
μ = 0,15	**Bottom inclined section (F1)**	F1 =	0		N
	Top inclined section (F2)	F2 = F1 + (W*L)*g*(cos α ± μ*sin α)			
		2 = F1 + (W(drillpipe)*(L Inc-(L HWDP+L DC))+(W(HWDP)*L HWDP)+(W(DC)*L DC))*g*(cos(10)+0,15*sin(10			
		F2 =	112502,4		N
	Top drop section (F3)	F3 = F2*(e^(±0,15*(70*(π/180))-1)+F2+W*g*0,5*L*(cos(α1)+cos(α2))*RF			
		F3 = F2*(e^(+0,15*(70*(π/180))-1)+F2+W(drillpipe)*g*0,5*ΔDT*(cos(80)+cos(10))*RF			
		F3 =	369430,6		N
	Top hold section (F4)	F4 = F3 + (W*L)*g*(cos α ± μ*sin α)			
		F4 = F3 + (W(drillpipe)*L hold)*g*(cos(80)+0,15*sin(80))			
		F4 =	1082287,4		N
	Top build-up section (F5)	F5 = F4*(e^(±0,15*(80*(π/180))-1)+F4+W*g*0,5*L*(cos(α1)+cos(α2))*RF			
		F5 = F4*(e^(+0,15*(80*(π/180))-1)+F4+W(drillpipe)*g*0,5*ΔBC*(cos(80)+cos(0))*RF			
		F5 =	1618904,9		N
	Top Well (F6)	F6 = F5 + W*L*g			
		F6 = F5 + (W(drillpipe)*L vertical)*g			
		F6 =	1921384,7		N

μ = 0,2	**Bottom inclined section (F1)**	F1 =	0		N
	Top inclined section (F2)	F2 = F1 + (W*L)*g*(cos α ± μ*sin α)			
		F2 = F1 + (W(drillpipe)*(L Inc-(L HWDP+L DC))+(W(HWDP)*L HWDP)+(W(DC)*L DC))*g*(cos(10)+0,2*sin(10)			
		F2 =	113468,7		N
	Top drop section (F3)	F3 = F2*(e^(±0,2∗(70*(π/180))-1)+F2+W*g*0,5*L*(cos(α1)+cos(α2))*RF			
		F3 = F2*(e^(+0,2∗(70*(π/180))-1)+F2+W(drillpipe)*g*0,5*ΔDT*(cos(80)+cos(10))*RF			
		F3 =	379176,3		N
	Top hold section (F4)	F4 = F3 + (W*L)*g*(cos α ± μ*sin α)			
		F4 = F3 + (W(drillpipe)*L hold)*g*(cos(80)+0,2*sin(80))			
		F4 =	1201257,5		N
	Top build-up section (F5)	F5 = F4*(e^(±0,2∗(80*(π/180))-1)+F4+W*g*0,5*L*(cos(α1)+cos(α2))*RF			
		F5 = F4*(e^(+0,2∗(80*(π/180))-1)+F4+W(drillpipe)*g*0,5*ΔBC*(cos(80)+cos(0))*RF			
		F5 =	1872690,9		N
	Top Well (F6)	F6 = F5 + W*L*g			
		F6 = F5 + (W(drillpipe)*L vertical)*g			
		F6 =	2175170,8		N

μ = 0,25	**Bottom inclined section (F1)**	F1 =	0		N
	Top inclined section (F2)	F2 = F1 + (W*L)*g*(cos α ± μ*sin α)			
		2 = F1 + (W(drillpipe)*(L Inc-(L HWDP+L DC))+(W(HWDP)*L HWDP)+(W(DC)*L DC))*g*(cos(10)+0,25*sin(10			
		F2 =	114435,0		N
	Top drop section (F3)	F3 = F2*(e^(±0,25∗(70*(π/180))-1)+F2+W*g*0,5*L*(cos(α1)+cos(α2))*RF			
		F3 = F2*(e^(+0,25∗(70*(π/180))-1)+F2+W(drillpipe)*g*0,5*ΔDT*(cos(80)+cos(10))*RF			
		F3 =	389613,6		N
	Top hold section (F4)	F4 = F3 + (W*L)*g*(cos α ± μ*sin α)			
		F4 = F3 + (W(drillpipe)*L hold)*g*(cos(80)+0,25*sin(80))			
		F4 =	1320919,1		N
	Top build-up section (F5)	F5 = F4*(e^(±0,25∗(80*(π/180))-1)+F4+W*g*0,5*L*(cos(α1)+cos(α2))*RF			
		F5 = F4*(e^(+0,25∗(80*(π/180))-1)+F4+W(drillpipe)*g*0,5*ΔBC*(cos(80)+cos(0))*RF			
		F5 =	2157181,9		N
	Top Well (F6)	F6 = F5 + W*L*g			
		F6 = F5 + (W(drillpipe)*L vertical)*g			
		F6 =	2459661,8		N

μ = 0,3	**Bottom inclined section (F1)**	F1 =	0		N
	Top inclined section (F2)	F2 = F1 + (W*L)*g*(cos α ± μ*sin α)			
		F2 = F1 + (W(drillpipe)*(L Inc-(L HWDP+L DC))+(W(HWDP)*L HWDP)+(W(DC)*L DC))*g*(cos(10)+0,3*sin(10)			
		F2 =	115401,3		N
	Top drop section (F3)	F3 = F2*(e^(±0,3∗(70*(π/180))-1)+F2+W*g*0,5*L*(cos(α1)+cos(α2))*RF			
		F3 = F2*(e^(+0,3∗(70*(π/180))-1)+F2+W(drillpipe)*g*0,5*ΔDT*(cos(80)+cos(10))*RF			
		F3 =	400791,0		N
	Top hold section (F4)	F4 = F3 + (W*L)*g*(cos α ± μ*sin α)			
		F4 = F3 + (W(drillpipe)*L hold)*g*(cos(80)+0,3*sin(80))			
		F4 =	1441320,8		N
	Top build-up section (F5)	F5 = F4*(e^(±0,3∗(80*(π/180))-1)+F4+W*g*0,5*L*(cos(α1)+cos(α2))*RF			
		F5 = F4*(e^(+0,3∗(80*(π/180))-1)+F4+W(drillpipe)*g*0,5*ΔBC*(cos(80)+cos(0))*RF			
		F5 =	2475635,9		N
	Top Well (F6)	F6 = F5 + W*L*g			
		F6 = F5 + (W(drillpipe)*L vertical)*g			
		F6 =	2778115,7		N

μ = 0,35	**Bottom inclined section (F1)**	F1 =	0		N
	Top inclined section (F2)	F2 = F1 + (W*L)*g*(cos α ± μ*sin α)			
		2 = F1 + (W(drillpipe)*(L Inc-(L HWDP+L DC))+(W(HWDP)*L HWDP)+(W(DC)*L DC))*g*(cos(10)+0,35*sin(10			
		F2 =	116367,6		N
	Top drop section (F3)	F3 = F2*(e^(±0,35∗(70*(π/180))-1)+F2+W*g*0,5*L*(cos(α1)+cos(α2))*RF			
		F3 = F2*(e^(+0,35∗(70*(π/180))-1)+F2+W(drillpipe)*g*0,5*ΔDT*(cos(80)+cos(10))*RF			
		F3 =	412760,2		N
	Top hold section (F4)	F4 = F3 + (W*L)*g*(cos α ± μ*sin α)			
		F4 = F3 + (W(drillpipe)*L hold)*g*(cos(80)+0,35*sin(80))			
		F4 =	1562514,3		N
	Top build-up section (F5)	F5 = F4*(e^(±0,35∗(80*(π/180))-1)+F4+W*g*0,5*L*(cos(α1)+cos(α2))*RF			
		F5 = F4*(e^(+0,35∗(80*(π/180))-1)+F4+W(drillpipe)*g*0,5*ΔBC*(cos(80)+cos(0))*RF			
		F5 =	2831642,8		N
	Top Well (F6)	F6 = F5 + W*L*g			
		F6 = F5 + (W(drillpipe)*L vertical)*g			
		F6 =	3134122,7		N
μ = 0,4	**Bottom inclined section (F1)**	F1 =	0		N
	Top inclined section (F2)	F2 = F1 + (W*L)*g*(cos α ± μ*sin α)			
		F2 = F1 + (W(drillpipe)*(L Inc-(L HWDP+L DC))+(W(HWDP)*L HWDP)+(W(DC)*L DC))*g*(cos(10)+0,4*sin(10)			
		F2 =	117333,9		N
	Top drop section (F3)	F3 = F2*(e^(±0,4∗(70*(π/180))-1)+F2+W*g*0,5*L*(cos(α1)+cos(α2))*RF			
		F3 = F2*(e^(+0,4∗(70*(π/180))-1)+F2+W(drillpipe)*g*0,5*ΔDT*(cos(80)+cos(10))*RF			
		F3 =	425576,8		N
	Top hold section (F4)	F4 = F3 + (W*L)*g*(cos α ± μ*sin α)			
		F4 = F3 + (W(drillpipe)*L hold)*g*(cos(80)+0,4*sin(80))			
		F4 =	1684555,2		N
	Top build-up section (F5)	F5 = F4*(e^(±0,4∗(80*(π/180))-1)+F4+W*g*0,5*L*(cos(α1)+cos(α2))*RF			
		F5 = F4*(e^(+0,4∗(80*(π/180))-1)+F4+W(drillpipe)*g*0,5*ΔBC*(cos(80)+cos(0))*RF			
		F5 =	3229158,7		N
	Top Well (F6)	F6 = F5 + W*L*g			
		F6 = F5 + (W(drillpipe)*L vertical)*g			
		F6 =	3531638,5		N

,

Appendix B.5 Analytical Model for S-Profile – Tripping in Scenario

DRILLSTRING CHARACTERISTICS:									
Nominal Diameter of Drillpipe	Nominal Unit Mass of Drillpipe	Grade	Type of Tooljoint	Appr. Unit Mass incl. Tooljoint	Nominal Diameter of HWDP	Connection HWDP	Nominal Unit Mass HWDP	Drill Collar (OD & ID)	Nominal unit mass of Drill Collar
(inch)	(lb/ft)			(kg/m)	(inch)	NC50 (4 1/2 IF)	(kg/m)	(inch)	(kg/m)
5	25,6	S-135	5 1/2 FH	43,73	5		73,4	8 x 3	218,77
	in air			*in air*			*in air*		*in air*

Additional														
MW	ρ(steel)	g	Inclination 1	Build-up angle	Vertical length down to KOP	Build-up bend (ΔBC)	Lenght of Hold/sail section	Drop bend (ΔDT)	Inclined section to target	Total length (MD)	Radius (R)	Length of HWDP	Length of DC	Inclination 2
(kg/m^3)	(kg/m^3)	(m/s^2)	(degree)	(degree/m)	(m)	(m)	(m)	(m)	(m)	(m)	(m)	(m)	(m)	(degree)
1700	7850	9,81	80	2/30	900	1200	6600	1050	150	9 900	859,44	90	30	70
					MD & TVD	*MD*	*MD*							

Buoyancy Factor		
β	1 - (ρmud / ρsteel)	0,783

Buoyed Weight			
W(HWDP)	β * W(HWDP)	57,5	(kg/m)
W(drillpipe)	β * W(app.incl.tolljoint)	34,26	(kg/m)
W(DC)	β * W(DC)	171,4	(kg/m)

Angles in Radians:	
0*(π/180) =	0
10*(π/180) =	0,1745
70*(π/180) =	1,2217
80*(π/180) =	1,3963

Weight of Topdrive		
W(Top Drive)	25	tons
	25000	kg
	245250	N

Ratio Factor:	
RF = (80°)	1,202
RF = (70°)	1,146

	Drag force calculations (Tripping in)				
μ = 0,1	Bottom inclined section (F1)	F1 =	0		N
	Top inclined section (F2)	F2 = F1 + (W*L)*g*(cos α ± μ*sin α)			
		F2 = F1 + (W(drillpipe)*(L Inc-(L HWDP+L DC))+(W(HWDP)*L HWDP)+(W(DC)*L DC))*g*(cos(10)-0,1*sin(10))			
		F2 =	107670,9		N
	Top drop section (F3)	F3 = F2*(e^(±0,1*(70*(π/180))-1)+F2+W*g*0,5*L*(cos(α1)+cos(α2))*RF			
		F3 = F2*(e^(-0,1*(70*(π/180))-1)+F2+W(drillpipe)*g*0,5*ΔDT*(cos(80)+cos(10))*RF			
		F3 =	329589,2		N
	Top hold section (F4)	F4 = F3 + (W*L)*g*(cos α ± μ*sin α)			
		F4 = F3 + (W(drillpipe)*L hold)*g*(cos(80)-0,1*sin(80))			
		F4 =	496324,5		N
	Top build-up section (F5)	F5 = F4*(e^(±0,1*(80*(π/180))-1)+F4+W*g*0,5*L*(cos(α1)+cos(α2))*RF			
		F5 = F4*(e^(-0,1*(80*(π/180))-1)+F4+W(drillpipe)*g*0,5*ΔBC*(cos(80)+cos(0))*RF			
		F5 =	716103,8		N
	Top Well (F6)	F6 = F5 + W*L*g			
		F6 = F5 + (W(drillpipe)*L vertical)*g			
		F6 =	1018583,6		N
μ = 0,15	Bottom inclined section (F1)	F1 =	0		N
	Top inclined section (F2)	F2 = F1 + (W*L)*g*(cos α ± μ*sin α)			
		F2 = F1 + (W(drillpipe)*(L Inc-(L HWDP+L DC))+(W(HWDP)*L HWDP)+(W(DC)*L DC))*g*(cos(10)-0,15*sin(10))			
		F2 =	106704,6		N
	Top drop section (F3)	F3 = F2*(e^(±0,15*(70*(π/180))-1)+F2+W*g*0,5*L*(cos(α1)+cos(α2))*RF			
		F3 = F2*(e^(-0,15*(70*(π/180))-1)+F2+W(drillpipe)*g*0,5*ΔDT*(cos(80)+cos(10))*RF			
		F3 =	323138,1		N
	Top hold section (F4)	F4 = F3 + (W*L)*g*(cos α ± μ*sin α)			
		F4 = F3 + (W(drillpipe)*L hold)*g*(cos(80)-0,15*sin(80))			
		F4 =	380649,1		N
	Top build-up section (F5)	F5 = F4*(e^(±0,15*(80*(π/180))-1)+F4+W*g*0,5*L*(cos(α1)+cos(α2))*RF			
		F5 = F4*(e^(-0,15*(80*(π/180))-1)+F4+W(drillpipe)*g*0,5*ΔBC*(cos(80)+cos(0))*RF			
		F5 =	593179,9		N
	Top Well (F6)	F6 = F5 + W*L*g			
		F6 = F5 + (W(drillpipe)*L vertical)*g			
		F6 =	895659,7		N
μ = 0,2	Bottom inclined section (F1)	F1 =	0		N
	Top inclined section (F2)	F2 = F1 + (W*L)*g*(cos α ± μ*sin α)			
		F2 = F1 + (W(drillpipe)*(L Inc-(L HWDP+L DC))+(W(HWDP)*L HWDP)+(W(DC)*L DC))*g*(cos(10)-0,2*sin(10))			
		F2 =	105738,3		N
	Top drop section (F3)	F3 = F2*(e^(±0,2*(70*(π/180))-1)+F2+W*g*0,5*L*(cos(α1)+cos(α2))*RF			
		F3 = F2*(e^(-0,2*(70*(π/180))-1)+F2+W(drillpipe)*g*0,5*ΔDT*(cos(80)+cos(10))*RF			
		F3 =	317117,0		N
	Top hold section (F4)	F4 = F3 + (W*L)*g*(cos α ± μ*sin α)			
		F4 = F3 + (W(drillpipe)*L hold)*g*(cos(80)-0,2*sin(80))			
		F4 =	265403,6		N
	Top build-up section (F5)	F5 = F4*(e^(±0,2*(80*(π/180))-1)+F4+W*g*0,5*L*(cos(α1)+cos(α2))*RF			
		F5 = F4*(e^(-0,2*(80*(π/180))-1)+F4+W(drillpipe)*g*0,5*ΔBC*(cos(80)+cos(0))*RF			
		F5 =	485196,4		N
	Top Well (F6)	F6 = F5 + W*L*g			
		F6 = F5 + (W(drillpipe)*L vertical)*g			
		F6 =	787676,3		N
μ = 0,25	Bottom inclined section (F1)	F1 =	0		N
	Top inclined section (F2)	F2 = F1 + (W*L)*g*(cos α ± μ*sin α)			
		F2 = F1 + (W(drillpipe)*(L Inc-(L HWDP+L DC))+(W(HWDP)*L HWDP)+(W(DC)*L DC))*g*(cos(10)-0,25*sin(10))			
		F2 =	104772,0		N
	Top drop section (F3)	F3 = F2*(e^(±0,25*(70*(π/180))-1)+F2+W*g*0,5*L*(cos(α1)+cos(α2))*RF			
		F3 = F2*(e^(-0,25*(70*(π/180))-1)+F2+W(drillpipe)*g*0,5*ΔDT*(cos(80)+cos(10))*RF			
		F3 =	311497,5		N
	Top hold section (F4)	F4 = F3 + (W*L)*g*(cos α ± μ*sin α)			
		F4 = F3 + (W(drillpipe)*L hold)*g*(cos(80)-0,25*sin(80))			
		F4 =	150559,8		N
	Top build-up section (F5)	F5 = F4*(e^(±0,25*(80*(π/180))-1)+F4+W*g*0,5*L*(cos(α1)+cos(α2))*RF			
		F5 = F4*(e^(-0,25*(80*(π/180))-1)+F4+W(drillpipe)*g*0,5*ΔBC*(cos(80)+cos(0))*RF			
		F5 =	390655,6		N
	Top Well (F6)	F6 = F5 + W*L*g			
		F6 = F5 + (W(drillpipe)*L vertical)*g			
		F6 =	693135,4		N

μ = 0,3	**Bottom inclined section (F1)**	F1 =	0		N
	Top inclined section (F2)	F2 = F1 + (W*L)*g*(cos α ± μ*sin α)			
		F2 = F1 + (W(drillpipe)*(L Inc-(L HWDP+L DC))+(W(HWDP)*L HWDP)+(W(DC)*L DC))*g*(cos(10)-0,3*sin(10))			
		F2 =	103805,7		N
	Top drop section (F3)	F3 = F2*(e^(±0,3*(70*(π/180))-1)+F2+W*g*0,5*L*(cos(α1)+cos(α2))*RF			
		F3 = F2*(e^(-0,3*(70*(π/180))-1)+F2+W(drillpipe)*g*0,5*ΔDT*(cos(80)+cos(10))*RF			
		F3 =	306253,2		N
	Top hold section (F4)	F4 = F3 + (W*L)*g*(cos α ± μ*sin α)			
		F4 = F3 + (W(drillpipe)*L hold)*g*(cos(80)-0,3*sin(80))			
		F4 =	36091,2		N
	Top build-up section (F5)	F5 = F4*(e^(±0,3*(80*(π/180))-1)+F4+W*g*0,5*L*(cos(α1)+cos(α2))*RF			
		F5 = F4*(e^(-0,3*(80*(π/180))-1)+F4+W(drillpipe)*g*0,5*ΔBC*(cos(80)+cos(0))*RF			
		F5 =	308198,9		N
	Top Well (F6)	F6 = F5 + W*L*g			
		F6 = F5 + (W(drillpipe)*L vertical)*g			
		F6 =	610678,8		N
μ = 0,35	**Bottom inclined section (F1)**	F1 =	0		N
	Top inclined section (F2)	F2 = F1 + (W*L)*g*(cos α ± μ*sin α)			
		F2 = F1 + (W(drillpipe)*(L Inc-(L HWDP+L DC))+(W(HWDP)*L HWDP)+(W(DC)*L DC))*g*(cos(10)-0,35*sin(10)			
		F2 =	102839,4		N
	Top drop section (F3)	F3 = F2*(e^(±0,35*(70*(π/180))-1)+F2+W*g*0,5*L*(cos(α1)+cos(α2))*RF			
		F3 = F2*(e^(-0,35*(70*(π/180))-1)+F2+W(drillpipe)*g*0,5*ΔDT*(cos(80)+cos(10))*RF			
		F3 =	301359,3		N
	Top hold section (F4)	F4 = F3 + (W*L)*g*(cos α ± μ*sin α)			
		F4 = F3 + (W(drillpipe)*L hold)*g*(cos(80)-0,35*sin(80))			
		F4 =	-78027,0		N
	Top build-up section (F5)	F5 = F4*(e^(±0,35*(80*(π/180))-1)+F4+W*g*0,5*L*(cos(α1)+cos(α2))*RF			
		F5 = F4*(e^(-0,35*(80*(π/180))-1)+F4+W(drillpipe)*g*0,5*ΔBC*(cos(80)+cos(0))*RF			
		F5 =	236594,8		N
	Top Well (F6)	F6 = F5 + W*L*g			
		F6 = F5 + (W(drillpipe)*L vertical)*g			
		F6 =	539074,6		N
μ = 0,4	**Bottom inclined section (F1)**	F1 =	0		N
	Top inclined section (F2)	F2 = F1 + (W*L)*g*(cos α ± μ*sin α)			
		F2 = F1 + (W(drillpipe)*(L Inc-(L HWDP+L DC))+(W(HWDP)*L HWDP)+(W(DC)*L DC))*g*(cos(10)-0,4*sin(10))			
		F2 =	101873,1		N
	Top drop section (F3)	F3 = F2*(e^(±0,4*(70*(π/180))-1)+F2+W*g*0,5*L*(cos(α1)+cos(α2))*RF			
		F3 = F2*(e^(-0,4*(70*(π/180))-1)+F2+W(drillpipe)*g*0,5*ΔDT*(cos(80)+cos(10))*RF			
		F3 =	296792,8		N
	Top hold section (F4)	F4 = F3 + (W*L)*g*(cos α ± μ*sin α)			
		F4 = F3 + (W(drillpipe)*L hold)*g*(cos(80)-0,4*sin(80))			
		F4 =	-191817,8		N
	Top build-up section (F5)	F5 = F4*(e^(±0,4*(80*(π/180))-1)+F4+W*g*0,5*L*(cos(α1)+cos(α2))*RF			
		F5 = F4*(e^(-0,4*(80*(π/180))-1)+F4+W(drillpipe)*g*0,5*ΔBC*(cos(80)+cos(0))*RF			
		F5 =	174726,8		N
	Top Well (F6)	F6 = F5 + W*L*g			
		F6 = F5 + (W(drillpipe)*L vertical)*g			
		F6 =	477206,6		N

Drag Forces inluding Topdrive				
$\mu = 0,1$	Top Vertical section incl. Topdrive	F7 = F6 + W(topdrive)		
		F7 =	1263833,6	kN
$\mu = 0,15$	Top Vertical section incl. Topdrive	F7 = F6 + W(topdrive)		
		F7 =	1140909,7	kN
$\mu = 0,2$	Top Vertical section incl. Topdrive	F7 = F6 + W(topdrive)		
		F7 =	1032926,3	kN
$\mu = 0,25$	Top Vertical section incl. Topdrive	F7 = F6 + W(topdrive)		
		F7 =	938385,4	kN
$\mu = 0,3$	Top Vertical section incl. Topdrive	F7 = F6 + W(topdrive)		
		F7 =	855928,8	kN
$\mu = 0,35$	Top Vertical section incl. Topdrive	F7 = F6 + W(topdrive)		
		F7 =	784324,6	kN
$\mu = 0,4$	Top Vertical section incl. Topdrive	F7 = F6 + W(topdrive)		
		F7 =	722456,6	kN

Appendix B.6 Analytical Model for S-Profile – Static (Rotating off Bottom) Scenario

DRILLSTRING CHARACTERISTICS:									
Nominal Diameter of Drillpipe	Nominal Unit Mass of Drillpipe	Grade	Type of Tooljoint	Appr. Unit Mass incl. Tooljoint	Nominal Diameter of HWDP	Connection HWDP	Nominal Unit Mass HWDP	Drill Collar (OD & ID)	Nominal unit mass of Drill Collar
(inch)	(lb/ft)	S-135	5 1/2 FH	(kg/m)	(inch)	NC50 (4 1/2 IF)	(kg/m)	(inch)	(kg/m)
5	25,6			43,73	5		73,4	8 x 3	218,77
	in air			*in air*			*in air*		*in air*

Additional														
MW	ρ(steel)	g	Inclination 1	Build-up angle	Vertical length down to KOP	Build-up bend (ΔBC)	Lenght of Hold/sail section	Drop bend (ΔDT)	Inclined section to target	Total length (MD)	Radius (R)	Length of HWDP	Length of DC	Inclination 2
(kg/m^3)	(kg/m^3)	(m/s^2)	(degree)	(degree/m)	(m)	(m)	(m)	(m)	(m)	(m)	(m)	(m)	(m)	(degree)
1700	7850	9,81	80	2/30	900	1200	6600	1050	150	9 900	859,44	90	30	70
					MD & TVD	*MD*	*MD*							

Additional					
ΔL Build section	ΔL Hold section	ΔL Drop section	ΔL inclined section	ΔL HWDP	ΔL DC
(m)	(m)	(m)	(m)	(m)	(m)
846,4	1146,1	697,1	147,7	88,6	29,5
TVD	*TVD*	*TVD*	*TVD*	*TVD*	*TVD*

Buoyancy Factor		
β	1 - (ρmud / ρsteel)	0,783

Buoyed Weight			
W(HWDP)	β * W(HWDP)	57,5	(kg/m)
W(drillpipe)	β * W(app.incl.tolljoint)	34,26	(kg/m)
W(DC)	β * W(DC)	171,4	(kg/m)

Angles in Radians:	
0*(π/180) =	0
10*(π/180) =	0,1745
70*(π/180) =	1,2217
80*(π/180) =	1,3963

Ratio Factor:	
RF = (80°)	1,202
RF = (70°)	1,146

	Drag force calculations (Static (Rotating off bottom))				
μ = 0,1-0,4	**Bottom inclined section (F1)**	F1 =	0		N
	Top inclined section (F2)	F2 = F1 + (W*L)*g			
		F2 = F1 + (W(drillpipe)*(ΔL Inc-(ΔL HWDP+ΔL DC))+(W(HWDP)*ΔL HWDP)+(W(DC)*ΔL DC))*g			
		F2 =	109603,5		N
	Top drop section (F3)	F3 = F2 + (W*L)*g			
		F3 = F2 + (W(drillpipe)*ΔL drop section)*g			
		F3 =	343904,5		N
	Top hold section (F4)	F4 = F3 + (W*L)*g			
		F4 = F3 + (W(drillpipe)*ΔL hold section)*g			
		F4 =	729088,4		N
	Top build-up section (F5)	F5 = F4 + (W*L)*g			
		F5 = F4 + (W(drillpipe)*ΔL build-up section)*g			
		F5 =	1013547,1		N
	Top Well (F6)	F6 = F5 + (W*L)*g			
		F6 = F5 + (W(drillpipe)*ΔL vertical)*g			
		F6 =	1316027,0		N